THESIS FOR THE DEGREE OF DOCTOR OF PHILOSOPHY

Usability of Textile Reinforced Concrete: Structural Performance, Durability and Sustainability

NATALIE WILLIAMS PORTAL

Department of Civil and Environmental Engineering
Division of Structural Engineering
Concrete Structures
CHALMERS UNIVERSITY OF TECHNOLOGY
Gothenburg, Sweden, 2015

Usability of Textile Reinforced Concrete:
Structural Performance, Durability and Sustainability

NATALIE WILLIAMS PORTAL

Doktorsavhandlingar vid Chalmers tekniska högskola
Ny serie Nr. 3914
ISBN no. 978-91-7597-233-6
ISSN no. 0346-718X

Department of Civil and Environmental Engineering
Division of Structural Engineering
Concrete Structures
Chalmers University of Technology
SE-412 96 Gothenburg
Sweden
Telephone: + 46 (0)31-772 1000

Cover:
The cover picture shows the association of structural performance, durability and sustainability, which is the foundation of this thesis.

Chalmers Repro Service/Department of Civil and Environmental Engineering
Gothenburg, Sweden, 2015

Usability of Textile Reinforced Concrete:
Structural Performance, Durability and Sustainability

NATALIE WILLIAMS PORTAL

Department of Civil and Environmental Engineering
Division of Structural Engineering, Concrete Structures
Chalmers University of Technology

ABSTRACT

Textile reinforced concrete (TRC) is an innovative high performance composite material consisting of open multi-axial textiles embedded in a fine-grained concrete matrix. Despite the fact that TRC-based research has revealed many promising attributes, it has yet to reach its recognition due to a lack of available design tools, standards and long-term behaviour. To be able to reach this next stage, consistent test methods and reliable models need to be established to reduce uncertainty and the need for individual and extensive experimental studies.

This thesis aims to investigate structural performance, durability and sustainability aspects of TRC for its usability in the built environment. The structural performance was experimentally and analytically evaluated for the individual material constituents, material interaction, as well as global TRC components. The linking of the structural performance of these various levels was investigated by means of non-linear finite element analysis (FEA). The durability of TRC was characterized according to the influence of accelerated ageing based on alkali resistance on the structural performance of textile reinforcement. Furthermore, the environmental sustainability of TRC was evaluated in comparison to conventional RC using a Life Cycle Assessment (LCA).

The experimental quantification of the structural performance on the material and interaction levels was found to be decisive to understand the composite behaviour. In general, the bond behaviour in TRC has been identified as a critical feature affecting the global behaviour. Particularly for carbon textiles, the bond behaviour needs to be improved; an enhancement of the load bearing behaviour was successfully observed using surface coatings, short fibres, and high performance concrete. Linking the experimental data from the material and interaction levels to the global level in FEA led to promising results such that further insight on the actual failure behaviour could be gained. The accelerated testing was generally too aggressive for textiles made of basalt and AR-glass leading to extensive degradation; however, carbon textiles were found to be a promising alternative as they have superior durability properties in an alkaline environment without undergoing any strength loss. Through accelerated testing, it was found that the exposure time, temperature and test solution need to be material specific. The applied sizing or coating on the textiles also had a considerable influence on the extent of degradation. Based on the conducted LCA, the reduction of the concrete cover in a TRC panel significantly decreased its environmental impact compared to traditionally reinforced solutions. Ultimately, the experimental and modelling approaches developed in this work can be applied to further characterize the short- and long-term behaviour of TRC for the built environment.

Keywords: Textile reinforced concrete (TRC), experimental methods, finite element analysis (FEA), durability, sustainability, life cycle assessment (LCA).

Användbarhet av textilarmerad betong –
Konstruktionstekniska aspekter, beständighet och hållbarhet

NATALIE WILLIAMS PORTAL

Institutionen för bygg- och miljöteknik
Avdelningen för konstruktionsteknik, Betongbyggnad
Chalmers tekniska högskola

SAMMANFATTNING

Textilarmerad betong (TRC) är ett innovativt och högpresterande kompositmaterial bestående av multi-axiella textilarmeringsnät inbäddade i en finkornig betongmatris. Trots att forskning om TRC indikerar att det är lovande, så har det ännu inte fått sitt erkännande på grund av att det saknas dimensioneringsverktyg, standarder och tillräckliga kunskaper om dess långsiktiga beteende. För att kunna uppnå de målen krävs enhetliga testmetoder och tillförlitliga modeller för att minska osäkerheten och behovet av individuella och omfattande experimentella studier.

I avhandlingen undersöks konstruktionstekniska, beständighets- och hållbarhetsaspekter av TRC för dess användbarhet i den byggda miljön. Den konstruktionstekniska prestandan evaluerades både experimentellt och analytiskt, dels för de enskilda materialkomponenterna, men också för interaktionen mellan dem och det globala beteendet. Kopplingen mellan dessa olika nivåer studerades med hjälp av icke-linjära finita element (FE) analyser. Beständigheten hos TRC karaktäriserades genom dragförsök på provkroppar utsatta för ett accelererat åldringsförfarande med alkali. Därutöver utvärderades den miljöbetingade hållbarheten av TRC i en livscykelanalys (LCA), där TRC jämfördes med konventionellt armerad betong.

Försöken på material- och interaktionsnivåerna var viktiga för att kunna förstå den sammansatta strukturens beteende på global nivå. Vidhäftningen mellan textilarmeringen och betongmatrisen är en av de kritiska faktorer som påverkar böj- och draghållfastheten på den globala nivån och behöver förbättras, särskilt för kolfibertextiler. En signifikant förbättring av bärförmågan nåddes genom att ytbehandla textilarmeringen samt genom användning av korta fibrer och högpresterande betong. Kopplingen mellan försöksresultaten från både material- och interaktionsnivå i en förenklad FE-modell på global nivå ledde till goda resultat och ytterligare insikt om de faktiska brottmekanismerna. De accelererade åldringstesterna var i allmänhet alldeles för aggressiva för textilarmeringen gjord av basalt- och AR-glasfibrer – de uppvisade omfattande nedbrytning. Kolfiberprodukterna däremot hade mycket god alkalibeständighet utan någon hållfasthetsförlust. Åldringstesterna visade att exponeringstid, temperatur och kemiskt lösningsmedel bör anpassas materialspecifikt. Den applicerade ytbehandlingen hade betydande inverkan på beständigheten. Beträffande TRC:s inverkan på miljön, så visade LCA-studien att det minskade betongtäckskiktet och elementets totala betongtjocklek signifikant reducerade miljöeffekterna för en TRC-panel jämfört med en med konventionell armering. Slutligen, de experimentella och numeriska metoder som utvecklats i detta arbete kan användas för att karakterisera TRC:s användbarhet i den byggda miljön både på kort och på lång sikt.

Nyckelord: Textilarmerad betong, experimentell metodik, finit elementanalys, beständighet, hållbarhet, livscykelanalys.

LIST OF PUBLICATIONS

This thesis is primarily based on the work contained in the following papers:

Paper I

Williams Portal N., Flansbjer M., Johannesson P., Malaga K. and Lundgren K. (2015): Tensile Behaviour of Textile Reinforcement under Accelerated Ageing Conditions. Submitted for publication to *Journal of Building Engineering*.

Paper II

Williams Portal N., Perez Fernandez I., Thrane Nyholm L. and Lundgren K. (2014): Pull-out of Textile Reinforcement in Concrete. *Construction and Building Materials*, Vol. 71, pp. 63-71, (doi: http://dx.doi.org/10.1016/j.conbuildmat.2014.08.014), *License number 3682010911209.*

Paper III

Williams Portal N., Lundgren K. and Thrane Nyholm L. (2015): Flexural Behaviour of Textile Reinforced Concrete Composites: Experimental and Numerical Evaluation. Submitted for publication to *Materials and Structures.*

Paper IV

Williams Portal N., Lundgren K., Wallbaum H. and Malaga K. (2014): Sustainable Potential of Textile-Reinforced Concrete. *Journal of Materials in Civil Engineering*, Vol. 27(7), With permission from ASCE. ISSN (print): 0899-1561, (doi: http://dx.doi.org/10.1061/(ASCE)MT.1943-5533.0001160).

THE AUTHOR'S CONTRIBUTIONS TO JOINTLY PUBLISHED PAPERS

The contribution of the author of this doctoral thesis to the appended papers is described here:

I. The author was responsible for the structure and a large part of the writing. The experimental program was primarily established by the author for EU funded project H-House (EeB.NMP.2013-2-608893) and Formas Tekocrete II (IQS). The author conducted the accelerated testing and Mathias Flansbjer was responsible for the development of the tensile test setup at SP Technical Research Institute of Sweden. The author analysed the presented results with the assistance of Pär Johannesson concerning the statistical analyses.

II. The author was primarily responsible for the planning and writing of the paper with the assistance of the co-authors. The experimental work was conducted at Danish Technological Institute (DTI) within the EU funded project TailorCrete (NMP2-LA-2009-228663). The experimental program was handled by the author, while the laboratory technicians at DTI, led by Lars Nyholm Thrane, developed and performed the pull-out tests. The author evaluated the experimental data and analysed the data according to the 1D model in collaboration with Ignasi Perez Fernandez who developed the 3D FE-model.

III. The author of this thesis planned and wrote the majority of the paper with input from the co-authors. The first test series (1A) was conducted by Ane Mette Walter from DTI and was previously published in Williams Portal et al. (2013). The second test series (1B) was linked to that presented in Paper II, wherein the experiments were planned and conducted at DTI with the involvement of the author. The author was responsible for the analysis of the experimental results and conducted the FE-analysis included in the paper.

IV. The author of this thesis was accountable for a major part of the background research, Life-cycle analysis (LCA) analysis, structuring and writing of this paper. The co-authors supported the technical content and outcome of the paper.

ADDITIONAL PUBLICATIONS & CONTRIBUTIONS BY THE AUTHOR

Licentiate Thesis

Williams Portal N. (2013): *Sustainability and flexural behaviour of Textile Reinforced Concrete*. Degree for Licentiate of Engineering, Licentiate Thesis, Civil and Environmental Engineering, Chalmers University of Technology, pp. 53.

Master's Thesis

Williams Portal N. (2011): *Evaluation of heat and moisture induced stress and strain of historic building materials and artefacts*. Masters of Engineering Thesis, Civil and Environmental Engineering, Chalmers University of Technology, pp. 99.

Technical Articles

Hodicky K., Williams Portal N., Hulin T. and Stang H. (2015): Assessment of risk of early age cracking in thin-walled sandwich panels. Submitted for publication to *Engineering Fracture Mechanics*.

Williams Portal N., van Schijndel A.W.M. and Sasic Kalagasidis A. (2013): The multiphysics modelling of heat and moisture induced stress and strain historic building materials and artefacts. *Building Simulation, An International Journal.* Vol. 7 (3), p. 217-227. ISSN (print): 1996-3599, (doi: http://dx.doi.org/10.1007/s12273-013-0153-4)

Conference Papers

Miccoli L., Johansson G., Zandi K., Williams Portal N., Fontana P. and Mueller U. (2015): Numerical modelling of UHPC and TRC sandwich elements for building envelopes: assessment of different modelling approaches. In *Proceedings of International Association for Bridge and Structural Engineering (IABSE) Conference 2015 – Structural Engineering*, Geneva, Switzerland, 23-25 September 2015.

Chozas V., Larraza I., Vera-Agullo J., Williams Portal N., Mueller U., and Flansbjer M. (2015): Synthesis and characterization of reactive powder concrete for its application on thermal insulation panels. In *Proceedings of 2nd International Conference "Innovative Materials, Structures and Technologies"*, Riga, Latvia 30 September-02 October 2015.

Mueller U., Williams Portal N., Flansbjer M., Silva N., Malaga K., Larraza I. and Vera-Agullo J. (2015): Reactive powder concrete for façade elements – A sustainable approach. In *Proceedings of VII International Congress on Architectural Envelopes*, San Sebastian-Donostia, Spain, 27-28 May 2015.

Flansbjer M., Mueller U., Wlasak L., Honfi D., Williams Portal N., Edgar J.O. and Larraza I. (2015) Structural behaviour of RPC sandwich façade elements with GFRP connectors. In *Proceedings of VII International Congress on Architectural Envelopes*, San Sebastian-Donostia, Spain, 27-28 May 2015.

Williams Portal N., Silva N., Mueller U., Malaga K. and Billberg P. (2015): Durability Study of Textile Fibre Reinforcement. In *Proceedings of Concrete 2015 27th Biennial National Conference of the Concrete Institute of Australia*, Melbourne, Australia, 30 August-02 September 2015.

Williams Portal N., Flansbjer M., Lundgren K. and Malaga K. (2015): Implementation of Experimental Data in Analyses of Textile Reinforced Concrete Structures. In *Proceedings of 3rd ICTRC International Conference on Textile Reinforced Concrete*, Aachen, Germany, 7-10 June 2015.

Williams Portal N., Flansbjer M., Tammo K. and Malaga K. (2014): Alkali Resistance of Textile Reinforcement for Concrete Façade Panels. In *Proceedings of the XXII Concrete Research Symposium*, Reykjavik, Iceland, 13-15 August 2014.

Williams Portal N., Lundgren K. and Malaga K. (2014): Evaluation of Pull-out Behaviour in Textile Reinforced Concrete. In *Proceedings of the 10th fib International PhD Symposium in Civil Engineering*, Quebec City, Canada, 21-23 June 2014, pp. 97-102.

Williams Portal N., Lohmeyer R. and Wallbaum H. (2014): Sustainability of Reinforcement Alternatives for Concrete. In *Proceedings of the Concrete Innovation Conference 2014 (CIC 2014)*, Oslo, Norway, 10-12 June 2014.

Williams Portal N., Lundgren K., Walter A.M., Frederiksen J.O. and Nyholm Thrane L. (2013): Numerical Modelling of Textile Reinforced Concrete. In *Proceedings of the VIII International Conference on Fracture Mechanics of Concrete and Concrete Structures*, Toledo, Spain, 10-14 March 2013.

Williams Portal N., Sasic Kalagasidis A. and van Schijndel J. (2011): Simulation of heat and moisture induced stress and strain of historic building materials. In *Proceedings of Building Simulation 2011: 12th Conference of International Building Performance Simulation Association*, Sydney, Australia, 14-16 November 2011, pp. 24-31.

Williams Portal N., van Aarle M. and van Schijndel J. (2011): Simulation and Verification of Coupled Heat and Moisture Modelling. Comsol Conference, Stuttgart, Germany, 25-27 October 2011.

Magazines

Fall D., Lundgren K. and Williams Portal N. (2013): Provning av betongplattor – inverkan av olika armeringstyper (Testing of concrete slabs: the influence of different reinforcement types). In Swedish. *Tidskriften Betong*. Vol. 5/November 2013.

Contents

”Teachers open the door but you must enter by yourself.” – Chinese Proverb

Preface

The research that is presented in this thesis was carried out in two parts, whereby the first part took place from September 2011 to February 2013 at the Division of Structural Engineering, Chalmers University of Technology (CTH), Sweden and the second part from February 2013 to July 2015 at The Swedish Cement and Concrete Research Institute (CBI), Sweden in connection to CTH. Several projects were coupled to this research including EU projects *H-House* (EeB.NMP.2013-2-608893) and *SESBE* (EeB.NMP.2013-1-608950), Formas project *Tekocrete II* (IQS), Formas project *Homes for Tomorrow* and EU project *TailorCrete* (NMP2-LA-2009-228663).

The time marking the grand finale of my academic journey has at last come. Nearly a decade ago, this journey began at the University of Waterloo in Canada where I completed my bachelor studies in Civil engineering. Curiosity and urge to learn brought me to Sweden as well as the Netherlands. Along the way, I have been graced with so many meaningful people who have shaped me into who I am today. It is impossible to mention everyone in this short discourse, but I trust that you know who you are.

The realization of my Ph.D. studies was certainly not accomplished alone. I am grateful to have had Prof. Karin Lundgren as a supervisor and examiner. She was present along the entire process participating in long discussions providing valuable advice and academic guidance. I am also thankful to my co-supervisor, Adj. Prof. Katarina Malaga, who offered both technical and personal guidance along the way along with the resources to complete my work. From these two important people, I have been taught to believe in my own efforts and research ideas.

My grateful thanks are extended to colleagues at CBI and CTH particularly Urs Mueller, Ph.D., and Nelson Silva, Ph.D., as well as Adj. Prof. Mathias Flansbjer who enabled my research to gain new insights. I would like to further express my appreciation to all the collaborative partners involved in the EU projects (H-House and SESBE), Pär Johannesson, Ph.D., for his expert knowledge and guidance regarding statistical analysis, Ignasi Fernandez Perez, Ph.D. for our fruitful cooperation, Lars Nyholm Thrane, Ph.D., for making our experimental collaboration possible at Danish Technical Institute (DTI), Prof. Holger Wallbaum for his assistance with sustainability evaluations and Prof. Kent Gylltoft for being my co-supervisor at the beginning of my studies.

I am grateful for having numerous colleagues at both CTH and at CBI who have become great friends over time. Special acknowledgments are sent out to Valbona Mara for being present from the beginning to the end. To all my connections all over the world, it is a pleasure to have managed to stay in touch.

As a final point, I am indebted to my parents, my brother and Elyse, as well as Thomas for their undying love and understanding during this rewarding process. This work is dedicated to my *grand-maman* Rita, *tante* Carmen and *tío* Alberto who believe in me for eternity.

NATALIE WILLIAMS PORTAL

Gothenburg, August 2015

1 Introduction

1.1 Background

The middle of the 19th century marked the beginning of the use of reinforced concrete in structural building applications (Shaeffer, 1992). To this day, research and development concerning this common building material continues. Concrete is known for having high compressive strength yet it requires reinforcement to compensate for its low tensile strength. Steel reinforcement bars are considered as the universal reinforcement solution but various alternatives have been applied more recently, such as fibre-reinforced polymer (FRP) bars, steel welded-wire mesh, discrete fibres (steel or synthetic) (ACI Education Bulletin E2-00, 2000), as well as textile reinforcement. Alternative reinforcement materials have been exploited primarily due to the fact that conventional reinforced concrete (RC) has a history of being vulnerable to corrosion attack leading to loss of structural integrity if the protective medium of concrete were to be weakened (Domone et al., 2010). Secondarily, the use of alternative reinforcements could reduce the need for a thick concrete cover mandated by *EC2* (EN 1992-1-1, 2008), thus leading to potential reduction of self-weight and material resources. Other reasons to deviate from conventional steel reinforcement could be to facilitate structural versatility and simplify casting and production methods.

Textile reinforcement is an alternative reinforcement material consisting of natural or synthetic singular technical fibres processed into yarns or rovings which are woven into multi-axial textile fabrics having an open mesh or grid structure. When textile reinforcement is incorporated into concrete, it is most often termed as Textile Reinforced Concrete (TRC). Research and development pertaining to this innovative high performance composite material is thought to have commenced at the end of the 20th century. Research clusters involved in the use of woven or continuous fibres in a cementitious matrix were primarily situated in Germany (Curbach et al., 1999, Brameshuber, 2006, Scheerer et al., 2015), Israel (Peled et al., 1994), United States of America (Mobasher, 2012), United Kingdom (Ohno et al., 1994) and Japan (Hayashi et al., 1990, Fujisaki et al., 1993). Overtime this research area has globally progressed within Europe, Brazil and China. The extent of research has led to a variety of applications: façade panel solutions (Hegger, 2009, Malaga et al., 2012, Shams et al., 2015), shell structures (Tysmans et al., 2011, Scholzen et al., 2012), pedestrian bridges (Hegger et al., 2010b), strengthening applications (Täljsten et al., 2006, Papanicolaou et al., 2008, Dai et al., 2009, D'Ambrisi et al., 2011, Ortlepp et al., 2011, Schladitz et al., 2012, Si Larbi et al., 2012) and corrosion protection (Tang et al., 2012, Lohaus et al., 2015).

For the application of new materials, it becomes of great importance to understand the key features and their underlying interaction. In this work, it was of interest to focus on the particular application of TRC in the built environment. Accordingly, critical features pertinent to TRC in this context could include, e.g. the complex bond behaviour between the textile reinforcement and concrete matrix, characterization of material variability, and long-term performance. Unfortunately, the current design codes or recommendations pertaining to RC, fibre reinforced concrete (FRC) or use of FRP bars in concrete are to a certain degree inapplicable to the design of TRC due to the aforementioned critical features. Besides, no design standards are yet formalized for TRC, such that extensive experimental programs are still needed to acquire approval for each individual application (Orlowsky et al., 2011, Lorenz et al., 2015).

There exists however a few registered associations, e.g. TUDALIT e.V., thriving towards general construction approvals for TRC in Germany. In essence, TRC cannot reach its recognition without standardized structural design methods and experimental methods.

1.2 Research objectives

The aim of this thesis is to investigate *structural performance*, *durability* and *sustainability* aspects of textile reinforced concrete (TRC) for its usability in the built environment. Each of these investigated subjects constitutes an exhaustive array of related topics of which most relevant ones were incorporated in this work as highlighted in Figure 1.1. Both *structural performance* and *durability* are defined as subsets of *sustainability*, as the application of new materials often revolves around holistic and sustainable decision making. *Structural performance* aspects are further classified in this thesis at various levels, namely *material*, *interaction* and *global* levels. Since TRC is a composite material with a complex heterogeneous structure, it is of key importance to evaluate the individual constituents (*material*) and their composite action (*interaction*) in order to be able to gain an adequate understanding of the composite behaviour of a structure (*global*). Flexural and tensile behaviours of TRC were investigated because they are prevailing in typical structures applied in the built environment, e.g. façade solutions and slabs. Furthermore, to enable the application of a material in the built environment, a wide range of design parameters typically need to be fulfilled, yet when dealing with innovative materials in particular, the long-term performance (*durability*) and environmental consequences (*sustainability*) are often most uncertain and thus need to be investigated.

The specific objectives of the work presented in this thesis are:

1. To quantify the *structural performance* of TRC on *material*, *interaction* and *global* levels.
2. To interconnect the *structural performance* of TRC on *material* and *interaction* levels to the *global* level.
3. To determine the *durability* of textile reinforcement through the effect of accelerated ageing on the *structural performance* on the *material* level.
4. To evaluate the *sustainability* of TRC versus conventional reinforced concrete through the *environmental* impact from *cradle-to-gate*.

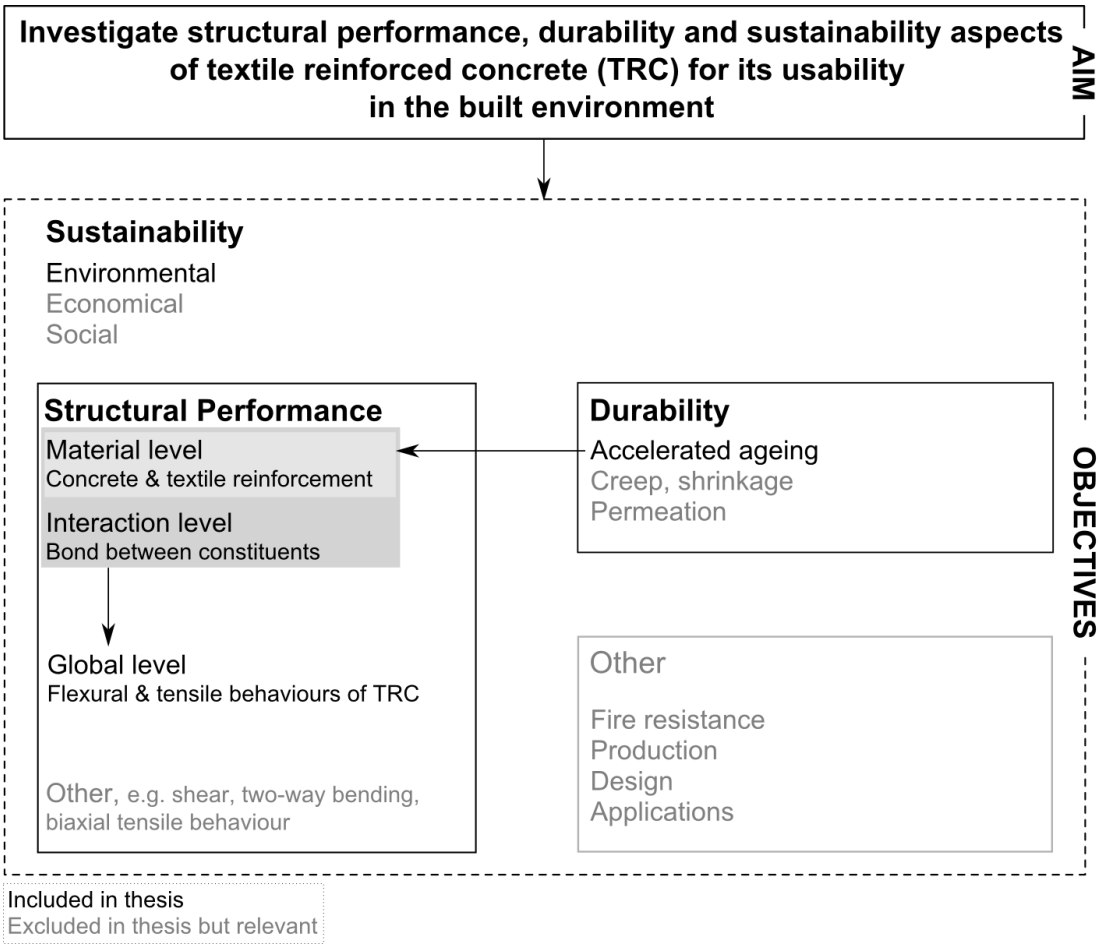

Figure 1.1 Schematic illustration of the research objectives.

1.3 Methodology

The methodology of this thesis is presented for each of the key features investigated in this work. A detailed description of the individual methodologies is provided in the following sections.

1.3.1 Structural performance

The methodology applied for s*tructural performance*, related to *Objectives 1* and *2*, encompassed experimental methods on three levels i.e. *material*, *interaction* and *global* and numerical modelling was used to link these levels as depicted in Figure 1.2. The experimental methods conducted on the various levels are:

> Material Level
  - Concrete matrix: General short-term mechanical properties were quantified, such as compressive and tensile properties.
  - Textile reinforcement: Mechanical properties were measured by uniaxial tensile testing.

> Interaction Level
  - Bond behaviour between concrete and textile reinforcement was quantified through pull-out tests.

> Global Level
    - Four-point bending tests were conducted to quantify the flexural behaviour of TRC.
    - The tensile behaviour of TRC was quantified by means of uniaxial tensile tests.

Available standard or recommended experimental test methods were applied in this work and are documented accordingly. Test methods which have no standardized documentation were primarily developed based on published scientific research results related to TRC or similar research fields, e.g. fibre reinforced polymers (FRP) in concrete or fibre reinforced concrete (FRC). Deviations in the experimental test methods are justified where applicable.

The experimental results obtained through the applied experimental methods were processed and thereafter applied in finite-element analysis (FEA) at a *global* level. The experimental methods needed to be adapted such that they could be applied as input data, which will be further explained throughout the thesis. When applicable, parameters were calculated using existing empirical equations from, e.g. fib Model Code 2010 (2013), in place of characterizing the given behaviour experimentally.

On the *global* level, FEA was applied to gain a deeper understanding regarding the failure mode and to identify difficulties and uncertainties in the modelling of TRC. The commercial software DIANA (DIsplacement ANAlyser) was used to perform the analyses. Through modelling, it was also identified whether the experimental methods applied were adequate or required further development to be able to better capture a given aspect of the relevant structural behaviour. Overall, FEA was applied as a complement to experimental investigations.

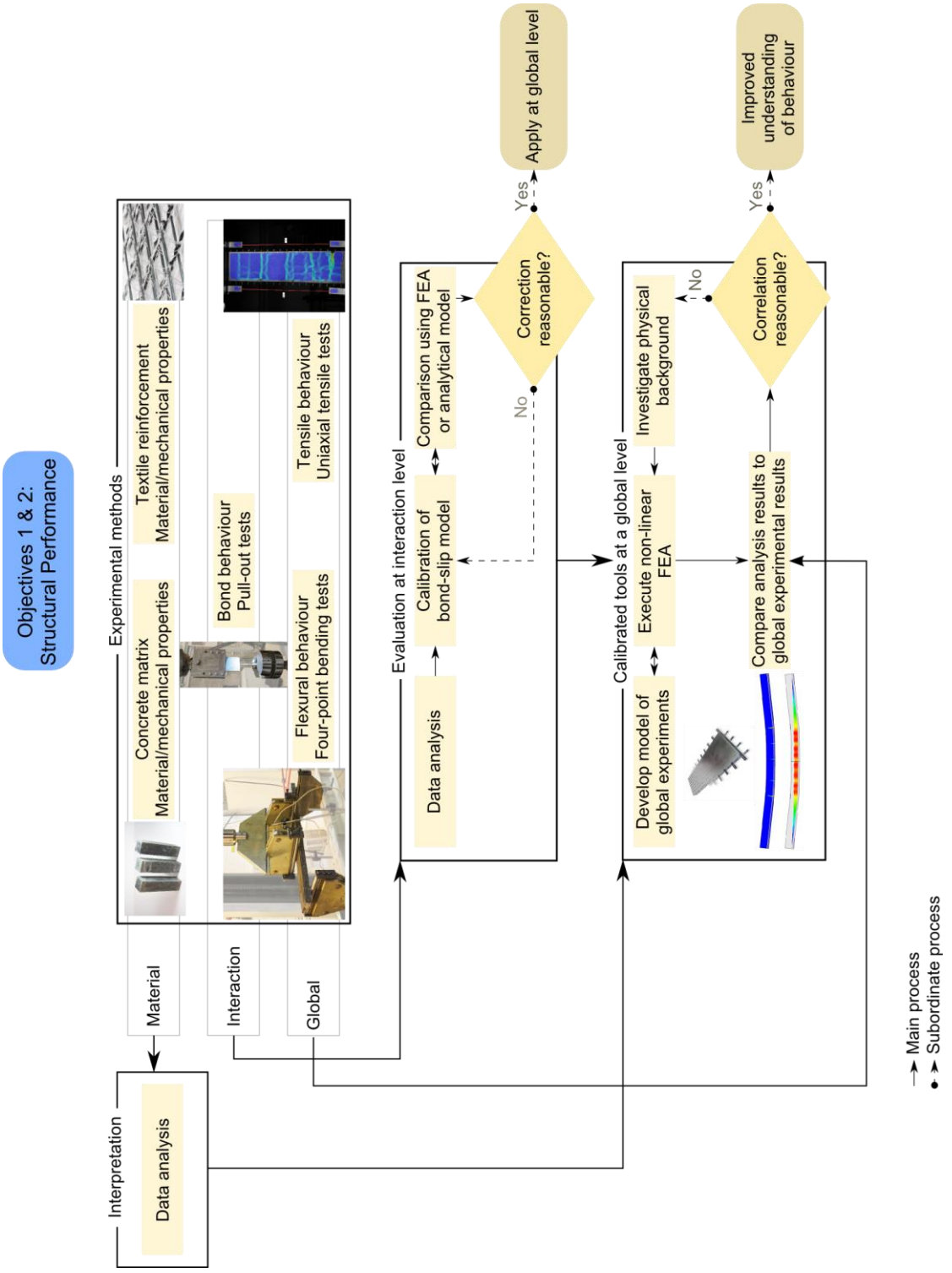

Figure 1.2 *Schematic illustration of the methodology pertaining to structural performance (Objectives 1 and 2).*

1.3.2 Durability

The methodology applied for *durability*, pertaining to *Objective 3*, included two main processes (see Figure 1.3): experimental methods and interpretation of results. In this work, durability was investigated on the *material* level and related to the chemical resistance, viz. alkali resistance, of textile reinforcement. Various commercial textile reinforcement materials underwent accelerated ageing tests paired with tensile tests in accordance with ISO 10406-1 (2008). Textile reinforcement specimens were aged in a simulated concrete pore solution and exposed to the standard specified boundary conditions. Alternative boundary conditions were also included in the scope of work to investigate the discrete influence of two key variables on material ageing, i.e. temperature and pH of a simulated pore solution. Tensile tests were conducted on specimens before and after ageing given that the materials could be tested based on their level of degradation. Furthermore, the interpretation of the experimental results involved the documentation of visual observations before and after testing, data processing, as well as statistical analysis of the data to understand the significance and variability of the results. Degradation curves in terms of tensile strength versus time were established for the given materials. When considered statistically beneficial, additional accelerated tests were conducted to further refine the degradation curve. It is to say that the selected boundary conditions of these additional tests could statistically improve the certainty and correlation of the curves.

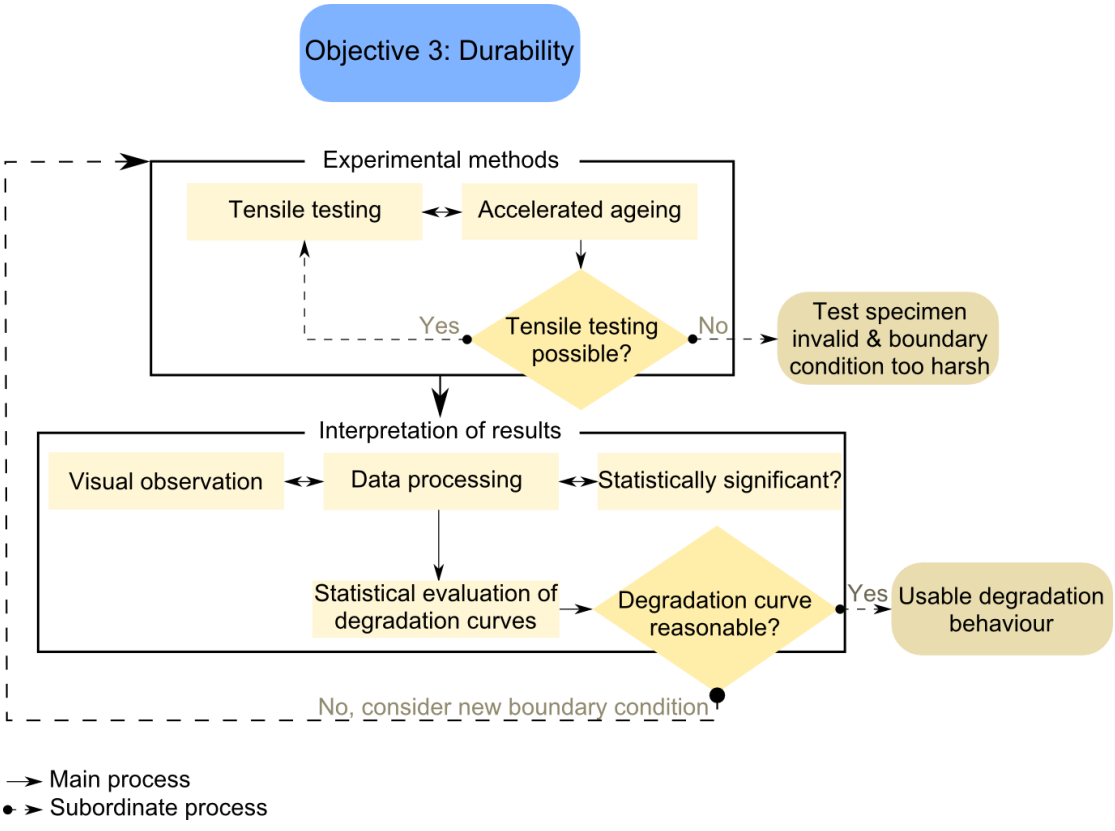

Figure 1.3 Schematic illustration of the methodology pertaining to durability (Objective 3).

1.3.3 Sustainability

The methodology used to evaluate the s*ustainability* of TRC according to an environmental context, related to *Objective 4*, is presented in Figure 1.4. The evaluation was conducted by means of a Life Cycle Assessment (LCA) in accordance with ISO 14040 (2006) and ISO 14044 (2006). This method is used to evaluate the environmental impact of e.g. building materials. A cradle-to-gate perspective was assumed, such that the impact of the extraction to production processes was included in the assessment. By doing so, the environmental impact of reducing e.g. the concrete cover in TRC structures could be observed when compared to RC. SimaPro (Version 7.3.3) was used to execute the analysis and a functional unit of 1 m^2 of reinforced concrete was assumed throughout the study. Moreover, to be able to *equally* compare various reinforced concrete alternatives, the one-way bending capacity of an RC section of 1 m x 1 m x 0.08 m was selected as a reference. It was assumed that the concrete cover could be reduced for textile reinforcement to a minimal value providing sufficient bond. The cradle-to-gate inventory data used in this study were taken from readily available databases: European Reference Life Cycle Database 3.0 (ELCD) (European Commission, 2013) and EcoInvent version 3.0 (Swiss Centre for Life Cycle Inventories, 2013).

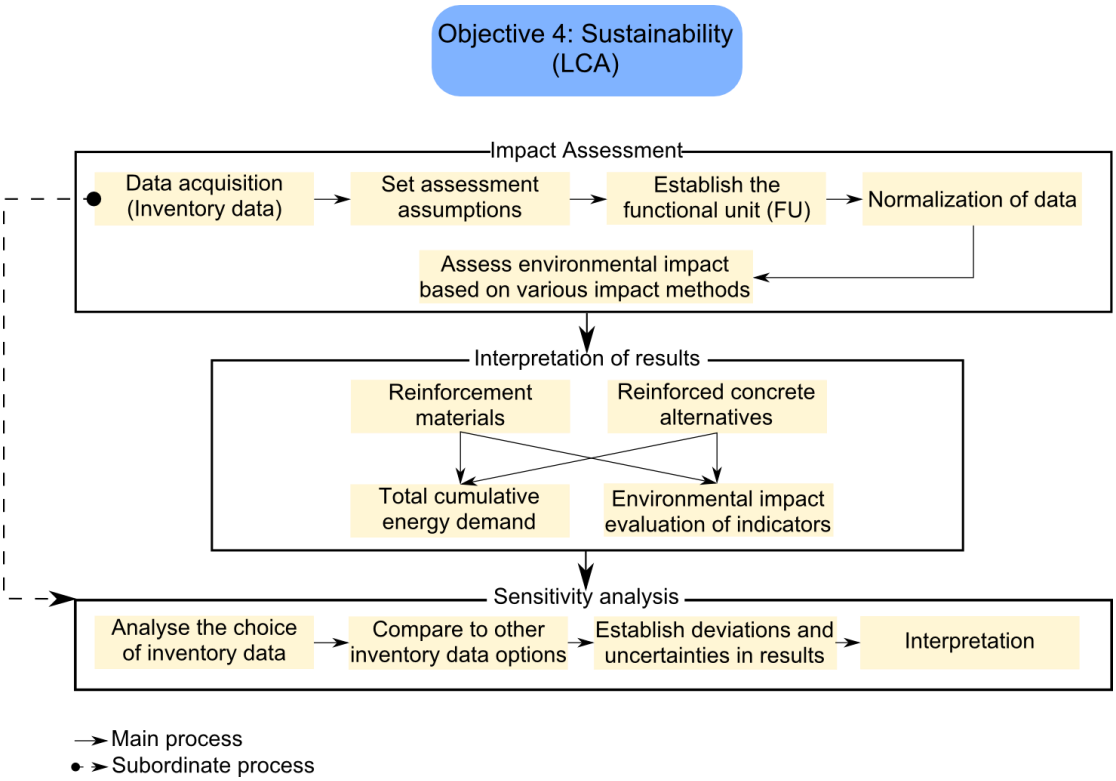

Figure 1.4 Schematic illustration of the methodology pertaining to sustainability (Objective 4).

1.4 Limitations

Limitations concerning the overall scope of work revolve around key aspects of *structural performance*, *durability* and *sustainability*, as previously illustrated in Figure 1.1. Limitations related to more detailed aspects of this thesis and papers can be summarized as follows:

- Long-term tests due to, e.g. creep and shrinkage, were not carried out to characterize the mechanical properties of fine-grained concrete (Durability – *material* level)
- The change in chemical composition on the surface of the aged textile reinforcements was not studied.
- Accelerated ageing of textile reinforcement in a concrete matrix was not a part of this thesis. Accordingly, changes in bond between the textile reinforcement and concrete matrix were not investigated (Durability – *interaction* level).
- Experimental sample sizes were restricted by the available resources.
- The material inventory data for the LCA were taken from available databases; however, the actual materials produced and applied in TRC could have differing inventory data which should ideally be obtained or verified by producers.
- The comparative scenario in the LCA was not experimental verified.
- The material's use and end-of-life stage, e.g. maintenance, demolition and waste management, were not included in the LCA. Scenarios for the maintenance and demolition phases deserve considerable attention, deeper analysis and knowledge about the long-term performance of the material.

1.5 Outline of thesis

The thesis contains a synopsis of four papers, denoted as **Paper I-IV**, as well as an introductory section providing the background and methodology concerning the topics treated in the papers. Additional experimental findings and discussion are also included in the thesis to give emphasis to certain aspects which are related but were not covered in the scope of the papers. The following summarizes the outline and contents of the thesis:

Chapter 1 – Introduction
Background information, research objectives, methodology and limitations are provided as the framework of this thesis.

Chapter 2 – Material Level: Concrete & Textile Reinforcement
An introduction to relevant properties pertaining to the *material level* is provided. The applied experimental methods and assumptions are also elaborated. This chapter primarily refers to **Objective 1** and makes reference to **Papers I, III** and **IV**.

Chapter 3 – Durability
An outlook on the durability of textile reinforcement is covered. Also, the investigation of the chemical resistance of textile reinforcement on the *material level* is discussed. This chapter relates to **Objective 3** and **Paper I**.

Chapter 4 – Interaction Level: Pull-out Behaviour
The bond behaviour of TRC and typical pull-out test methods are addressed. The applied experimental and numerical methods to determine the bond behaviour (*interaction level*) are explained. This chapter is associated to **Objective 1** and **Paper II**.

Chapter 5 – Global Level: Flexural Behaviour
The experimental and numerical analysis of the flexural behaviour of TRC on the *global level* is presented. This chapter refers to **Objectives 1** and **2** and **Paper III**.

Chapter 6 – Global Level: Tensile Behaviour
Experimental findings and methods related to the quantification of the tensile behaviour of TRC are discussed in addition to the enclosed papers. This chapter touches upon **Objective 1**.

Chapter 7 – Sustainable Potential
A summary of the conducted LCA study comparing TRC to conventional reinforced concrete is included. An outlook on economic and social aspects revolving around TRC is discussed. This chapter is related to **Objective 4** and **Paper IV**.

Chapter 8 – Conclusions and Future Outlook
The main conclusions of this thesis are discussed in this section along with the author's future outlook on the work.

References
Literature included in this thesis is listed alphabetically.

Appendices
Additional experimental methods and findings are provided here in **Appendices A** and **B**. **Papers I-IV,** acting as the foundation of this thesis, are also enclosed in respective appendices.

2 Material Level: Concrete & Textile Reinforcement

At first, the meaning of *Textile Reinforced Concrete* may not necessarily be obvious as it has been designated by various acronyms and terminology overtime:

- *Textile Reinforced Concrete* (TRC) (Brameshuber, 2006, Hegger et al., 2011, Mechtcherine, 2012),
- *Textile reinforced cement composites* (Mobasher, 2012),
- *(Textile) fabric-cement composites* (Cohen et al., 2012),
- *Textile reinforced engineered cementitious composites* (TR-ECC) (Dai et al., 2009),
- *Textile Reinforced Mortar* (TRM) (Triantafillou et al., 2006),
- *Mineral-Based Composites* (MBC) (Täljsten et al., 2006, Orosz, 2013),
- *Fibre reinforced cementitious mortar* (FRCM) (D'Ambrisi et al., 2013),
- Categorized as a *Cement-based composites* (Mechtcherine, 2013).

In this thesis, the most common terminology being *Textile Reinforced Concrete* (TRC) is applied. It refers to a composite material encompassing discrete textile reinforcement in the form of a grid or open mesh structure made of non-corrosive technical fibres embedded in a fine-grained cementitious matrix (see Figure 2.1). A main aspect differentiating TRC from other types of cement-based composites e.g. FRC is that fibres are bundled and arranged in a discrete open structure which can be positioned according to the imposed tensile stresses similar to conventional RC thus increasing the load capacity and effectiveness of the fibres in comparison to random short fibres in concrete. Accordingly, TRC is often claimed to combine the benefits of both RC and FRC as schematically illustrated in Figure 2.2 (Hegger et al., 2006).

It is important to provide an account of the individual constituents of TRC, namely *concrete matrix* and *textile reinforcement*, to be able to further comprehend TRC as a composite material. The quantification of the mechanical properties of these singular materials constitutes the *material* level of *structural performance* in this work, previously described in Section 1.2. An overview of the applied materials, along with the selected experimental methods and assumptions are discussed in Sections 2.1 and 2.2. Definitions and acronyms provided in this section are consistent with Brameshuber (2006) and ACI 440.1 R-06 (2006), unless stated otherwise.

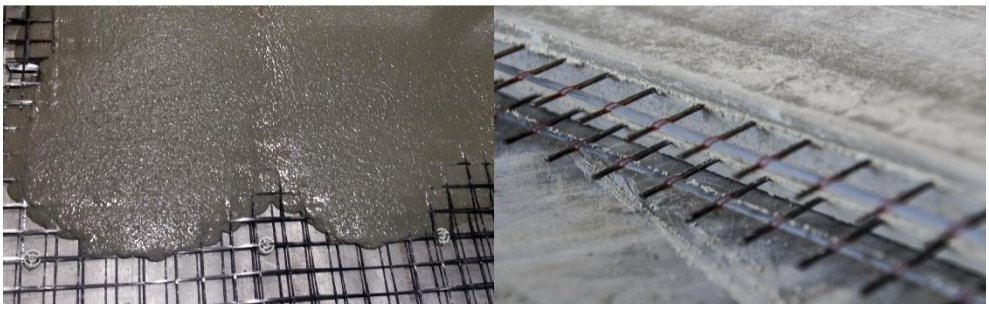

Figure 2.1 Overview of Textile Reinforced Concrete: casting process (left) and hardened TRC component (right).

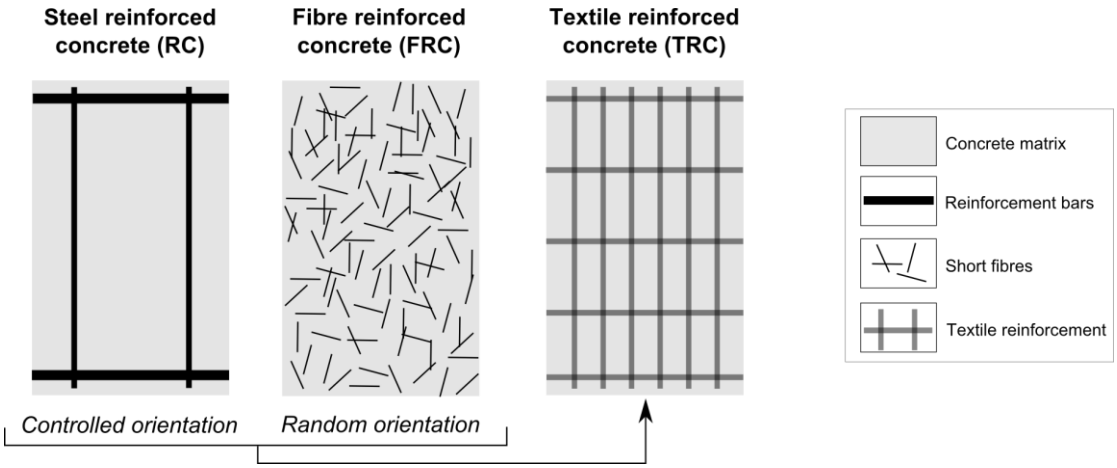

Figure 2.2 Combined effects of RC and FRC forming TRC [Adopted from (Hegger et al., 2006)]

2.1 Concrete matrix

The concrete matrix applied in TRC differs from that typically used in conventional steel reinforced concrete. Fine-grained concrete also defined as *mortar* is typically prescribed for TRC, where the maximum aggregate size is typically < 2 mm. Self-compacting and highly flowable concrete is primarily needed to adequately penetrate the openings of the textile reinforcement structure to allow for adequate bond and load transfer from the concrete to the reinforcement. This minimal aggregate size could however increase shrinkage and the need for larger quantities of cement paste; as such, a slight increase in maximum aggregate size to 4-6 mm could be considered while bearing in mind the desired design thickness of the TRC structure.

Moreover, the matrix should be designed to be chemically compatible with the selected reinforcement, i.e. in terms of alkalinity, while providing the required strength properties, mechanical behaviour and suitable characteristics for the specimen geometry and production method (Brameshuber, 2006). For instance, the concrete matrix could also be designed such that the alkalinity and hydration kinetics be altered (Butler et al., 2009) or by modifying the morphology at the interface of the textile reinforcement by means of polymer coatings along with nanoclay (Scheffler et al., 2009d). Additions of silica fume or high alumina cement, for example, can be incorporated in the mix to lower the alkalinity (Bentur et al., 2006).

For the past several decades, there have been concerns about the sustainability and reduction of CO_2 gas emissions as a consequence of cement production. According to statistics from 2013, the production causes the generation of approximately 700 kg CO_2 per ton of cement (Svensk Betong, 2015), which is why the substitution of cement with pozzolans like fly ash has been explored. For example, Mueller et al. (2015) investigated the use of reactive powder concrete (RPC) with textile reinforcement, whereby a large portion of the clinker was replaced by class F fly ash without causing a loss of performance. Another environmentally friendly concrete applied in TRC included the use of so-called *green concrete* which is made of a blast furnace slag binder from a by-product in the production of iron and a liquid sodium silicate solution as an activator (Bentland, 2015).

2.1.1 Concrete composition

Concrete, defined as a composite material, comprises aggregates or particles which are embedded into a binding medium. The binding medium most often consists of hydraulic cement, i.e. Portland cement, mixed with water (Mehta et al., 2006). In so-called modern concrete mixtures which were included in this work, admixtures were incorporated to modify concrete properties in a variety of ways. The concrete mixtures used throughout the work in this thesis differed due to the fact that experimental tests were conducted within various project frameworks. The source of the constituents also varied, such that a direct comparison of all experimental results is not applicable. However, a general description of the concrete mixtures used is given in the following.

In general, the applied mixes were self-compacting with a w/c of approximately 0.4 and a maximum aggregate size, d_{max}, of 4 mm. The *chemical* admixture applied was a polymer-based *superplasticizer* which reduces the surface tension of water during mixing, thus allowing the concrete consistency to increase without additional water. Using such high range water-reducing admixtures gives way to the reduction of the water-cement ratio, which in turn increases the strength of the concrete. *Mineral* admixtures in the form of natural pozzolanic materials, e.g. fly ash and silica fume, were also included as concrete components in this work. These admixtures are primarily applied to improve the workability of fresh concrete, enhance the resistance of concrete to e.g. thermal cracking, reduce costs when replacing large amounts of cement (Mehta et al., 2006), and potentially reduce the associated environmental impact. Furthermore, filler materials, particularly derived from quartz, were incorporated in the developed mixtures to improve the particle size distribution of the mix. An overview of the constituents used in the fine-grained concrete mixtures developed is illustrated in Figure 2.3 and exemplified in Table 2.1. The fresh concrete properties, e.g. slump, particle density, yield stress and plastic viscosity, were investigated to be able to make appropriate adjustments to reach a suitable concrete mix for certain cases. These methods are, however, not further described here as they are beyond the scope of this thesis.

Figure 2.3 Common constituents used in the fine-grained concrete mixtures.

*Table 2.1 Exemplified fine-grained concrete mix for TRC (**Paper III**).*

Constituent category	Material	Quantity (kg/m^3)	Density (kg/m^3)	Abs/moist	m^3/m^3
Cement	Low-alkali cement CEM I 52.5 R	406	3200		0.127
Mineral admixture	Fly ash	121	2300		0.053
Mineral admixture (silica fume)	Microsilica	22	2200		0.010
Fine aggregate	0/4 sand	1400	2640	0.2	0.530
Chemical admixture (Superplastizer)	Glenium SKY 532-SU	7.6 (1.4-wt%B)	1100	68.0	0.007
Chemical admixture (Air entrainment)	Amex SB 22	3	1010	98.2	0.003
Water	Water	170.56	1000		0.171
Entrapped	Air				0.100
Total		2130.16			1.000

2.1.2 Mechanical properties

Mechanical properties related to the fine-grained concrete were either quantified using short-term standardized experimental methods or calculated, using e.g. fib Model Code 2010 (2013) [fib MC 2010] or EN 1992-1-1 (2008) [EC2], depending on the extensity of the experimental program in each project. Ideally, it is most exact to characterize the mechanical properties of concrete experimentally and thereafter compare these to the outcome of the available empirical expressions, as is exemplified later. These expressions are based on certain underlying assumptions, e.g. cement type and aggregate size, such that they should be verified using experimental results. The relations presented in fib MC 2010 are said to be adequate as a first approximation for self-compacting concrete and to a certain degree apply to green concrete, i.e. replacement of a ration of cement by pozzolans.

Moreover, when quantifying the properties at the *material* level, it was important to understand which parameters are the most critical to further interpret the behaviour at the *interaction* (Section 4) and *global* levels (Sections 5 and 6), as well as those necessary to conduct non-linear finite element analysis (FEA) (Section 5.3). For plain concrete, the investigated mechanical properties, categorized according to *compression* and *tension*, are summarized in Table 2.2. The *compression* properties include compressive strength, ultimate strain, modulus of elasticity and Poisson's ratio, while *tensile* properties comprise tensile strength and softening behaviour, i.e. crack-opening curve. It is important to clarify that the tests presented in Table 2.2 were conducted under varying conditions, wherein the projects, test equipment, methods and concrete mix differed. The experimental work included in the papers associated to this thesis was conducted at the Danish Technological Institute (DTI). Experiments in addition to these were conducted at SP Technical Research Institute of Sweden (SP) and The Swedish Cement and Concrete Research Institute (CBI). The details pertaining to these additional experiments are reported in **Appendix A**. The purpose of discussing these additional tests is to demonstrate that the mechanical

properties of concrete can be obtained using an array of approaches which all provide varying levels of output and accuracy.

Table 2.2 Summary of mechanical properties quantified for concrete.

Category	Method	Outcome/Result	Reference
Compression	1.Cylinder test – method 1 (e.g. Ø 150/300 mm & Ø 100/200 mm) *Test method:* EN 12390-3 (2009) *Recommendations & calculations:* EN 1992-1-1 (2008) fib Model Code 2010 (2013)	Compressive strength, f_c	**Paper III**
	2.Cylinder test – method 2 (e.g. Ø 54/110 mm) *Test methods:* EN 12390-3 (2009) EN 12390-13 (2013)	Compressive strength, f_c Ultimate Strain, ε_{cu} Axial strain, ε_a Radial strain, ε_r Volumetric strain, ε_{vol} Poisson's ratio, ν Elastic properties: Modulus of elasticity, E_c Poisson's ratio, ν_c	Williams Portal et al. (2015) **Appendix A**
Tension	1. Indirect splitting test (e.g. Ø 150/300 mm) *Test method:* EN 12390-6 (2009)	Tensile splitting strength, $f_{ct,sp}$	**Paper III**
	2. Direct tensile test (e.g. Ø 54/110 mm) *Test method:* SS 13 72 31 (2005)	Tensile strength, f_t	**Appendix A**
	3. Uniaxial tension test (e.g. Ø 100/100 mm) *Recommendations & calculations:* RILEM TC 187-SOC (2007) RILEM TC 162-TDF (2001)	Tensile strength, f_t Fracture energy, G_F Softening curve	Williams Portal et al. (2015) **Appendix A**

Compressive properties

The compressive strength of a concrete mix should be quantified experimentally as a minimum, particularly at an age of 28 days, as most empirical equations estimate other mechanical properties from the characteristic or mean compressive strength at 28 days. It could also be important to examine the early stages of compressive strength development when concerned with production and installation. In this work, two methods were applied to characterize the compressive strength, i.e. basic and more elaborate cylinder compressive tests, denoted as *Methods 1* and *2*, respectively. Other related properties, being the modulus of elasticity, Poisson's ratio and ultimate strain were also measured using *Method 2* (see **Appendix A**). When concerned with the design of thin structures, the need to evaluate the size and slenderness effects as a function of the test specimen geometry could arise (Brockmann, 2006). These effects were however not further experimentally investigated in this scope of work.

Method 1: Cylinder test (**Paper III**): The compressive strength of hardened concrete, f_c, is typically determined experimentally by means of cylindrical test specimens as per EN 12390-3 (2009) with varying acceptable nominal sizes, refer to e.g. EN 12390-1 (2012). This test method, denoted as *Method 1*, is rather straightforward to conduct yet it generates but a single value corresponding to the applied compressive force. The maximum applied compressive force at failure, F, is divided by the cross-sectional area of the specimen, A_c, to yield the compressive strength. In this work, compressive tests were conducted on cylindrical specimens (Ø150/300 mm and Ø100/200 mm) at DTI. Due to the limited output of this method, other mechanical properties were estimated using available empirical expressions.

Method 2: Cylinder test (**Appendix A**): The compressive properties of hardened concrete in addition to the compressive strength can be characterized using more comprehensive test methods. Using *Method 2*, the compressive strength, axial and radial strains, Modulus of elasticity as well as Poisson's ratio, etc. can be determined due to the inclusion of a more detailed experimental setup. It is beneficial to generate such detailed material properties primarily for the sake of yielding more accurate analyses results and to be able to proceed with design. The preparation time and need for more complex measurement equipment are disadvantages of this method. In this work, these tests were carried out at SP in accordance with EN 12390-3 (2009) and EN 12390-13 (2013), on small cylinders (Ø54/110 mm) after 28 days of curing. The use of small cylinders was justified due to the small aggregate size (d_{max} < 4 mm) and experimental setup constraints. Further details pertaining to the experimental setup and procedure are described in Williams Portal et al. (2015a) and **Appendix A**.

Tensile properties – Tensile strength & softening behaviour

The tensile properties of plain concrete, i.e. tensile strength and fracture energy, can be estimated using the compressive strength of the concrete at 28 days. As previously mentioned, however, it is more accurate to experimentally quantify the mechanical properties of concrete, particularly if the mixture encompasses unconventional constituents. As such, determining the fracture properties of plain concrete in tension can be achieved using various experimental methods, e.g. uniaxial tension tests or indirect methods. The tensile properties of fine-grained concrete for TRC have been measured using different methods. For instance, notched beams tested in three point bending in combination with FEA (Brockmann, 2007) as well as uniaxial tensile tests on cylinders and thin dog-bone specimens have been investigated (Brockmann, 2006). When concerned with TRC as a strengthening material, the quantification of tensile properties of the composite could be of greater interest. Orosz et al. (2010) have studied these aspects using wedge-splitting tests and uniaxial tensile tests on dog-bone specimens.

In this work, three different methods were applied which produce varying levels of experimental output. Firstly, the tensile strength was obtained by means of indirect splitting tests (**Paper III**) and direct tensile tests (**Appendix A**), indicated as *Methods 1* and *2*. *Method 2* is a simplified method only allowing for the quantification of the tensile strength due to the nature of the test setup. The uniaxial tensile test (UTT) (*Method 3)*, a direct and reliable method (RILEM TC 187-SOC, 2007), was performed to quantify both the tensile strength and softening behaviour, i.e. stress-crack opening curve (**Appendix A**). Furthermore, there could also be a need to evaluate if there is an underlying effect of the specimen or notch size on the results; however, these effects have not been further studied in this work.

Method 1: Indirect splitting tests (**Paper III**): The indirect method of tensile splitting is often applied as an alternative to uniaxial tension tests. This method consists of loading a concrete cylinder placed on its side in a similar testing machine to that used for compression testing. The tensile cylinder splitting strength or tensile strength, $f_{ct,sp}$, can be calculated based on the maximum yielded load and specimen geometry using the denoted standard. A limitation of this method is such that the state of stress of the cylinder is biaxial (σ_x and σ_y) which results in the tensile strength to be higher than the uniaxial tensile strength, i.e. direct tensile strength, but lower than the flexural strength, i.e. modulus of rupture. This method however provides consistent results (minimal scatter), and is practical since it requires the same equipment and specimen

as the compressive strength test (Domone et al., 2010). The axial tensile strength, f_{ctm}, is thought to have a linear relationship with $f_{ct,sp}$, which is independent of the concrete grade (fib Bulletin No. 42, 2008). A correlation coefficient describing this relationship has been debated overtime and has been specified as 1.0 in this work according to fib MC 2010. Moreover, *Method 1* was applied in this work on cylinders (Ø150/300 mm) at DTI as per EN 12390-6 (2009). Concerning the input data applied in FEA, the yielded tensile strength value was included in conjunction with a calculated fracture energy value and an existing concrete softening relationship available in commercial software, as further described in Section 5.3.

Method 2: Direct tensile test (**Appendix A**): Direct tensile tests included in this work generate the axial tensile strength of the plain concrete. The outcome of this test is the applied tensile load and corresponding machine displacement. The tensile strength, f_t, is determined by dividing the failure load by the cross-sectional area of the specimen. The softening behaviour could not be characterized due to the nature of the experimental setup (hinged end supports). Using the tensile strength obtained from this method to calculate the fracture energy could likely yield more reasonable results in comparison to applying the converted splitting tensile strength from *Method 1*. Furthermore, *Method 2* was performed on cylindrical specimens (Ø54/100 mm) according to SS 13 72 31 (2005) at CBI. The same concrete was also tested using *Method 3*, such that a comparison between these methods could be effectuated. *Method 2* was observed to yield a lower tensile strength by 37 %, which could be due to the difference in specimen diameter or influence of the notch size. The result of this method can be applied in FEA similarly to that specified for *Method 1*.

Method 3: Uniaxial tension test (UTT) (**Appendix A**): UTTs are a direct and reliable test method to determine the tensile properties of plain concrete. The stress-deformation curve is obtained using this detailed method, which can be used to derive the softening behaviour of the concrete. As well, the fracture energy, G_F, can be calculated from the area under the stress-crack opening relationship. Similar to *Method 2: cylinder test*, the characterization of these additional data is valuable for the outcome of analysis and design, however at the expensive of time and level of test difficulty. In this work, *Method 3* was performed on notched cylinders (Ø 100/100 mm) with fixed end conditions at SP based on RILEM TC 187-SOC (2007) and RILEM TC 162-TDF (2001). More details related to this experiment are provided in **Appendix A**.

Comparison with empirical equations

The experimental results were compared to the outcome of selected available empirical expressions for fracture energy and tensile strength (see Table 2.3). The average compressive strength (71.5 MPa) resulting from *Method 2: cylinder tests* (**Appendix A**) corresponding to the same concrete tested in the UTTs was applied in the calculations. Through this comparison, it becomes clear that a) equations for normal weight or lightweight aggregate concrete are not entirely suitable for fine-grained concrete and b) that the maximum aggregate size, d_{max}, is an important parameter which should be reflected in the equations to yield more comparable results to that of the experiments for fine-grained concrete.

Table 2.3 Experimental results versus estimated values.

Category	Method	Result (Std dev)	Difference (%)	Comment
Fracture energy, G_F (N/m)	Experimental value Method 3: uniaxial tension test	96 (9)	–	Reference value
	CEB-FIP MC 1990 Maximum aggregate size d_{max}=8 mm	99	3	Within standard deviation of sample
	fib MC 2010 Normal weight concrete	157	63	Overestimation
	fib MC 2010 Lightweight aggregate concrete	74	-23	Underestimation
Mean tensile strength, f_{ctm} (MPa)	Experimental value Method 3: uniaxial tension test	3.2 (0.1)	–	Reference value
	CEB-FIP MC 1990 Various concrete grades	4.8	41	Overestimation Equations are valid for normal weight concrete and neglects effect of d_{max}.
	fib MC 2010 Concrete grades > C50	4.4	52	Overestimation Equations are valid for normal weight concrete and neglects effect of d_{max}

Idealized models

Despite the fact that concrete is a complex heterogeneous material, it has been idealized as a homogeneous material on the macroscale in modelling related to TRC (Hartig, 2011), as well as in this work. Both the material and cracking behaviour of the concrete matrix need to be incorporated in modelling to yield a realistic composite behaviour. The cracking behaviour is characterized by the linear-elastic uniaxial tensile behaviour of the matrix, while the post-cracking resistance can be described by a tension softening curve or brittle failure (Hartig, 2011). Furthermore, the crushing behaviour of concrete is described by the compressive stress-strain relationship. There exists various types of tension softening and compression functions available in TNO DIANA (2014) which have been applied in this work due to limited experimental data. As well, a constitutive crack model (*Total Strain*) was implemented to describe both tensile and compressive behaviours with one stress-strain relationship. When having access to measured detailed material properties, these data can be incorporated directly as input in modelling without the need for idealized models. More information related to the applied material models are provided in Section 5 and **Paper III**.

2.2 Textile reinforcement

Textile reinforcement is a composite material consisting of a heterogeneous structure. To understand the complex behaviour of this material, it should be examined at several observational levels, e.g. macroscopic to microscopic (see Figure 2.4). *Fibres* are categorized according to their origin as being either naturally occurring, e.g. jute and flax, or man-made, e.g. nylon, carbon and glass (Fangueiro, 2011). The

production differs depending on the nature of the *fibre*, i.e. inorganic or organic, and selected details pertaining to the production are covered later on. *Fibres* can be used to produce individual *fibres* of continuous length, also known as *filaments*, which are characterized by a diameter ranging between 7-27 µm depending on the material type (Bentur et al., 2006, Brameshuber, 2006). A sizing material is typically applied to the *filaments* to provide surface protection and improve the interaction between them in an assembled group (Dejke, 2001). The assembling of continuous filaments can be achieved by either twisting or grouping filaments together parallely. Based on the method applied, the terminology differs, wherein *yarn* often describes the group of twisted filaments, while *tow* or *roving* denotes bundled filaments in parallel. The parallel *filament* bundles are often used for reinforcing applications as they present smaller structural elongation in comparison to other forms of assemblies (Brameshuber, 2006). For improved bond in concrete, the surface features and volume of a yarn can be modified by texturing or crimping using added crimps, coils or loops along its length (Fangueiro, 2011). Furthermore, the number of filaments incorporated in a bundle is based on the desirable end thickness (Mahadevan, 2009), strength properties and application. The *fineness of a yarn* is measured in *tex* (g/1000 m) and is a function of the number of *filaments*, average *filament* diameter and density. The number of *filaments* in a bundle is often denoted as, e.g. *24K* meaning 24 000 filaments. *Fibres* and *yarns/rovings* can be further grouped to create textile structures using numerous methods to produce nonwoven, woven, knitted or braided fabrics. Regardless of the grouping method, textile reinforcement are typically classified as being two-dimensional planar or conventional (2D), three-dimensional (3D), directionally oriented (DOS) or hybrid structures. These structures are further described based on the direction of the *yarns/rovings*: mono, bi-, tri- or multi-axial (Fangueiro, 2011). In the case of a bi-axial case, the *mesh*/*grid* comprises two groups of *yarns/rovings*, *warp* (0°) and *weft* (or fill) (90°), interconnected orthogonally (see Figure 2.5). In tri and multi-axial cases, there are intermediate *yarns/rovings* diagonally placed in reference to the warp and weft directions. A 3D *mesh* generally consists of two individual 2D layers of woven *yarns/rovings* which are connected by, e.g. a spacer warp knit (Fall, 2011), made of a different fibre material (see Figure 2.5). For a detailed discourse on the common manufacturing techniques and influential factors related to fibres, yarns and textile reinforcement structures refer to Fangueiro (2011).

A suitable fibre for use in textile reinforcement should fulfil some basic requirements (Brameshuber, 2006): high fibre/yarn tensile strength at break (i.e. tenacity), high ultimate elongation at break, a modulus of elasticity superior to that of the cementitious matrix, as well as being resistant to an alkaline environment. Without these basic properties, the textile reinforcement cannot adequately take tensile stresses and allow for sufficient crack development in a concrete structure. Long-term properties which are important to consider consist of, e.g. consistent bond between the reinforcement and matrix and small relaxation under permanent load. Furthermore, the initial production cost, material availability and the ease of production are critical factors that also come into consideration.

Benefits of incorporating a *mesh/grid* structure in concrete include a homogeneous microcracking state dissipating energy over the entire volume, a notable increase in ductility and a low-weight to strength ratio (Mobasher, 2012). The geometric characteristics of the *mesh/grid* in terms of, e.g. yarn/roving bundle size, cross-sectional area, spacing of open structure (i.e. density), warp/weft cross-points (i.e.

junctions) and stability of the woven structure, greatly impact the interaction between the reinforcement and concrete. For instance, the *mesh/grid* spacing will primarily influence the crack spacing and width, while the stability of the woven structure as well as the strength and stiffness of the cross-points can influence the bond strength. The type of woven structure and yarn crimp has also been observed to have a significant influence the bond behaviour and flexural performance (Peled et al., 2003).

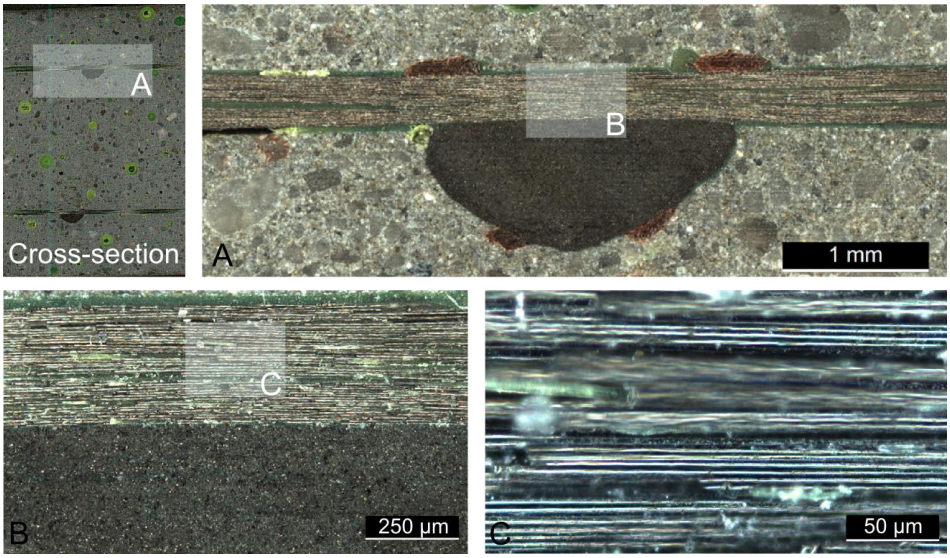

Figure 2.4 *The different levels of the heterogeneous structure of textile reinforcement embedded in a matrix: a) photo of cross-section of embedded 2D carbon grid in matrix; b) magnification of warp and weft roving node (1 mm); c) magnification of roving-matrix interface (250 µm); d) magnification of filaments in weft roving (50 µm).*

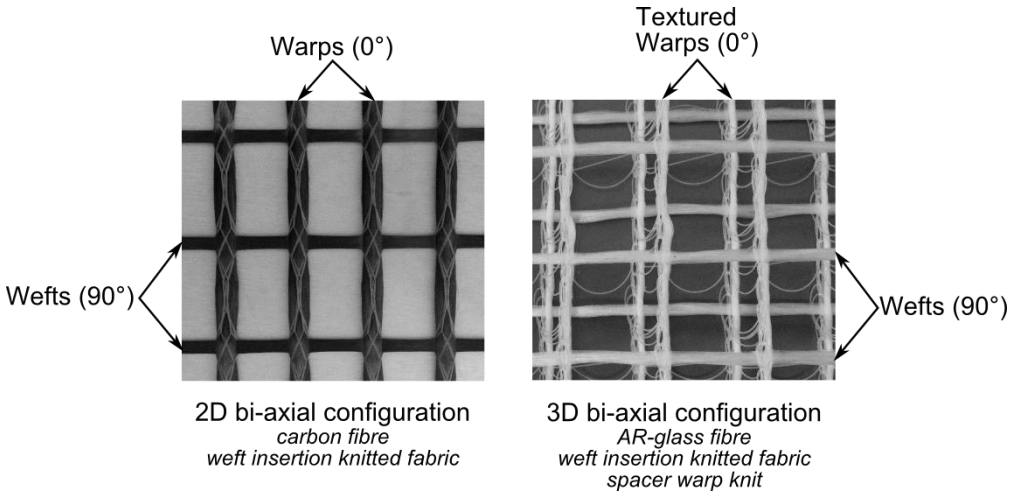

Figure 2.5 *Examples of applied textile reinforcement structures in TRC.*

2.2.1 Applied fibre materials

Fibres which have generally been used and explored in TRC include, but are not limited to: alkali-resistant glass (AR-glass), carbon, basalt, aramid, polypropylene, polyvinyl-alcohol (PVA) with polyvinyl chloride (PVC) coating as well as hybrid variants. The work presented in this thesis primarily focused on the application of

AR-glass, basalt and carbon, because these materials have been most readily available (see Figure 2.6). Besides, TRC building applications have primarily focused on the use of AR-glass and carbon fibre materials (Mechtcherine, 2012). Brief descriptions of the applied materials are provided in the following and for additional information related to commonly applied fibres in concrete, the reader can turn to, e.g. Brameshuber (2006), Bentur et al. (2006), Mobasher (2012) and Wulfhorst et al. (2006).

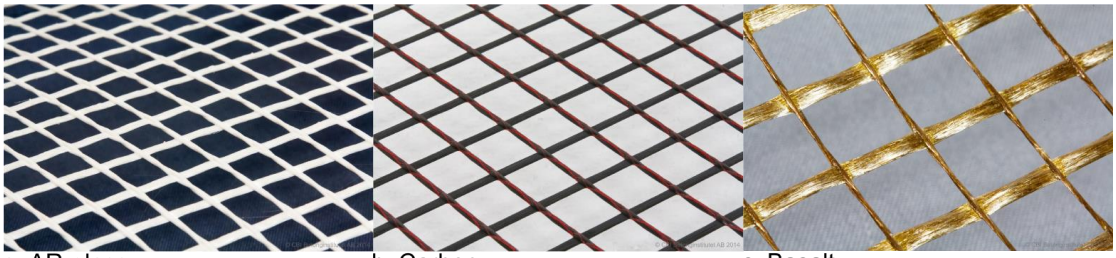

Figure 2.6 Examples of investigated textile reinforcements: a) AR-glass, b) carbon, c) basalt.

AR-glass

AR-glass is often coined as the most cost effective and readily available textile reinforcement solution in comparison to carbon (Büttner et al., 2010). Glass fibres are chemical fibres derived from inorganic non-metallic raw materials (Wulfhorst et al., 2006). The raw materials needed to produce AR-glass are primarily silica sand (SiO_2) and the addition of up to 15-16 wt-% zirconium oxide (ZrO_2) to provide a superior alkali resistance (Bentur et al., 2006, Brameshuber, 2006), which are proportioned through a batching process. The production of AR-glass yarns consist of the following processes (Brameshuber, 2006, Wulfhorst et al., 2006):

- Melting process of raw materials between 1250-1350 °C → molten glass
- Fiberization of molten glass, i.e. wet-spinning process (25-150 m/s) → filaments (Ø 9-27 µm)
- Sizing/coating (organic polymers) on filament → surface wetting and bonding of filaments (Parnas et al., 2007).
- Bundling of filaments → yarns (e.g. 400-6600 number of filaments)

Carbon

Carbon fibres are synthetic chemical fibres that can be produced by two methods: 1) based on polyacrylonitrile (PAN) and 2) based on meso phases pitch (petroleum). Production method 1 is discussed here as this one is most commonly used in TRC applications and is also reflected in the LCA (Section 7); nevertheless, each method aims for carbon fibres having at least 90 % carbon content (Wulfhorst et al., 2006). The production of carbon yarns involve the following processes (Brameshuber, 2006, Wulfhorst et al., 2006):

- Wet-spinning, i.e. polymerization, of organic polymer resin polyacrylonitrile → chemical fibres
- Thermal stabilization of fibres (200-300 °C), i.e. removal of non-carbon atoms through oxidation → unmeltable fibres
- Carbonization and graphitization of fibres (1000-3000 °C), i.e. aligning graphite layers parallel to fibres → carbon fibres from PAN, i.e. High tenacity

(HT)-fibres (1500-1700 °C) or High modulus of elasticity (HM)-fibres (2200-3000 °C)
- > Drawing of processed fibres → filament (Ø 7 to 15 µm)
- > Sizing/coating on filaments
- > Bundling of filaments → *yarns/rovings*

Basalt

Basalt fibres can be categorized as mineral non-organic or man-made fibres. The origin of the mineral derives from volcanic rock. Due to its natural formation process, its raw material content and morphology can differ greatly depending on its source. This variability in raw materials poses a challenge, as it can have a large influence on the chemical and mechanical properties and durability of the fibres (Förster et al., 2010). As a consequence of this uncertainty, man-made modified basalt fibres have even been explored in work by Förster et al. (2011). Accordingly, the production of basalt yarns is similar to that of glass due to their chemical composition, such that simple and conventional processes and equipment can be applied which makes it cost-effective (Sim et al., 2005, Wei et al., 2010). The diameter of basalt filaments can range between 9-22 µm (Soukhanov et al., 2014). The applied sizing and coating applied at the end of the production process particularly influence the durability and bond behaviour of basalt fibres in a concrete matrix (Hempel et al., 2015)

Qualitative assessment

A qualitative assessment of general mechanical and chemical properties including corrosion and temperature resistance, bond quality, in addition to demand and production cost for selected reinforcement materials is presented in Table 2.4 (from **Paper IV)**. Each criterion is assessed on a scale from *Low* to *High* (1-3) based on a relative comparison between conventional steel reinforcement, uncoated AR-glass, carbon and basalt textile reinforcements for use in concrete. All criteria were also weighted equally in this evaluation; however, depending on the application at hand, there could be a need to consider a different evaluation scheme. For example, temperature resistance may not be of a concern for certain applications, such that this criterion could be weighted according to the importance level.

The main highlights which can be drawn from the quantitative evaluation summarized in Table 2.4, as well as further remarks are mentioned in the following:

- > Carbon fibre is a superior solution in terms of chemical durability but drawbacks are relatively high initial cost and low availability for use in construction applications. The bond properties of carbon can be improved by means of polymer-based coatings.
- > Steel reinforcement is a relatively good solution but has a known risk of corrosion. It also has the disadvantage of having a high environmental impact, which is further discussed in Section 7.
- > AR-glass is the least favourable mainly due to it being instable under increasing temperature loads. It is however seen as the most cost-effective and readily available textile reinforcement alternative.
- > Despite the fact that basalt and AR-glass are similar chemically, basalt scored higher primarily due to the temperature resistance properties. Basalt appears to be a promising solution due to the availability of raw materials and affordable production methods; however, it is important to note that the applied sizing or coating is a critical factor influencing the durability properties.

*Table 2.4 Qualitative assessment of selected reinforcements (**Paper IV**).*

Reinforcement Material	Corrosion Resistance	Temperature Resistance	Bond Quality	Demand/Production Cost	Total Score* (Norm. score)
Conventional steel reinforcement	-**High** to high alkaline solutions (passive film) -**Low** to low alkaline, neutral or realistic acidic outdoor conditions	-**Average** -**High** thermal expansion and conductivity (Saertex 2013)	-**Low-High**, based on mechanical deformations	-**High/Average,** commonly used	8.5 (1.00)
AR-Glass	-**Average-High** to alkali attack -**High** to neutral or realistic acidic outdoor conditions	-**Low** -**Average** thermal expansion (Saertex 2013; Vetrotex 2011) -**Low** thermal conductivity (Saertex 2013; Vetrotex 2011)	-**Average**, depends on density of yarn -Improve with coatings	-**Average/Average**, particularly produced for use in alkaline environments	7.75 (0.91)
Carbon	-**High** to acid, alkaline and organic solvents (inert)	-**High** -**Low** thermal expansion, shortens when heated -**Average** thermal conductivity (Saertex 2013)	-**Low-Average** -Smaller filament diameter leads to weaker adhesion -Improve with coatings	-**Low/High**, compared to all other reinforcement materials	9.5 (1.12)
Basalt	-Comparable to unsized E-glass and AR-glass in high alkaline solutions (Scheffler, Förster, et al. 2009; Förster et al. 2010)** -**High** to neutral or realistic acidic (Wei, Cao, and Song 2010) and alkaline outdoor conditions (Van de Velde, Kiekens, and Van Langenhove 2003)	-**High** resistance -**Low** thermal expansion -Geometrically stable (Smarter Building Systems 2010) -**Low** thermal conductivity (Smarter Building Systems 2010)	-**Average** -Unsized filaments (Scheffler, Förster, et al. 2009) -Low friction coefficient, improve with coatings (Scheffler, Förster, et al. 2009)	-**Low/Average,** easily extractable natural resource (Förster et al. 2010; Smarter Building Systems 2010)	9.25 (1.09)

**Low = 1, Low to Average = 1.5, Low to High = 2, Average = 2, Average to High = 2.5, High = 3.*

***Uncertainties exist due to unknown chemical formulation of basalt and fibre sizing, which as result caused observations of high standard deviation values in tensile strength after ageing.*

2.2.2 Microstructure

TRC is differentiated from ordinary steel reinforced concrete mainly by its complex heterogeneous structure (Möller et al., 2005, Häußler-Combe et al., 2007). A textile reinforcement yarn consists of numerous filaments which inhibit the even penetration of the fine-grained concrete matrix between the filaments. The inner filaments, as a result, have less contact with the fine-grained concrete matrix depending on the size of the *fill-in zone*. The *fill-in zone* is the depth at which adhesive load transfer can take place between the filaments and the matrix. The inner zone, i.e. core, is defined as the filaments having less contact with the matrix but assuming that frictional load transfer between the filaments remains possible (Hartig et al., 2008). The yarn structure embedded in a matrix along with these abovementioned associated zones is conceptualized in Figure 2.7 (left).

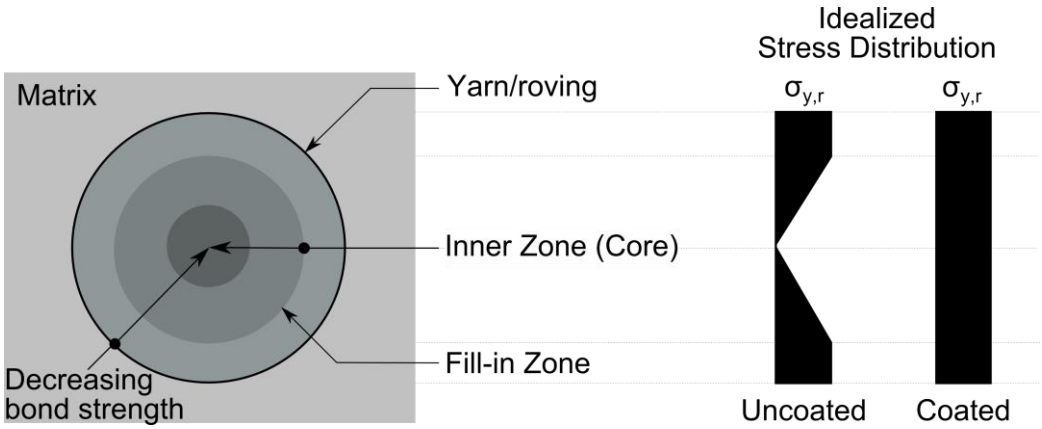

Figure 2.7 Conceptualized yarn/roving structure (left) [Adopted from (Hartig et al., 2008)] and idealized stress distribution across uncoated and coated yarn/roving (right).

The heterogeneous bond between the textile reinforcement mesh/grid and matrix can differ greatly depending on, e.g. fibre type, binding type, surface smoothness, and rheology of the concrete matrix. The impregnation of the textile mesh/grid using, e.g. polymer-based coatings, is often used to eliminate the highly heterogeneous structure of the yarn/roving. The penetration of the coating into the yarn/roving activates more internal filaments, which in turn improves the load transfer between the filaments (Morales Cruz et al., 2015). Ideally, the aim is to activate the entire yarn/roving to achieve a constant stress distribution across the yarn/roving cross-section as illustrated in Figure 2.7 (right). This configuration can be seen as analogous to a uniform bond surface between the cement matrix and reinforcement. Enhanced bond strength and composite tensile strength due to added surface coatings has been reported in various studies, e.g. in Büttner et al. (2008) and Scheffler et al. (2009c). The modification of the surface roughness using sand fillers and coatings has also been found to have a positive impact on the bond (Morales Cruz et al., 2015). Coatings applied to entire sections of textile reinforcement mesh/grid can furthermore influence the stiffness and draping characteristics. Other benefits include added surface protection during handling and within an alkaline environment. A more detailed account of how the tensile strength of a TRC member could be potentially altered by utilizing different textiles, binding types, and surface modifications is further discussed in **Paper IV**.

2.2.3 Mechanical properties

Textile reinforcement is primarily incorporated into concrete to carry the tensile stresses developed under loading of a TRC member. The characterization of the tensile behaviour of textile reinforcement under a uniaxial tensile stress state was focused on in this work. In general, textile reinforcement under uniaxial tensile loading has linear-elastic and brittle behaviour such that it undergoes a so-called sudden failure upon reaching ultimate stress.

Due to the fact that textile reinforcement consists of a heterogeneous structure of interwoven yarns/rovings made up of single filaments, it is important to specify the corresponding component level of the examined tensile properties. For instance, an unprocessed filament has been shown to have greater tensile strength in comparison to a yarn due to the fact that processing causes so-to-say a loss of material strength through material defects and uneven stress distribution between the individual filaments (Brameshuber, 2006). Further loss of strength occurs for yarns/rovings processed in a mesh/grid structure as well as for the finalized mesh/grid embedded into a matrix (Morales Cruz et al., 2015). In the composite form, the bond between the individual filaments and cementitious matrix becomes the primary factor influencing the resulting *effective* tensile strength of the textile reinforcement (**Paper IV**). In various cases, the tensile properties have been determined or idealized at the yarn/roving level (see *Idealized models*). This level is however inadequate to describe the composite behaviour of a TRC member in, e.g. macroscale modelling or component design. Consequently, the tensile behaviour of the textile reinforcement mesh/grid was characterized in this work.

Measurements

General material and mechanical properties are commonly provided by the textile reinforcement producers/suppliers, which include geometric parameters of the mesh, weight, applied coating, tensile strength, modulus of elasticity and elongation (ultimate break), but are not limited to these parameters. However, the experimental methods used to obtain the mechanical properties related to the textile reinforcement are not standardized; they vary based on the source and are sometimes undisclosed. Whether the provided data represent characteristic or average values is also not provided. In effect, the quality of the available data and comparability of different materials remain uncertain.

As summarized in Table 2.5, examples of available standards pertaining to the investigation of the tensile behaviour of single-filaments, yarns or textile fabrics mainly derive from the textile industry. It should be pointed out that there are, however, no all-encompassing standard methods to characterize the tensile behaviour of a mesh/grid structure made of technical fibres. In this work, the extensive standards established for fibre reinforced polymer (FRP) reinforcement for concrete, namely ISO 10406-1 (2008) and ISO 10406-2 (2008), were applied as they were to some extent more applicable to textile reinforcement mesh/grids. To make use of the provisioned tensile test method in ISO 10406-1 (2008), adaptations of the method were necessary, e.g. end anchorage and strain measurement technique, which are further described in **Paper I**.

Based on the standard test method for tensile testing provisioned in ISO 10406-1 (2008), individual rovings were cut from a grid structure with a remaining 2 mm projection of the cross-points (cross-threads). The tests were carried out using a

universal testing machine (Sintech 20D) depicted in Figure 2.8. The deformation was measured by a Messphysik video extensometer ME46 with backlight technique in the background and digital camera in the foreground. The main benefit of using this deformation measurement technique is such that the ultimate strain could be captured. Further details pertaining to this experiment are documented in **Paper I** and Williams Portal et al. (2014a).

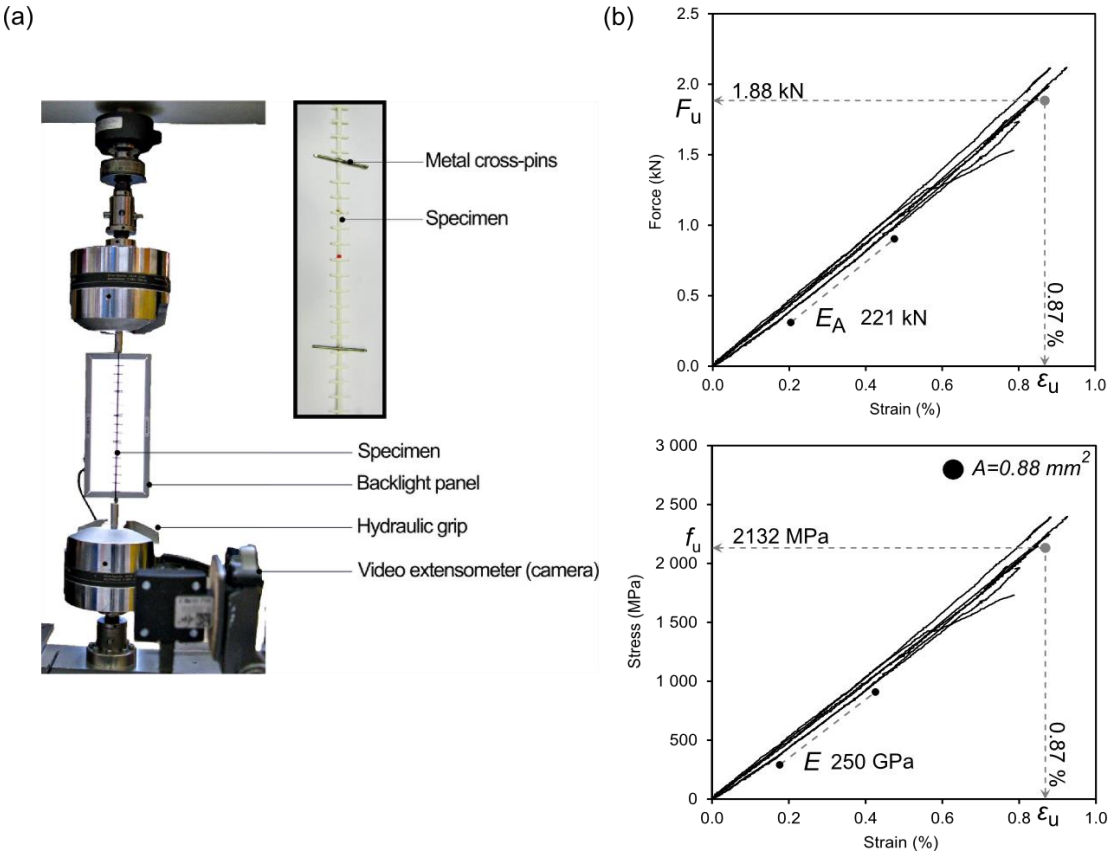

*Figure 2.8 Overview of the tensile test setup and reference metal cross-pins (from **Paper I**) (left) and exemplified results for carbon textile reinforcement (right).*

The maximum tensile force, F_u, tensile rigidity, E_A, and ultimate strain, ε_u, of the textile reinforcement were the general outputs of this test method, yet these can also be converted to tensile strength, f_u, and Young's modulus, E, of the material as indicated in ISO 10406-1 (2008). The tensile rigidity was calculated from the load-strain relation as the secant modulus between the load level at 20 % and 50 % of the tensile capacity. In this particular case, the tensile properties were determined for one direction of the grid. In the case of differing yarns/rovings along the warp and weft directions, the tests could be conducted in both directions to characterize more detailed data.

Table 2.5 Summary of relevant standard methods to measure tensile properties of fibre-based materials.

Evaluation level	Standard method	General focus	Relevant end results	Limitations
Reinforcement	ISO 10406-1 (2008) ISO 10406-2 (2008)	Test methods for fibre-reinforced polymer (FRP) reinforcement of concrete and upgrading of concrete members	Tensile properties (tensile strength, tensile rigidity/Young's modulus, ultimate strain)	FRP bars, grids (rigid array of interconnected FRP bars) and sheets made of continuous fibres of carbon, aramid and glass
Textile fabric	ISO 13934-1 (2013) ISO 13934-2 (2014)	Tensile properties of fabrics (textiles)	Maximum force and elongation at maximum force (strip and grab methods)	Woven textile fabrics with stretch characteristics (through elastomeric fibre, mechanical or chemical treatment)
Textile fabric	ISO 4606 (1995)	Tensile properties of woven fabric (textile glass)	Tensile breaking force and elongation at break (strip method)	Unimpregnated and impregnated textile glass fabrics (sizing or stiffening)
Yarn	ISO 3341 (2000)	Tensile properties of yarns from packages (textile glass)	Tensile breaking force and elongation at break	Glass yarns from packages (single, folded, cabled, rovings, etc.) Diameter < 2 mm
Yarn	ISO 2062 (2009)	Tensile properties of yarns from packages (or extracted from fabrics)	Tensile breaking force and elongation at break (Single-strand; Constant rate of extension tester)	All yarns except glass, elastomeric, aramid, high molecular polyethylene (HMPE), carbon yarns etc.
Yarn	ISO 6939 (1988)	Tensile properties of yarns from packages	Tensile breaking force and elongation at break (Skein method)	Not a reference test method (comparative)
Fibres (single filament)	ISO 5079 (1995)	Tensile properties of individual fibres	Tensile breaking force and elongation at break	All fibres (also crimped fibres)
Fibres (single filament)	ISO 11566 (1996)	Tensile properties of individual fibres (carbon)	Tensile strength and tensile modulus of elasticity	Carbon fibres from different sources (multifilament yarns, strands, woven fabrics, etc.)
Fibres (single filament)	ASTM D3379-75 (1989)	Test method for tensile strength and Young's modulus for high modulus single-filament materials	Tensile strength and Young's modulus of single filaments	High-modulus single-filament materials (> 21 x 10^9 Pa) Withdrawn

Idealized models

To model the composite behaviour of TRC, the material and failure behaviour of the textile reinforcement is required. The bond behaviour between the filaments, as well as between the concrete matrix and reinforcement is a critical input which is further covered in Section 4. Due to the highly heterogeneous structure of textile reinforcement, the accurate experimental quantification of the material and failure behaviour is a challenging task. Accordingly, idealized models have been applied in the modelling of TRC to attempt to describe the mechanical behaviour of textile reinforcement at various levels, i.e. micro, meso and macroscale. In this thesis, only an overview of selected models is included to recognize the related research efforts which have been made overtime. A detailed discourse of the various idealized models which have been applied to describe the behaviour of the textile reinforcement can be found in, e.g. Hartig (2011) and Peiffer (2008).

The choice of an appropriate idealized model can be made based on the level of modelling. At filament level (microscale), a linear-elastic stress-strain law has been typically proposed to describe the tensile behaviour (Banholzer, 2004). When it comes to the tensile behaviour of the textile *yarn/roving* (mesoscale/macroscale), however, various idealized stress-strain laws have been suggested and applied in numerical modelling:

- Linear-elastic material law similar to that describing a filament (see Figure 2.9a);
- Delayed activation of the filaments within a *yarn/roving* at load initiation due to initial crimping/undulation and post-strength resistance caused by successive filament rupture, applied by e.g. Richter (2005) (see Figure 2.9b);
- Linear-elastic material law and unloading curve considering gradual rupture of filaments, applied by e.g. Bruckermann (2007) (see Figure 2.9c);
- Linear-elastic material law and post-strength resistance from intact filaments, applied by e.g. Krüger (2004) (see Figure 2.9d).
- Two-branch curve with delayed activation and increase in stiffness, applied by e.g. Schladitz et al. (2012) on macroscale level modelling of TRC strengthened beams.

Another approach to describe the behaviour of textile reinforcement in TRC is the application of fibre bundle models and damage models, which were developed by e.g. Lepenies (2007). Fibre bundle models describe the load sharing and redistribution between the fibres, whereas this particular damage model describes the change in cross-sectional yarn/roving area due to the successive rupture of the filaments in the yarn/roving.

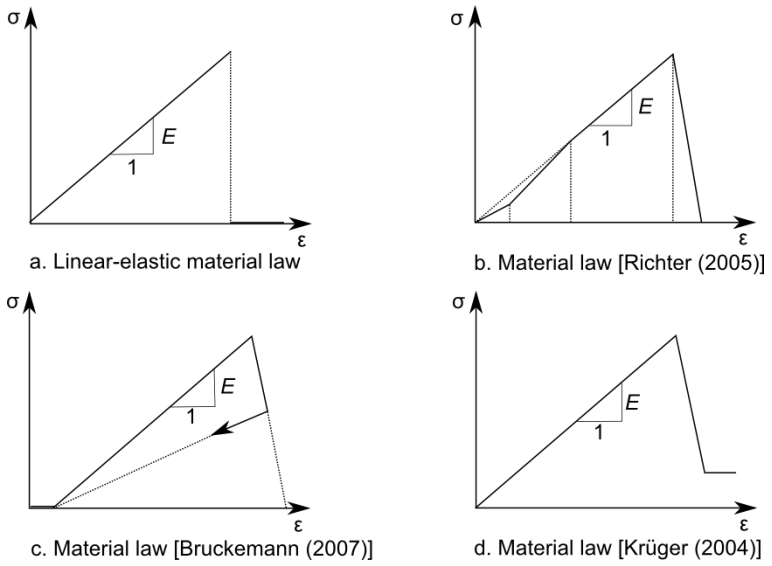

Figure 2.9 Constitutive laws for reinforcement yarns/rovings [Adopted from (Hartig, 2011)].

The geometrical representation of the yarns/rovings should also be considered in addition to the constitutive laws. As a first attempt to simplify the heterogeneous structure of a yarn/roving, a so-called smeared behaviour consisting of a homogeneous circular cross-section with one bond interface with the matrix can be assumed. This assumption was made in this work because there are underlying difficulties involved in defining internal bond interfaces and appropriate filament subdivisions, as well as to minimize the computation time of the analyses (Section 5). Numerous studies have focused on developing suitable subdivision schemes and associated models for yarns/rovings, e.g. Hegger et al. (2006) and Banholzer (2004). Such models are typically calibrated by comparing numerical and experimental results as well as by using parametric studies (Hartig, 2011). Further details pertaining to these models are not included in this thesis.

Research related to the modelling of textile reinforcement as a mesh/grid in a 2D space is vague, yet it is assumed that a smeared or bundled approach is typically implemented. It is to say that the idealized material behaviour and filament subdivision scheme that is applied for an individual yarn/roving also applies to all yarns/rovings present within a mesh/grid. For the case of a thin TRC specimen loaded in uniaxial tension or one-way bending, it could be appropriate to consider but the loaded longitudinal yarns/rovings in a model. Accordingly, the amalgamation of these individual loaded yarns/rovings into one compact yarn/roving can be effectuated as a smeared approach. This method was included in this work and is further elaborated in Section 5 and **Paper III**.

2.3 Summary

A general account of the two main constituents of TRC, *concrete matrix* and *textile reinforcement*, was given in this section. The experimental methods applied to quantify the mechanical properties pertaining to both the concrete matrix and textile reinforcement were also discussed (**Objective 1**). More specific findings and reflections are provided in the following:

- Simplified versus more complex experimental methods, e.g. tensile splitting tests versus uniaxial tensile tests, were presented in this work to quantify the compressive and tensile properties of fine-grained concrete.
    - Simplified methods yielded less output, such that empirical expressions were used to gain further material properties (**Paper III**).
    - Complex methods yielded more detailed output and understanding of the behaviour, whereby the empirical expressions could be verified by means of experimental results.
    - The extent of available resources is however most often the limiting factor governing the extensiveness of the applied experimental methods.
- Estimating mechanical properties for fine-grained concrete, e.g. fracture energy and tensile strength, using available empirical equations yielded overestimated values.
    - The equations for normal weight or lightweight concrete do not adequately predict the behaviour of fine-grained concrete.
    - A parameter such as the maximum aggregate size, d_{max}, should be reflected in the expressions in order to yield more appropriate estimations for fine-grained concrete.
- Concrete was idealized as a homogeneous material in modelling (**Paper III**).
    - Models describing the cracking and crushing behaviour of concrete were incorporated.
- A method to determine the tensile properties of a yarn/roving extracted from a textile reinforcement mesh/grid was successfully developed and applied (**Paper I**).
    - Mechanical properties of textile reinforcement fibres, yarns/rovings or mesh/grid are inconsistently characterized such that available data becomes uncertain.
    - Without consistency of the material and mechanical properties of textile reinforcement products, it remains difficult to proceed with design and application.
- The tensile behaviour of a yarn/roving extracted from a mesh/grid represents the most expected behaviour of the reinforcement in a TRC composite.
    - For 2D macroscale modelling of a TRC composite, the tensile behaviour of the extracted yarn/roving was applied in a smeared approach to reflect the loaded parts of the mesh/grid structure (**Paper III**).
    - These data can be used in combination with idealized models which describe the tensile behaviour of yarn/rovings.
- Textile reinforcement was idealized as having a compact circular cross-section in modelling (**Paper III**).
    - Complex yarn/roving subdivision schemes incorporate uncertainties, require validation and parametric studies, and they can become numerically expensive.
    - For more detailed levels of evaluation, e.g. multi, meso and microscales, the use of a more intricate yarn/roving cross-section can be justified.

3 Durability

A concrete structure should be designed, constructed and maintained to ensure durability over a required service life (CEB-FIP MC90, 1993). The durability of a structure is important so that it can fulfil a safe functionality, while reducing costs, energy, extraction and production of new materials, maintenance, rehabilitation, replacement and deconstruction. To incorporate durability into design, the long-term performance of the applied building materials should be known or should be projectable using experiments or models. In the case of TRC, however, the long-term performance of such a novel building material is rather limited. Research pertaining to the durability properties of similar fibre-based reinforced composites, namely FRC and FRP, has been referred to in this work. It is thought that these characteristics could to some degree provide some insight on the long-term performance of TRC.

Fibre-based reinforcements embedded in a concrete matrix are typically most affected by chemical attack due to the presence of an alkaline environment (Bentur et al., 1990). A universal method to assess the durability performance of fibre-based reinforcements in concrete is nonetheless non-formalized and applicable methods could vary depending on the nature of the fibre (Bentur et al., 1990). In this work, the effect of accelerated ageing on the tensile properties of textile reinforcement materials was investigated (**Objective 3, Paper I**). The conducted experiments were initially based on a standard method for FRP materials, yet a range of boundary conditions with respect to temperature and pH level were tested to investigate the loss of strength and physical changes.

3.1 Assessing durability

The durability performance is most accurately measured in real-time (Mechtcherine, 2012); though due to time constraints, accelerated aging tests or experimentally calibrated numerical models are typically applied to predict the long-term performance of materials. Durability is a broad term which consists of deteriorating processes such as chemical attack, fire resistance, freezing and thawing (ACI 544.5R-10, 2010). The durability performance pertaining to chemical attack on fibres is focused on in this context. A common method found in literature to accelerate the ageing of fibres in the form of FRP rods or textile reinforcement consists of immersing them in a simulated or an actual concrete pore solution, while simultaneously being exposed to high temperature (Micelli et al., 2004, Cuypers et al., 2007a). Others have exposed textile reinforcement cast in concrete to varying temperatures or moisture conditions (Butler et al., 2009, Scheffler et al., 2009d, Butler et al., 2010, Mumenya et al., 2010). A collection of other experimental methods applied to different types of fibres can be found in ACI 544.5R-10 (2010) and Bentur et al. (2006). Nonetheless, methods to assess the durability performance of common textile reinforcements used in TRC are not formalized.

When turning to existing recommendations for FRC and FRP, the level of description varies. For instance, in ACI 544.1R-96 (2002) related to FRC, it is stated that the durability performance is typically evaluated through changes in strength and toughness of the composite material exposed to either natural or accelerated ageing conditions. The accelerated tests could involve the immersion of a specimen in a hot water bath, yet no further guidelines are provided to carry out the assessment. In a

more recent document, ACI 544.5R-10 (2010), an overview of experimental studies applied to various types of fibres is provided. The compilation of an all-encompassing test method, e.g. related to degradation due to chemical attack, has not been attempted likely due to the differing degradation processes involved for each fibre type. In general, a systematic approach to develop an accelerated test to aid in predicting the service life of building components and materials was previously covered in ASTM E632-82 (1996), which has been withdrawn without being replaced.

Recommended experimental methods to assess durability seem to be primarily established for FRP. For instance, similar methods to assess the durability of FRP materials are presented in both ISO 10406-1 (2008) and Japan Society of Civil Engineers (1997). As per these guidelines, the durability performance related to the alkali-resistance of the reinforcement should be assessed through tensile testing of specimens aged by means of accelerated testing in a simulated alkaline environment at an elevated temperature. In this work, ISO 10406-1 (2008) was used as a guideline for accelerated testing on textile reinforcement.

3.2 Durability characteristics of fibres

An overview of pertinent durability characteristics and research related to fibre-based reinforcement for concrete is presented here. A focus on AR-glass, basalt and carbon fibres is taken as these materials have been studied in this thesis. Over time, a particular emphasis has been made on the durability aspects of glass fibres in concrete, such that a significant amount of research findings is available for this material compared to the other considered fibre types.

Common degradation processes related to fibre-based reinforcement in concrete are (Bentur et al., 2006): fibre degradation due to chemical attack, fibre-matrix interfacial physical interactions, fibre-matrix interfacial chemical interactions, and volume instability and cracking. These processes are important to highlight, as the characterization of the long-term performance of a TRC can be complex due to singular or combined degradation processes. For further details on these processes, refer to Bentur et al. (2006). Another critical factor influencing the durability and interface of fibre-based reinforcements in a concrete matrix is the applied surface sizing/coating. This topic can easily become elaborate particularly when overseeing solutions for various fibre types. Therefore, it is only briefly addressed in the following.

3.2.1 AR-glass fibres

AR-glass fibres undergo strength loss in cementitious matrices over a long-term perspective (Purnell, 1998). These fibres are in fact facing similar damage mechanisms which are present in glass-fibre reinforced concrete (Butler et al., 2009). Hydroxide ions (OH^-) present in an alkaline solution react with the silica groups (Si-O-Si) of the glass fibre network which build up hydrated surfaces and dissolved silica (Scheffler et al., 2009c). Furthermore, due to the production process, the AR-glass fibre surface is marked by small defects and/or weak zones which lead to strength loss. Consequently, these so-called weak zones make way for local displacements, pitting corrosion and stress concentrations when placed in an alkaline environment (Purnell, 1998, Orlowsky et al., 2005). It is important to note that the corrosion attack

of AR-glass fibres in terms of reactive products has been found to differ when exposed to a NaOH-solution compared, i.e. formation of brittle shell and spalling, to a cement solution, i.e. pitting (Scheffler et al., 2009a). As such, the extent of the reaction is said to be dependent on numerous factors such as the composition of the alkaline solution and of the glass fibre, as well as accelerated exposure time and temperature (Scheffler et al., 2009a). In addition, the densification of the matrix at the fibre interface due to the continued hydration process of the concrete has also been noted to cause potential degradation and change in bond properties (Zhu et al., 1997).

Attempts to improve the durability of AR-glass include the reduction of the pH-level in the cementitious matrix particularly near the fibres, as well as the inclusion of a hydrophobic protection layer, e.g. epoxy or styrene butadiene, around fibres or rovings to act as a diffusion barrier against the alkaline solution (Scheffler et al., 2009c, Büttner et al., 2011, Raupach et al., 2011). Further research on this topic included the incorporation of insoluble epoxy resins or chemically reactive dispersions, e.g. cement/silica fume/poly (vinyl acetate), on the AR-glass roving surface (Büttner et al., 2010). For instance, Büttner et al. (2009) examined the reduction of the long-term strength loss by means of adding coating to the reinforcement and polymers to the concrete to alter the water transport within the pore structure and decrease the alkali content around the textile reinforcement. The impact of varying the alkalinity, hydration kinetics and granulometry of binder on the durability of AR-glass fibres in concrete was studied in Butler et al. (2009) and Butler et al. (2010).

The time-dependent ageing effects of AR-glass yarns embedded in a matrix characterized using double-sided yarn pull-out tests were modelled in Butler et al. (2011). The microstructural changes at the fibre-matrix interface were correlated to the crack-bridging effect of a yarn on the mesoscale. The time-dependent strength loss of AR-glass fibres in concrete has been also investigated and predicted using developed corrosion models (Purnell, 1998, Orlowsky et al., 2005). For example, Orlowsky et al. (2005) verified the use of a mathematical approach including effects of initial pitting corrosion and diffusion controlled chemical attack in later stages of deterioration. These existing models were thereafter adapted to investigate weathering effects on strength loss with respect to humidity, temperature, pH level and composition of the glass fibres (Orlowsky et al., 2006, Cuypers et al., 2007b). The developed knowledge was later on applied to predict the long-term performance of an AR-glass reinforced TRC pedestrian bridge (Hegger et al., 2010b).

3.2.2 Basalt fibres

The published durability aspects revolving around basalt fibres have been rather contradictory. Basalt fibres have a distinct difference in chemical composition compared to AR-glass whereby the presence of high iron content has been found to decrease its alkali-resistance (Scheffler et al., 2009a, Scheffler et al., 2009b). Basalt fibres and yarns have been shown to have higher alkali resistance in comparison to E-glass when submerged in simulated concrete conditions of saturated calcium hydroxide, $Ca(OH)_2$, (pH = 13.2) (Van de Velde et al., 2003). Others have reported that basalt and E-glass fibres have rather similar alkali resistance, such that they both undergo surface damage, i.e. loss of volume, and lose tensile strength with increasing exposure to accelerated ageing in a sodium hydroxide (NaOH) solution (Sim et al., 2005, Wei et al., 2010). Nevertheless, it is thought that a comparison between the

alkali resistance of basalt and AR-glass fibres would lead to more conclusive remarks, as it is well-established that E-glass fibres are not suitable for use in concrete (Bentur et al., 2006). It has been reported by Scheffler et al. (2009b) that unsized basalt fibres age differently in NaOH (pH > 14) than in cement solution (pH = 12.8-12.9) (i.e. calcium containing solutions), whereby visible peeling of the fibre surface was caused by the former and pitting/hole formation due to the latter conditions. Moreover, it is interesting to note that the rate of alkaline attack for basalt fibres in both NaOH and cement solution occurred more rapidly than for the AR-glass fibres. Similar degradation observations were noted for unsized basalt fibres by Förster et al. (2010). The mechanical performance of unsized commercial basalt fibres to chemically modified fibres before and after undergoing accelerated ageing in an alkaline media was investigated by Förster et al. (2011). In which, the degradation of the fibres was observed to be similar in both a 3-ionic (NaOH, KOH, $Ca(OH)_2$) and NaOH solution, i.e. progressive formation of a peeling shell. However, the addition of certain compounds, i.e. Al_2O_3, MgO, was observed to moderately improve the tensile strength or modulus after accelerated ageing. Furthermore, to overcome these degradation issues, attempts to improve the durability of basalt fibres using similar surface coatings applied to AR-glass fibres, e.g. styrene butadiene, have been recently investigated (Hempel et al., 2015). In general, the applied coating or sizing (Hempel et al., 2015) and chemical composition (Förster et al., 2010, Förster et al., 2011) of basalt fibres are critical factors influencing the durability properties of basalt fibres in an alkaline environment.

3.2.3 Carbon fibres

Carbon fibres can be made from different components, i.e. PAN and pitch, as aforementioned in Section 2.2.1, whereby the given composition influences the characteristics of the fibres (Dejke, 2001). Most types of carbon fibres, e.g. HM-PAN, high performance (HP)-Pitch and HT-PAN, have been revealed to be highly resistant to acid, alkali and organic solvents (Machida et al., 1993). Likewise, carbon fibres have been generally categorized as being chemically inert (Micelli et al., 2004, Scheffler et al., 2009c), such that they can be suitable for environmental exposure. For instance, after immersion in an alkali solution (1 M NaOH) for 28 days, carbon fibres were marked by minimal tensile strength and volume reduction as well as an absence of reaction products at the surface (Sim et al., 2005). Remarkably, a slight increase of strength after undergoing accelerated testing has also been observed for carbon fibres by e.g. Hegger et al. (2010a) and in **Paper I**. The cause of the noted increase is likely related to the so-called stiffening or interlocking of the applied surface coating at high temperatures as reported in Hegger et al. (2010a) and de Andrade Silva et al. (2014).

Relating back to carbon-FRC, Katz et al. (1996) observed that HM-PAN carbon fibres embedded in a concrete matrix increased in tensile strength and toughness during early ages (< 30 days) which was followed by a drop in mechanical properties as a result of matrix densification. The extent of this degradation was found to be a function of the concrete composition. Others have reported that nearly negligible change in strength was noted for carbon-FRC composites aged in water at elevated temperatures for a year (ACI 544.1R-96, 2002). Moreover, the influence of elevated temperatures on the interfacial properties of uncoated and polymer-coated carbon yarns embedded in a concrete matrix was investigated by de Andrade Silva et al. (2014). Through double-sided pull-out tests, it was observed that the maximum pull-

out load remained unaffected for uncoated yarns exposed to a preheating load up to 200 °C. As for coated yarns, an increase in bond was noted after preheating up to 150 °C due to stiffening of the applied coating. As preheating loads were increased to 400 °C and 600 °C, matrix, fibre and polymer coating degradation became apparent.

3.3 Experimental work

Accelerated ageing tests paired with tensile tests were performed as per ISO 10406-1 (2008) to assess the durability performance of TRC in terms of alkali-resistance (**Paper I**). The change in physico-mechanical properties of various commercially available textile reinforcements was documented and evaluated. The ability for the reinforcements to retain their tensile capacity was also quantified in the form of empirical degradation curves.

3.3.1 Materials

The textile reinforcement materials tested consisted of commercially available products made of AR-glass, basalt and carbon as shown in Figure 3.1. General properties obtained from the producers/distributors for each product are summarized in Table 3.1. It is important to note that the tested materials are considered as products and the properties resulting from the accelerated ageing do not represent the overall properties of these reinforcement materials. Many influential factors need to be taken into consideration, such as the amount and type of applied coating/sizing, quality of the product and material defects, to name a few.

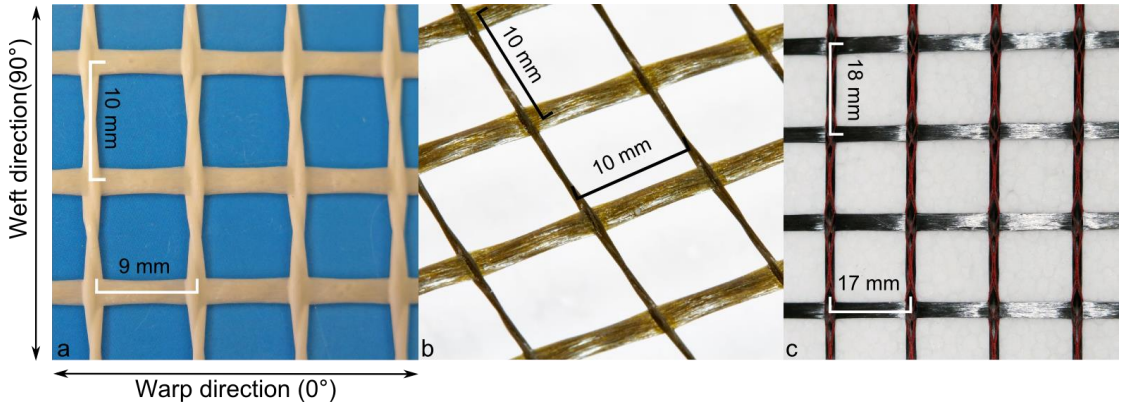

Figure 3.1 *Overview of textile reinforcement materials applied in accelerated ageing: a) AR-glass; b) basalt; c) carbon.*

*Table 3.1 General properties of the studied reinforcement materials (**Paper I**).*

Material (Product/Supplier)	Coating	Grid Spacing 0°/90° (mm)	Weight (g/m^2)	Tensile Strength of Yarn (N)
AR-glass (Glasfibervä v Grov), Sto Scandinavia AB	Styrene-butadiene resin (SBR), 20 %	7/8	210	>400
Basalt (Mesh-10-100), Sudaglass Fiber Technology Inc.	Undisclosed resin, 17 %	10/10	165	1152
Carbon (SIGRATEX Grid 250-24), SGL Group	Styrene-butadiene resin (SBR), 15 %	17/18	250	4243

3.3.2 Test description

The direct tensile tests applied in this series of tests were previously discussed in Section 2.2.3 and elaborated in **Paper I**. In order to yield a relative comparison, tensile tests were conducted on both reference and aged specimens, denoted as *pre-* and *post-immersed,* respectively. Accelerated tests were conducted on linear pieces of commercially available textile reinforcement products primarily using specifications provisioned in ISO 10406-1 (2008). The accelerated test boundary conditions specified in ISO 10406-1 (2008) consist of a prepared alkaline solution (pH > 13) and a temperature of 60 ±3 °C for 30 days. It was of further interest to gain an understanding as to whether the high alkaline solution or the temperature could be controlling degradation parameters for the tested textile reinforcement products. The effect of the exposure time of the specimens to the accelerated environment was also studied. The additional boundary conditions investigated in this work are summarized in Table 3.2 and a detailed account of the specimen and test preparations can be found in **Paper I**.

*Table 3.2 Experimental test matrix (**Paper I**).*

Case	Effect	Temperature [°C]	pH Value [-]	Time [days]	Carbon	Basalt	AR-glass
Reference	No exposure	20	-	0	C0	B0	A0
1	High temperature + high pH (ISO 10406-1)	60	14	5	C1-5	B1-5	A1-5
				10	C1-10	B1-10	A1-10
				20	C1-20	B1-20	A1-20
				30	C1-30	B1-30	A1-30
2	High temperature + neutral pH	60	7	30	C2	B2	A2
3	Low temperature + high pH	20	14	10	C3	B3	A3
4	Low temperature + neutral pH	20	7	10	C4	B4	A4

Performed ageing only
Performed ageing + tensile test
Not tested

3.3.3 Evaluation

Visual observations

Visual observations consisted of examining and reporting the external appearance of the pre- and post-immersion specimens in terms of colour, surface and shape. Documentation and discussion related to the visual observations can be found in **Paper I** and Williams Portal et al. (2015b)

Experimental results

The main measurements acquired from the direct tensile tests included the load versus strain, as aforementioned in Section 2.2.3. To further characterize the observed behaviour of the pre- and post-immersed materials, the ultimate tensile capacity, F_u, ultimate strain, ε_u, and tensile rigidity, E_A, were extracted from these results as recommended in ISO 10406-1 (2008). Moreover, to measure the relative mechanical degradation of the post-immersed reinforcement, the tensile capacity retention rate, R_{ET}, and tensile rigidity retention rate, R_{EA}, were calculated. The former is suggested in ISO 10406-1 (2008), while the latter was proposed in **Paper I** as an additional comparative parameter.

The applied load versus strain depicts a brittle material behaviour for all tested materials, see Figure 3.2 and **Paper I**. The carbon specimens were marked by a general increase in tensile strength for all tested cases, which could be perceived as this particular material can withstand the various exposure conditions. As for the basalt and AR-glass samples aged according to the standard conditions of Case 1, they were not measurable due to the extent of degradation, with the exception of specimens aged for five days (B1-5, A1-5). The tensile capacity and the ultimate strain were observed to significantly decrease for Cases 2 and 3. It was not possible to provide concluding remarks regarding the effect of Case 4 on AR-glass and basalt.

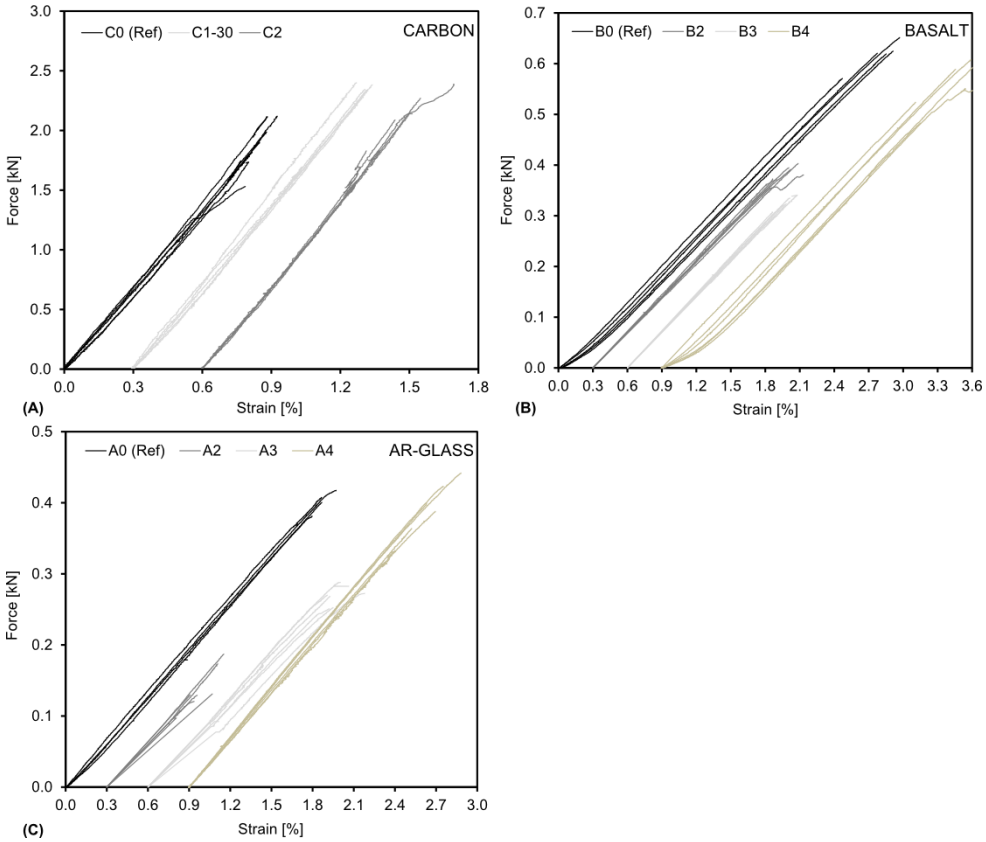

*Figure 3.2 Applied load versus strain of tested textiles: carbon (a), basalt (b) and AR-glass (c), note the differing scales (**Paper I**).*

Statistical evaluation

To determine the statistical significance of the experimental results and identify existing trends, confidence intervals were calculated for the tensile capacity and tensile rigidity retention rates as depicted in Figure 3.3 and further discussed in **Paper I**. A significant increase in tensile capacity was noted for the carbon specimens tested according to the standard conditions (Case 1). Major trends were identified for the AR-glass and basalt reinforcement products, such that AR-glass was found to be temperature sensitive particularly at 60 °C (Case 2) and could retain slightly more tensile strength (65 %) than basalt (52 %) while being exposed to 20 °C, pH 14, 10 days (Case 3). It was observed that the tensile rigidity did not provide any notable differences compared to the reference mean value.

Empirical exponential models of the degradation of the tensile retention rate were developed as a function of temperature and time, as detailed in **Paper I**. The developed degradation curves, illustrated in Figure 3.4, have an overall good correlation with the experimental findings. The use of such models could aid in describing expected behaviours for given textile reinforcement products based on the outcome of this experimental method.

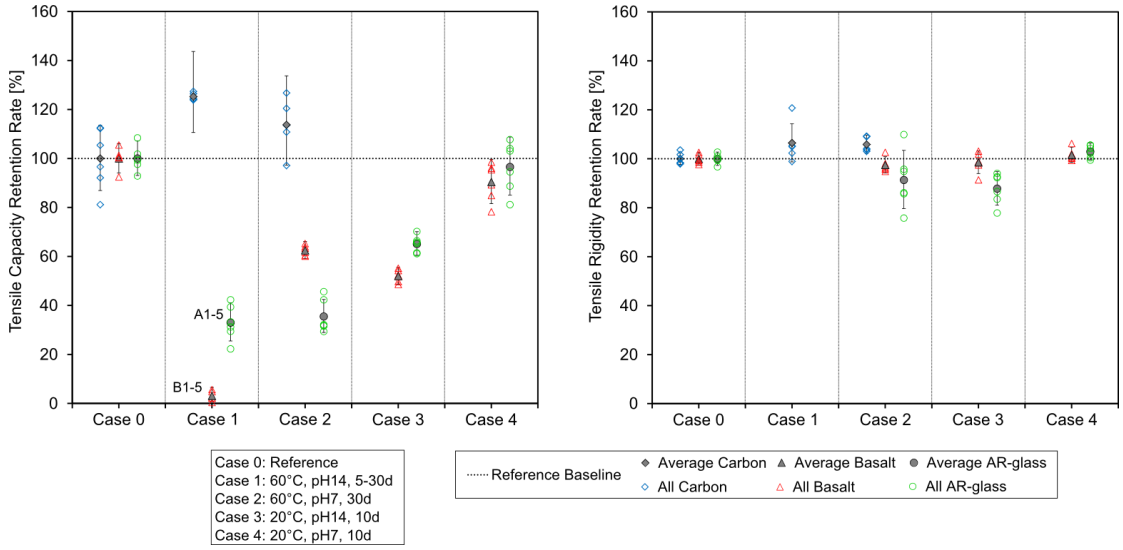

Figure 3.3 *The tensile capacity retention rate (left) and tensile rigidity retention rate (right) (**Paper I**).*

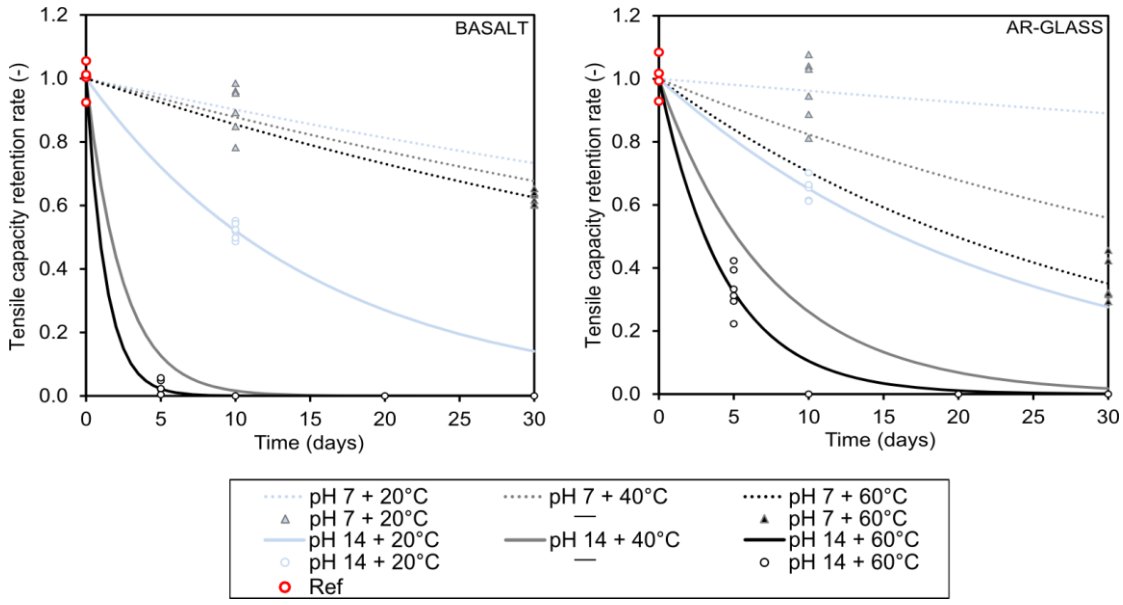

Figure 3.4 *Empirical degradation curves for the selected basalt and AR-glass products (**Paper I**).*

3.4 Summary

The effect of accelerated ageing in terms of chemical attack, viz. alkali-resistance, on the structural behaviour of textile reinforcement at the *material* level has been investigated (**Objective 3, Paper I**). Using a standard method typically applied to FRP along with certain adaptations, the change in physico-mechanical properties of various commercially available textile reinforcements was documented and evaluated using direct tensile tests. A method to describe the degradation of the tensile capacity based on the outcome of the experiments was proposed in this work.

Certain drawbacks and suggested modifications related to the applied accelerated ageing method specified in ISO 10406-1 (2008) are:

- The method does not provide any guidelines for the interpretation of the results.
  - Based on the output of this method, the use of empirical degradation models could aid in describing expected behaviours for given products, as demonstrated in this work.
  - Expected tensile strength loss limits could be defined based on previous knowledge related to FRP and FRC.
  - The chemical degradation and surface changes of the textile reinforcement could be investigated using microscopy.
- The method does not allow for the quantification of an actual lifespan of materials.
  - Could apply a similar approach used in e.g. (Dejke, 2001) to convert the test conditions to real-time conditions.
- The boundary conditions may overestimate or inadequately represent realistic boundary conditions of reinforcement in a concrete matrix.
  - Testing in an actual pore solution or reinforcement specimen cast in concrete could be an alternative.
  - Testing of the composite could include the effect of matrix densification at the reinforcement/matrix interface (Bentur et al., 1990).
- The boundary conditions are too aggressive and not suitable for all tested textile reinforcement materials.
  - Testing at different time intervals (e.g. minutes-weeks) and temperature ranges (e.g. 20-60°C).
  - The pH level of the test solution could be decreased (related to previous point to reflect actual pore solution).
  - Drying/wetting cycles could be more appropriate for certain types of fibres, e.g. natural fibres (Bentur et al., 2006).
  - Materials could be subjected to various tensioning loads during accelerated ageing, whereby time upon failure would become an independent variable.

Accordingly, the drawbacks and suggestions provided for this method along with findings from other relevant research efforts could be a good starting point towards the development of an experimental guideline which could be further applicable to TRC.

4 Interaction Level: Pull-out Behaviour

Textile reinforced concrete is a three-phase material consisting of textile reinforcement, concrete matrix and an interface. The force transferred from the brittle concrete matrix to the reinforcement is governed by the quality of the bond between the reinforcement and matrix (Mobasher, 2012). A critical factor influencing the global structural behaviour of TRC is in fact the complex compatibility between the textile reinforcement yarn/roving and the cementitious matrix (Zastrau et al., 2003), due to the heterogeneous structure of the yarn/rovings (see Section 2.2.2). This interfacial behaviour, categorized as the *interaction level* in this work, becomes a critical input parameter for numerical models developed to analyse the structural or component behaviour of TRC, denoted as the *global level* (**Paper III**).

Pull-out tests, a common method applied to study the bond or pull-out behaviour of reinforcement embedded in a matrix, have been developed and executed in this work (**Objective 1, Paper II**). It was of key interest to extract the local-bond stress-slip behaviour from pull-out tests of TRC reinforced by either basalt or carbon reinforcement grid. The local-bond behaviour was thereafter applied in both simple (1D) and more advanced models (3D) to yield global structural/component behaviour. The numerical results from the 1D and 3D models were compared to validate the simplifications assumed in the 1D model. A reasonable level of correlation was obtained between both numerical results and experimental findings. Moreover, the idealized local-bond behaviour established in **Paper II** was further applied as input in an FE-model of a one-way slab in **Paper III** (Section 5.3). A complementary study in addition to the papers was also conducted solely on carbon reinforcement grid to observe the use of an improved and modified pull-out testing technique. The influence of applied coatings and pull-out of a single roving versus single roving attached to a grid was investigated.

4.1 Bond behaviour

The interaction between the concrete matrix and reinforcement is characterized by the bond behaviour. The bond is responsible for different features of the structural behaviour at the serviceability and ultimate limit states (SLS, ULS) (fib Model Code 2010, 2013). It is to say that bond has an impact on the crack development (i.e. width and spacing), tension stiffening and curvature at SLS, while the strength at end anchorages are affected at ULS. It is important to note that the bond behaviour of textile reinforcement to concrete is inherently different from that of conventional steel reinforcement primarily due to the geometry and structure of the mesh/grid, surface roughness, applied coating, stiffness of yarn/roving, concrete matrix, as well as processing techniques. The effect of several of these parameters on the bond properties of TRC have been evaluated experimentally by e.g. Peled et al. (2003), (Krüger, 2004), Xu et al. (2007), Sueki et al. (2007), Ortlepp et al. (2008), Lorenz et al. (2012) and Zhang et al. (2013).

The stress transfer mechanisms occurring between the concrete matrix and textile reinforcement (or fibre) are typically divided into three stages, shown in Figure 4.1, after Mobasher (2012) and Richter et al. (2002):

- Stage I – Elastic:
  - The linear response signifies perfect bond between reinforcement and matrix (i.e. *adhesive bond*).
- Stage II – Non-linear:
  - Pre-peak, partial debonding starts (*external filaments*) and spreads along embedded length.
  - Post-peak, successive debonding until entire embedded length is debonded.
- Stage III – Dynamic:
  - Individual *filaments* start to slide out dynamically (i.e. *due to frictional bond*)

Overall, the force is transmitted by adhesion and friction between the reinforcement and the concrete. The load transfer between the filaments enclosed in the yarn/roving will however occur either based on adhesion or friction depending on the quality of the bond or so-called *fill-in zone* (refer to Section 2.2.2). The bond quality differs across the depth of yarn/roving which causes a complex failure mechanism involving the partial rupture and pull-out of singular filaments. This phenomenon has been coined as sleeve-core failure mechanism (Bentur et al., 2006) or telescopic failure (Bartos, 1987). A way to avoid complex failure is to impregnate or treat the yarn/roving with a coating, e.g. epoxy, which in turn helps create a homogeneous yarn structure leading to a more uniform bond interface between the yarn and the concrete matrix. This material alteration ideally results in a uniform pull-out failure of the yarn from the concrete and higher bond strength (Xu, 2004), however, it is believed at the expense of less deformation capacity due to a supposed increase in reinforcement stiffness.

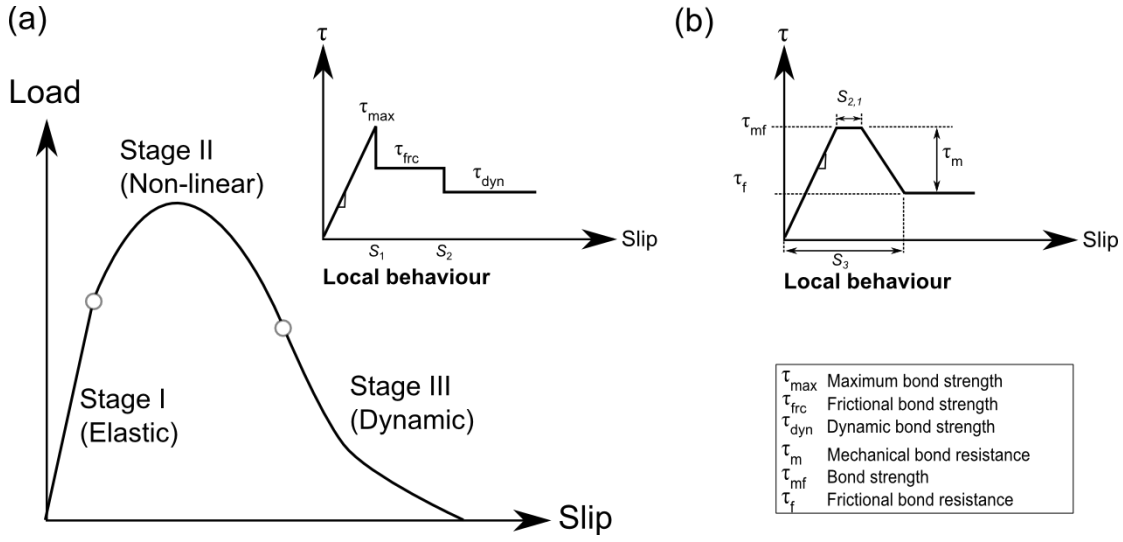

Figure 4.1 Idealized pull-out slip response of embedded textile reinforcement in concrete and local shear strength behaviour [Adopted from (Mobasher, 2012)](a) and an alternative local shear strength behaviour [Adopted from (Xu, 2004)] (b).

4.2 Pull-out testing

The characterization of the bond behaviour of textile reinforcement yarns embedded into a concrete matrix has been most commonly effectuated by means of two types of test configurations, namely one- or double-sided pull-out tests (Banholzer, 2004). It is to say that one-sided tests consist of applying a pull-out force on the free end of a yarn embedded in a concrete matrix while measuring the applied load and resulting active yarn displacement. As for double-sided tests, a crack bridging scenario is idealized by introducing a localized crack in the specimen which is bridged by one or more yarns. In this case, the successive crack opening is measured along with the load applied at the ends of the concrete specimen. Similar pull-out tests have also been applied on individual fibres/filaments to characterize the bond behaviour at another resolution of investigation. Another feature which is important to consider when concerned with the composite behaviour of a TRC structure is the bond behaviour of the textile reinforcement mesh in the concrete matrix. The presence of the transversal yarns in a textile reinforcement mesh introduces mechanical anchorage for the longitudinal yarns (Bentur et al., 2006, Mobasher, 2012) which is neglected when characterizing the bond behaviour of a smooth longitudinal fibre or yarn. This feature was exemplified in e.g. Peled et al. (1998) and Lorenz et al. (2012), wherein the pull-out behaviour of the textiles embedded in a matrix was tested.

In this work, it was of interest to determine the bond behaviour of a textile reinforcement grid embedded in a concrete matrix, such that a double-sided unsymmetrical pull-out test setup was developed and adapted based on relevant literature for this purpose (refer to Table 4.1). Thin panel specimens (400 x 100 x 15 mm) were reinforced by one centrically placed layer of reinforcement grid made of either carbon or basalt (see Figure 4.2). An individual roving was isolated by means of the defined crack bridge and loaded to obtain smeared pull-out behaviour (see Figure 4.3). The defined embedment length was generally decided according to the distance of the cross-threads, which is further specified in **Paper II**. Various embedment lengths were selected to be able to quantify the bond capacity and associated failure modes, e.g. pull-out and rupture. Additional information pertaining to these pull-out tests can be found in **Paper II** and Williams Portal et al. (2014b).

Table 4.1 Summary of experimental methods applied to characterize various levels of pull-out behaviour in textile reinforced concrete.

Test type	Investigation Level	Reference	Description	Limitations
One-sided	Fibre/filament	Banholzer (2004)	-Single fibre pull-out test -Result: applied force versus active filament displacement -Output used to idealize pull-out response of multifilament-yarn -Verified by one-sided tests of yarns	-Investigation/modelling of microscale
	Yarn	Banholzer (2004), Banholzer (2006), Aljewifi (2011)	-Embedded single yarns in a concrete matrix at one end and in an epoxy resin block or plates at the other -Result: Pull-out force versus displacement	-Neglects effect of lateral yarns/mesh structure -Investigation/modelling of mesoscale
	Textile mesh	Peled et al. (1998), Sueki et al. (2007), Mobasher (2012)	-Textile fabrics embedded in concrete matrix -Free sample end gripped to machine and loaded -Measurement: force versus slip	-Only considered for short embedment length -Influenced by free fabric length -Investigation/modelling of macroscale
Two-sided	Fibre/filament	Jun et al. (2010)	-Single fibre pull-out test -Fibre glued to mounting plates -Result: applied force versus machine displacement	-Investigation/modelling of microscale or mechanical behaviour of fibre-based composites (FRC, SHCC)
	Singular yarn	RILEM TC 232-TDT A.2 (Brameshuber et al., 2010)	-Symmetrical anchoring/ embedded length -Result: pull-out force versus pull-out displacement (i.e. crack opening displacement)	-Neglects effect of lateral yarns/mesh structure -Investigation/modelling of mesoscale
	Multiple yarns	Butler et al. (2009), Hempel et al. (2015)	-Symmetrical anchoring length -Narrowed prisms with defined breaking point (notch) -Reinforced by three yarns -Result: force, crack width and machine displacement	-Neglects effect of lateral yarns/mesh structure -Appropriate for relative comparison, i.e. change in bond after accelerated testing -Investigation/modelling of simplified macroscale
	Textile mesh	Krüger (2004), Xu (2004), Lorenz et al. (2012), Barhum et al. (2012), Lorenz et al. (2013), Lorenz et al. (2015)	-Unsymmetrical anchoring length - One yarn (connected to mesh) crossing the defined breaking point (notch) -Upper anchorage length = embedment length -Lower anchorage length = ensuring adequate yarn anchorage -Result: pull-out force versus pull-out displacement (i.e. crack opening displacement)	-Includes effect of lateral yarns/mesh structure -Investigation/modelling of macroscale (i.e. composite structure)
		Ortlepp et al. (2008)	-Upper anchorage length = clamping anchorage and load introduction -Lower anchorage length = several bond lengths in one specimen (45 ° angle cut) -Result: pull-out force versus average displacement	

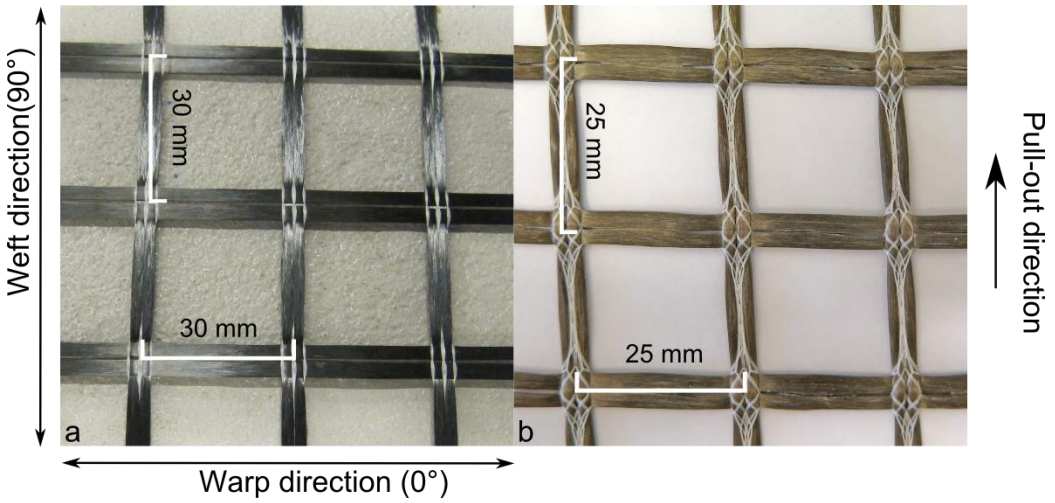

Figure 4.2 *Overview of textile reinforcement grids applied in the pull-out tests: a) Carbon; b) Basalt; (**Paper II**).*

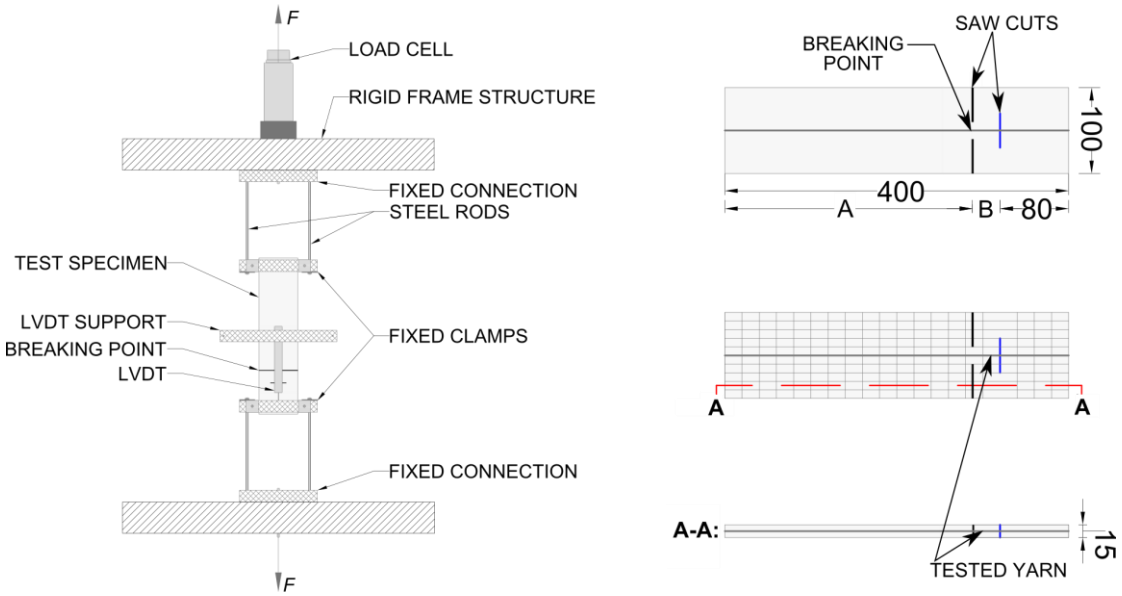

Figure 4.3 *Sketch of experimental setup (left) and specimen configuration (right) (**Paper II**).*

4.2.1 Experimental results

The outcome of the pull-out tests resulted in the applied force and crack-opening displacement (see **Paper II**). From these output, the average maximum force and the respective average crack-opening displacement, i.e. total slip, were calculated along with the standard deviation. Table 4.2 reports a summary of the experimental findings of this study. The failure mechanism denoted as *pull-out*, was often observed to be a telescopic failure (i.e. partial rupture and pull-out) which was previously explained as being a common failure phenomenon in Section 4.1.

Furthermore, these pull-out results were observed to have a rather large variability particularly as the embedment length increased, as can be noted by the standard deviation (Table 4.2). It is believed that the causes of variability can be associated to: uneven bond penetration through cross-section of roving, potential bond irregularities

along embedment length (weak zones), human error in sample preparation, defects along the reinforcement, limited experimental sample size (i.e. three samples), and even the measurement and loading precision.

Table 4.2 Experimental findings of the pull-out study – average values (std dev).

Reinforcement type	Embedded length (mm)	Maximum force (N)	Crack opening displacement at maximum force (mm)	Failure mechanism
Carbon	25 (Short)	629 (32)	0.05 (0.02)	Telescopic
	50 (Medium)	1050 (154)	0.36 (0.21)	Telescopic
	75 (Long)	1333 (298)	2.80 (2.29)	Telescopic
Basalt	35 (Short)	721 (79)	1.01 (0.20)	Telescopic
	70 (Medium)	1423 (63)	1.67 (0.14)	Rupture
	87.5 (Long)	1662 (139)	4.16 (1.41)	Rupture

The evaluation of the pull-out tests commenced with two primary inputs, namely the experimental pull-out results and material properties. A first estimation of the local bond-slip was thereafter derived from the experimental results as further explained in Section 4.2.2. By means of a 1D bond model, the calibration of the local bond-slip relationship was effectuated. The underlying assumptions included in the 1D bond model were thereafter verified using a more complex 3D FE-model. The numerical solutions in the form of force versus total-slip relationships were compared to the experimental results as described in the following sections.

4.2.2 Local bond stress-slip function

A suitable local bond stress-slip relationship should give results on the global level that correlate with the measured global bond behaviour. The shape of the local bond stress-slip function is dependent on numerous parameters, e.g. material properties of the concrete matrix, reinforcement geometry and surface, as well as the configuration and stiffness of the mesh cross-threads. Numerical or analytical methods are commonly applied to estimate a local bond-slip function. For instance, a suggested local bond-slip function shape pertaining to FRP rebar is provisioned in fib Model Code 2010 (2013), while a range of research efforts have focused on analytical solutions for TRC-based cases (Zastrau et al., 2003, Sueki et al., 2007, Lorenz et al., 2012). Within this scope of work, local bond stress-slip functions for both basalt and carbon reinforced TRC were calibrated to match the experimental results as presented in **Paper II**. A first estimate of a local bond-slip function was made according to the experimental results related to the test specimens constituting a short embedment length. This first estimate was then used as input in a global analysis resulting in a force versus crack opening relation. From comparisons with the measured results, the local bond versus slip was corrected in several steps until reasonable agreement was found on global level. Further details regarding the assumptions and corrections applied are mentioned in **Paper II**. This calibrated local behaviour, shown in Figure 4.4, was subsequently applied in numerical models simulating the pull-out behaviour (see Section 4.3), as well as input data in the analyses of the four-bending tests based on carbon reinforced TRC (see Section 5.2.1).

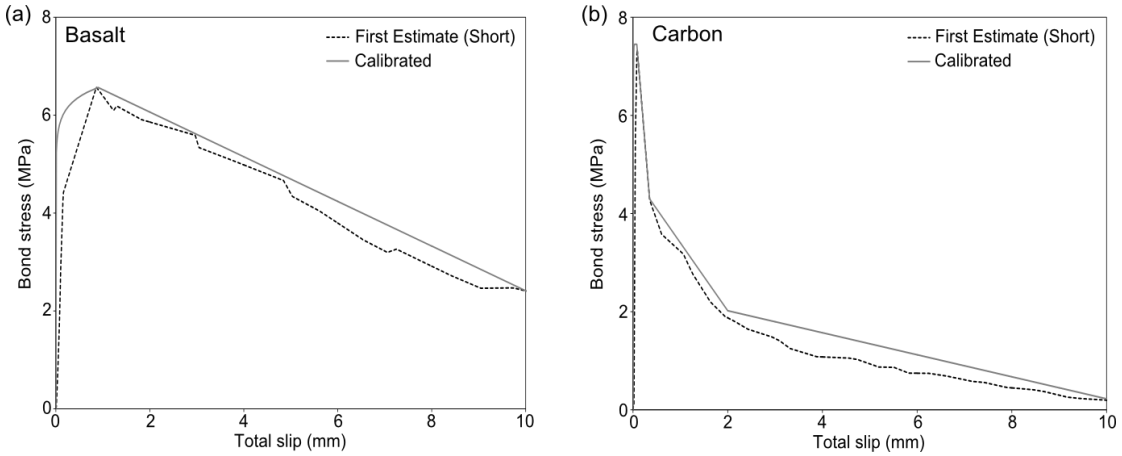

*Figure 4.4 Calibrated local bond-slip for basalt reinforced TRC (a) and carbon reinforced TRC (b) (**Paper II**).*

4.3 Numerical modelling

An analytical 1D bond-slip model developed by Lundgren et al. (2012), originally applied for corroded and uncorroded ribbed steel reinforcement, was adapted to describe a textile reinforcement yarn (see **Paper II**). The singular pull-out yarn, which uniformly bridged both anchorage ends (i.e. Short and Long zones) was idealized to have a homogeneous circular cross-section section and singular external bond interface. The geometric influence of the surrounding reinforcement mesh (lateral yarns) was not taken into account. In essence, the differential equation expressing equilibrium conditions along the reinforcement in tension was solved.

Furthermore, a 3D FE-model, as illustrated in Figure 4.5, was developed in DIANA based on the unsymmetrical double-sided pull-out test conducted. Further details related to the model development are provided in **Paper II**. The analyses were non-linear as they described the non-linear behaviour of the bond stress-slip relationship between the concrete matrix and textile reinforcement. An example of the numerical results from the 3D FE-model is depicted in Figure 4.6, where the reinforcement bond stress evaluation could be captured. Also, the numerical results obtained from these analyses were compared to the experimental results and 1D bond-slip model results as shown in **Paper II**. Main assumptions and differences between the 1D bond-slip model and 3D model are provided in Table 4.3.

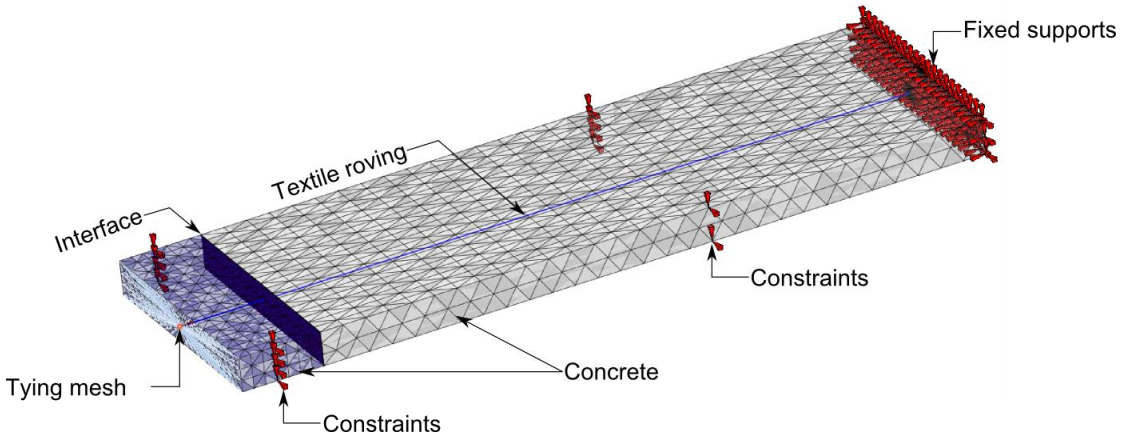

*Figure 4.5 Overview of 3D FE-model (**Paper II**).*

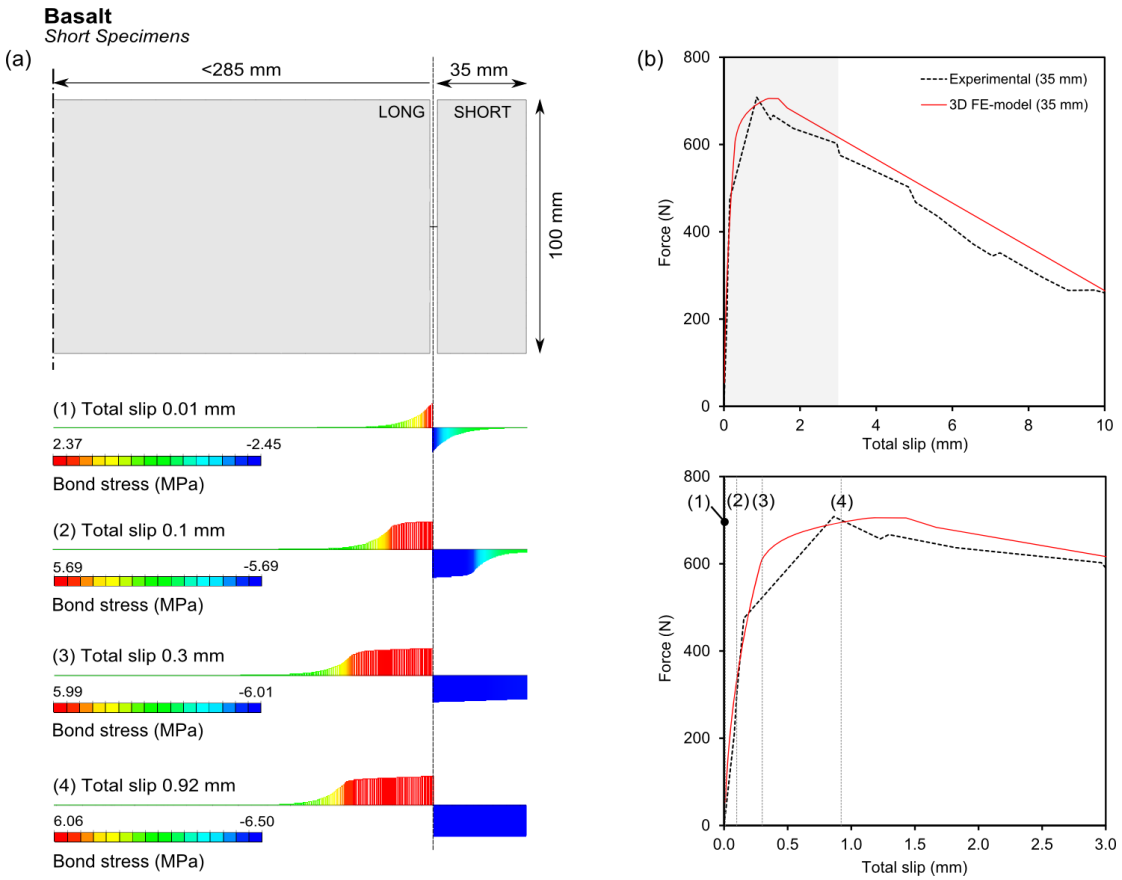

Figure 4.6 *Bond stress evolution captured by 3D FE-model for basalt Short specimens at different steps related to various slips (0.01 mm, 0.1 mm, 0.3 mm and 0.92 mm) (a) and force versus total slip curves with indicated slip steps (b).*

Table 4.3 *Key differences between the 1D and 3D models.*

Parameter/Property	Description	
	1D analytical model	3D FE-model
Idealization of reinforcement	Homogeneous yarn with circular cross-section	Homogeneous yarn with circular cross-section
Material model for reinforcement	Linear elastic (cannot capture rupture)	Linear elastic (cannot capture rupture)
Concrete strain	Not considered	Included
Local bond stress-strain relationship	Included	Included
Short and Long zones	Separate calculations and correlation	Interaction between zones Simultaneously captures bond stress distribution between zones
Unloading branch at peak	Considered additionally	Included

4.4 Additional investigations

An improved and modified pull-out testing technique was additionally studied in this work (see Figure 4.7). This content is in addition to the enclosed papers; highlights of

this preliminary study are presented here to provide further insight on the test method and bond behaviour. Detailed information related to these tests is provided in **Appendix B**. The main simplification of this method is such that the embedment length was defined by cutting away a part of the tested roving within the anchorage length. In the majority of the existing test methods, the embedment length is often defined in a secondary section of the specimen using a saw cut or prescribed breaking point as applied in **Paper II**. Furthermore, a valuable added feature was the use of a video extensometer technique to capture the active end-slip of the reinforcement relative to the concrete end. In a preliminary study, the pull-out tests were performed on several TRC specimens reinforced by either one layer of carbon textile grid or reinforced by a single carbon roving in order to determine the effect of the grid structure and cross-threads on the bond behaviour. In both tested cases, solely one roving was subjected to a pull-out force. The reinforcement surface was also modified using epoxy or a polymer based coating. A general observation from Figure 4.8 is such that the epoxy coated grid had on average superior bond strength and less active slip. This result indicates that the epoxy enhanced the stiffness of the cross-threads influencing the anchorage and allowed for a more homogeneous failure of the roving.

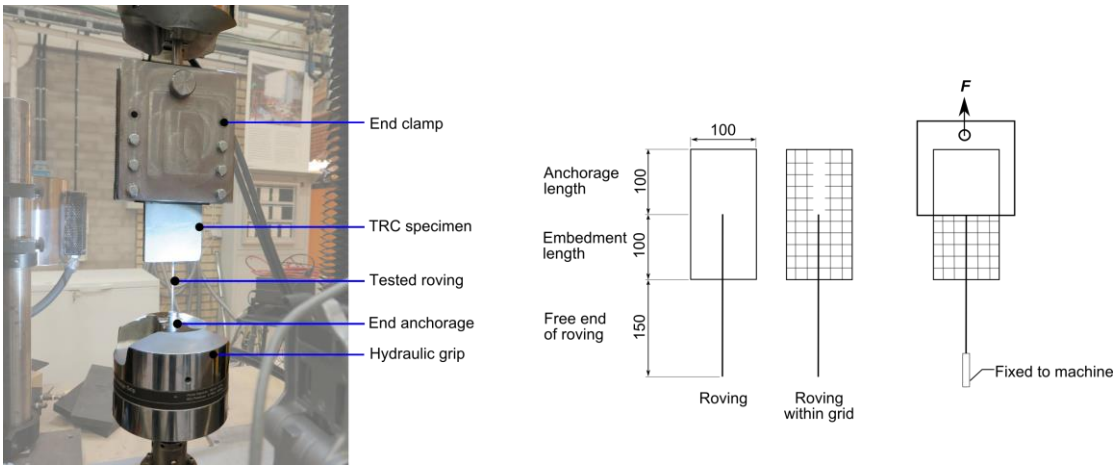

Figure 4.7 Experimental pull-out setup (left) and specimen configuration (right).

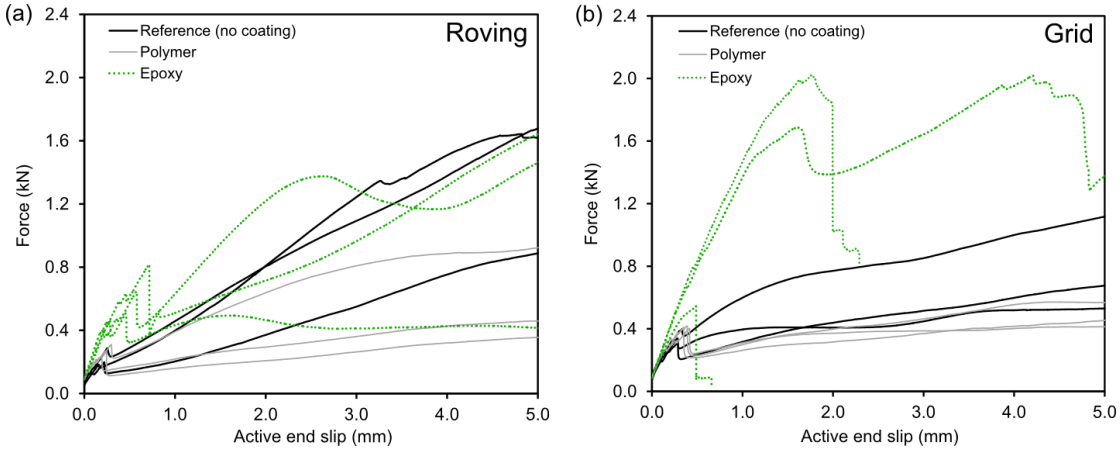

*Figure 4.8 Example force versus active end slip results for roving (a) and grid (b) (refer to **Appendix B**).*

4.5 Summary

It has been discussed that the interfacial bond between textile reinforcement and the concrete matrix is greatly heterogeneous. The characterization of the bond behaviour is thus critical in order to understand the global structural behaviour of TRC. The bond behaviour of textile reinforcement embedded in a concrete matrix was experimentally and numerically investigated in this work (**Objective 1, Paper II**). This level of evaluation involves the *interaction* level of the *structural performance* of TRC. The main findings of this section are presented in the following:

> The two-sided pull-out tests of an individual yarn from a textile mesh was successfully applied in this work.
  - The embedment length was varied, for both carbon and basalt textiles, to determine the differing failure modes, e.g. pull-out, rupture or combination (telescopic).
  - Larger standard deviation was generally observed as the embedment length increased which can be explained due to the potential inclusion of increased material defects.
  - Due to the inherent smoothness of the uncoated carbon textiles, much larger embedment lengths are required to yield rupture/anchorage in comparison to other textiles, e.g. basalt and AR-glass.
  - The measurement techniques could be further tailored to include an extensometer at the crack-opening location.
  - It could be worth investigating the influence of the end anchorage configuration on the bond behaviour, e.g. if there is an effect on the bond strength or introduction of eccentricities.

> The first assumption of a local bond stress-slip relationship based on the short embedment lengths appeared to be reasonable for both carbon and basalt. These first assumptions were verified using simplified (1D) and complex models (3D) to compute the so-called global force versus total slip behaviour. This output was thereafter compared to the experimental results.
  - Overall favourable agreement was noted between the applied 1D, 3D models and experimental results in terms of initial stiffness up to the peak load.
  - The post-peak behaviour was less accurately captured by the models especially as the embedment length increases which could be due to several reasons, e.g. assumption of constant reinforcement area after the peak and inaccurate experimental measurement of slip.

> The underlying assumptions in the 1D bond model, e.g. neglecting concrete strains, was successfully shown to have a minimal effect using the 3D FE-model.

> Additional studies showed that there are underlying differences between the bond behaviour of the grid structure versus the individual roving.
  - The cross-threads of the grid, especially when coated by epoxy, greatly increase the anchorage of the roving being pulled.
  - The level of investigation, i.e. macro, meso- or microscales, thus influences the chosen configuration and reinforcement arrangement of the pull-out test.
  - The use of video extensometers was shown to be a reliable way to accurately capture the end slip of the textile roving with respect to the concrete specimen.

5 Global Level: Flexural Behaviour

TRC in the form of a structural component was experimentally investigated in flexure. This level of investigation was defined as the *global* level of *structural performance* in this work as aforementioned in Section 1.2 (**Objective 1**). Furthermore, the ability to interconnect the *structural performance* on the *material* and *interaction* levels to the *global* level was studied by means of FEA (**Objective 2)**. The major findings presented in this section are presented in **Paper III**; however, additional experimental findings obtained by the author are also included to gain further insight.

The non-linear behaviour of TRC can be characterized by its flexure behaviour in combination with the tensile and bond behaviours. Based on the given application of the TRC structure, the applicable load combinations need to be taken into consideration. For example, in the case of a sandwich façade panel, which can be exposed to various load combinations, i.e. shear and tension forces and bending moments (Shams et al., 2014), the combined load effects need to be investigated. The one-way flexural behaviour of TRC in the form of thin slabs (Peled et al., 1999, Krüger, 2004) or as a beam strengthening solution (Schladitz et al., 2012) is typically studied by means of four-point bending tests which was also applied in this work.

5.1 Overview

We turn to a case of a one-way slab reinforced by textile reinforcement under four-point bending to discuss the flexural behaviour of TRC. The load versus midspan deflection is depicted in Figure 5.1 along with indicated loading states. There are technically three applicable states for TRC, but four are typically defined to draw a parallel between conventionally reinforced concrete and TRC (Brameshuber, 2006): *State I* (uncracked concrete), *State IIA* (crack formation), *State IIB* (crack stabilization), and State III (failure).

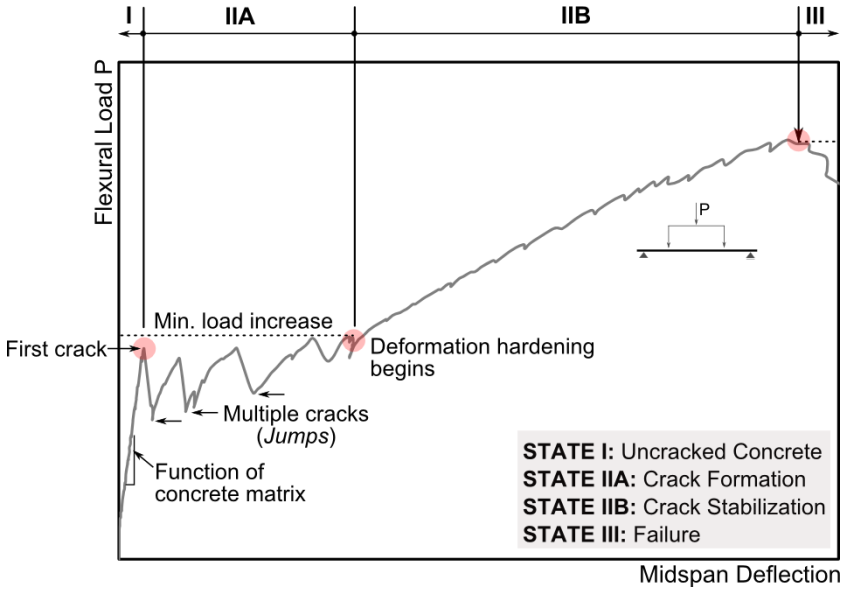

Figure 5.1 Load versus mid-span deflection for a TRC one-way slab under four-point bending, with indicated stages.

State I corresponds to the elastic state of the uncracked TRC member, where the stiffness is said to be entirely a function of the concrete matrix (Brameshuber, 2006).

First cracking takes place once the tensile strength of concrete is reached, which thereafter initiates tensile stresses in the textile reinforcement within the cracked region. The transfer of load from the concrete to the reinforcement in the crack location is effectuated by means of the bond. Multiple crack formation, marked by load *jumps* or *snap-back*, follows with a minimal increase in load, defined as *State IIa*. The initial size of the load jumps is also largely a function of e.g. the interfacial bond between textile and matrix, stiffness of textile and reinforcement ratio. Apparent loss of stiffness and decrease in load jump is observed within this state resulting from the crack formation. The crack formation eventually stabilizes in *State IIb*, which is marked by a gain of stiffness said to be governed by the properties of the textile reinforcement (Orosz et al., 2010). This gain in stiffness is often denoted as *strain hardening* in the case of uniaxial tension (Brameshuber, 2006) but can be seen as a form of *deformation hardening* in flexure. Ideally, when *State III* is reached, the failure of TRC occurs when the textile reinforcement undergoes linear elastic deformations until reaching its ultimate limit load causing a brittle failure. Nevertheless, despite the fact that carbon and AR-glass fibres have no plastic capacity, the heterogeneous yarn structure causes the uneven pull-out or slippage of individual filaments particularly in the case of non-coated yarns. As such, failure is typically marked by a combination of pull-out and rupture in practice (Bentur et al., 2006). Generally speaking, in the case of a pull-out failure, a more ductile failure (dashed line) could also take place at the expense of lower reinforcement utilization.

State I is essentially outlining the limit for serviceability limit state design for the case of TRC façade panels. Concerning the design of load bearing TRC structures, e.g. beam or slab, in the ultimate limit state, the flexural capacity applied for design should fall within *State IIb.* A certain safety factor would, however, need to be applied to the ultimate capacity in order to prevent brittle failure.

5.2 Experimental work

The experimental work related to the investigation of the flexural behaviour of TRC encompassed various studies listed in the following. It is important to highlight that there have been deviations in the use of materials, geometry and test setup in these studies. Accordingly, it is not the aim of the author to draw direct comparisons between all the results, yet to point out the observed flexural behaviours, bring along improvements and provide general remarks. The selected studies presented in this thesis are summarized in Table 5.1.

Table 5.1 Test series conducted to characterize the flexural behaviour of TRC.

Test series	Description
1A	TRC slab, thickness 80 mm, one textile layer (**Paper III)**
1B	TRC slab, thickness 50 mm, one textile layer (**Paper III)**
2A	High performance concrete (HPC) slab, thickness 20 mm, two textile layers
2B	HPC slab, thickness 20 mm, two textile layers + surface coating
3	Reactive powder concrete (RPC) slab, thickness 20 mm, two textile layers + short random fibres

5.2.1 Test series 1

Rectangular TRC one-way slabs were cast and tested at DTI in a two part test series, denoted as *Test series 1A* and *1B*. Firstly in *Test series 1A*, it was of interest to observe the application of different densities of carbon textiles in a conventional slab thickness (80 mm) commonly applied in façade panels. The reduction of the thickness to 50 mm in combination with commonly applied textile alternatives was studied in *Test series 1B* as well as the effect of mesh overlapping. In practice, it has been established that TRC slabs for façade panels can be produced having a thickness of 30 mm (Kulas et al., 2011). Further slab thickness reduction was explored in the subsequent *Test series 2* and *3*. The experimental results and related analysis associated to these tests have been documented in detail in Williams Portal (2013), (Williams Portal et al., 2013) and **Paper III**. As such, only a brief account of the work completed will be discussed here.

Experimental details

The flexural behaviour of rectangular one-way TRC slabs (800 x 200 x 80 mm and 1000 x 200 x 50 mm) reinforced by one layer of textile reinforcement (cover thickness 7.5 mm) was investigated using four-point bending tests. The four-point bending test consisted of the slab being placed upside down compared to when it was cast and the load was applied from beneath. The specimen geometry and test setup, however slightly differed due to attempted improvements in the test setup, yet a loaded span length of 400 mm remained constant.

Materials

The TRC specimens consisted of the concrete mixture previously specified in Table 2.1 (Section 2.1). In *Test series 1A*, three woven carbon textile meshes having differing linear densities and spacing were investigated, while carbon, AR-glass and basalt meshes were tested in *Test series 1B* (see Figure 5.2). Two mesh configurations were studied: a) whole mesh and b) spliced mesh with an overlap of 100 mm only for AR-glass and basalt. The purpose of investigating a spliced mesh with an overlap was to observe whether the selected length could adequately transfer loads. Splices are often introduced in the case of scaling-up structures and become critical in terms of defining anchorage and load transfer. The warp yarns were placed longitudinally in the specimens such that these yarns were loaded during the test. This loading direction also corresponds to the loading direction applied in the pull-out tests (Section 4.2). A test matrix for this test series is provided in Table 5.2. It should be noted that throughout this work the cross-sectional area of a yarn, A_f, was calculated as the ratio between the linear density of the yarn, *Tex*, and fibre density, ρ. Thereafter, this area was multiplied by the amount of longitudinal yarns positioned within the width of the specimen to yield the cross-sectional area of longitudinal reinforcement, $A_{t,l}$. Also, the reinforcement ratio was calculated as the ratio between $A_{t,l}$ and the gross specimen cross-sectional area, A_c.

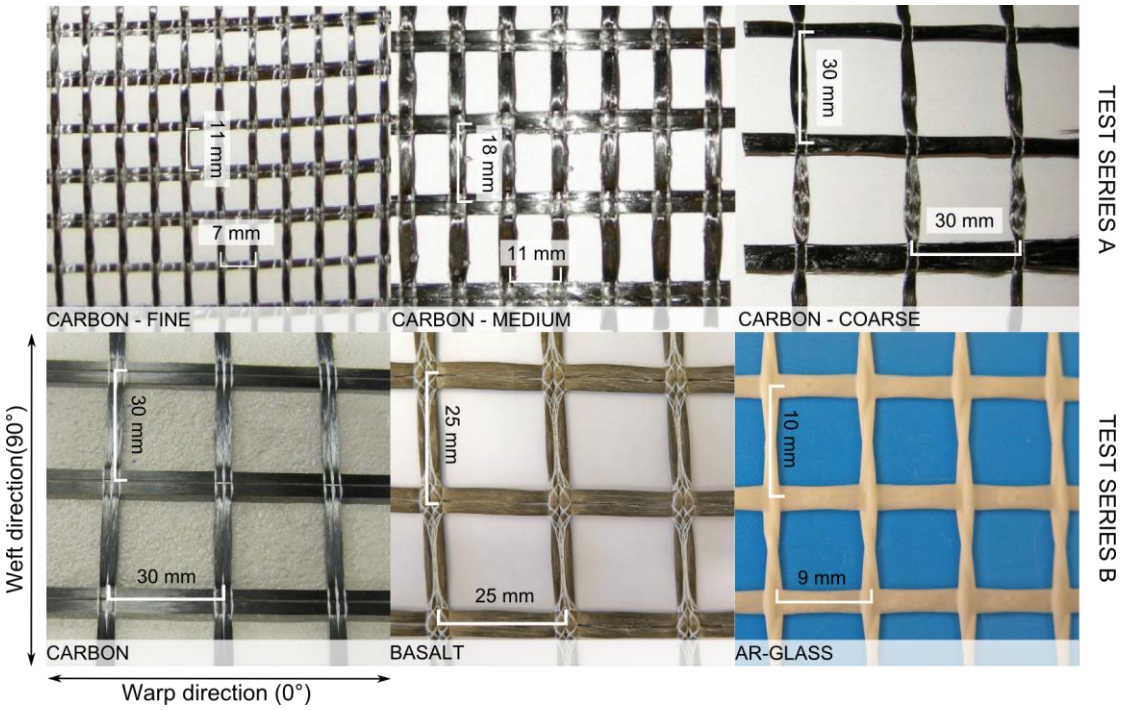

*Figure 5.2 Overview of textile reinforcement meshes used in Test Series 1 (**Paper III**).*

*Table 5.2 Test series 1 test matrix (**Paper III**).*

Test series	Specimen ID	No. specimens	Reinforcement	Average no. longitudinal yarns	Cross-sectional area of longitudinal reinforcement, $A_{t,l}$ (mm^2)	Reinforcement ratio, ρ (%)
1A	Fine	1	1 layer 2D carbon textile (fine)	29	12.7	0.08
	Medium	1	1 layer 2D carbon textile (medium)	18	35.4	0.22
	Coarse	1	1 layer 2D carbon textile (coarse)	7	13.0	0.08
1B	C1-C3	3	1 layer 2D carbon textile	7	12.8	0.13
	B1-B3	3	1 layer 2D basalt textile	8	5.9	0.06
	Bs1-Bs3 (splice)	3				
	A1-A3	3	1 layer 2D AR-glass textile	22	5.9	0.06
	As1-As3 (splice)	3				

Results: Test series 1A

The flexural load versus midspan deflection curves along with the crack formation for the TRC slabs reinforced by the various carbon textiles are depicted in Figure 5.3. The flexural load corresponds to the total load applied to the test specimen. General observations which can be drawn are:

> Pre-cracking behaviour (*State I*) was governed by concrete stiffness (≤ 10 kN).
> First cracking (*State IIa*) was marked by an unloading branch followed by multiple cracking indicated by the apparent load jumps.
> The stabilization of crack formation and resulting deformation hardening (*State IIb*) was not significantly apparent, yet a larger load increase was noted for the *Medium* specimen.
> The failure mechanisms (*State III*) included rupture and delamination.

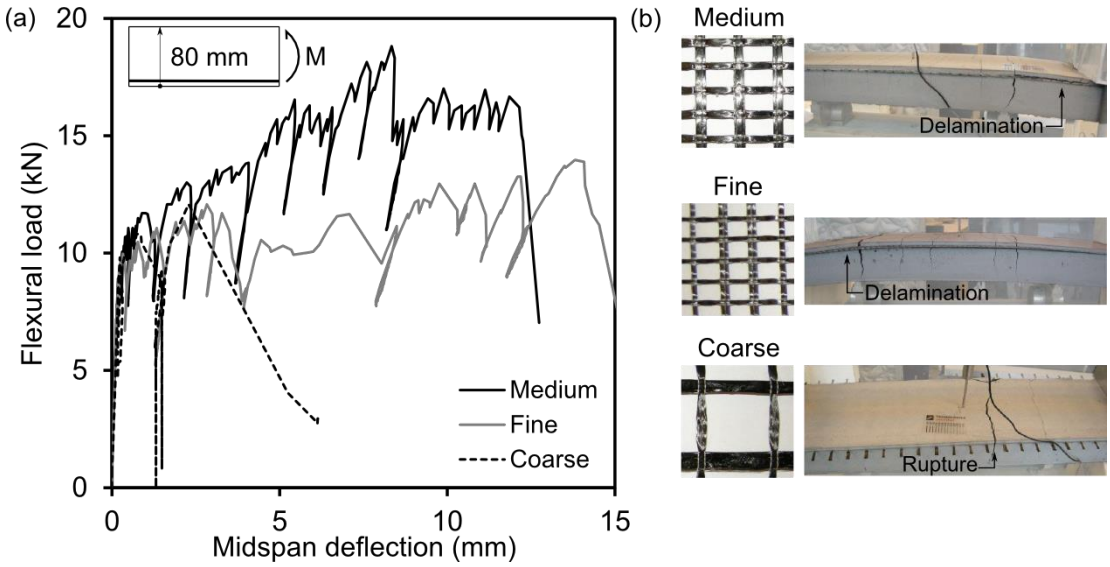

Figure 5.3 *Test series 1A – Experimental results for all specimens (Williams Portal et al., 2013) and* ***Paper III****.*

Results: Test series 1B

The flexural load versus midspan deflection curves for the TRC specimens reinforced by carbon, basalt and AR-glass are provided along with specific observations in Figure 5.4 to Figure 5.6, respectively. General observations pertaining to the results are:

> Pre-cracking behaviour (*State I*) was governed by concrete stiffness (≤ 4 kN).
> First cracking (*State IIa*) was marked by an unloading branch due to, e.g. the brittle nature of load redistribution to the textiles, low reinforcement ratio or poor bond. Multiple cracking took place solely for basalt and carbon.
> The stabilization of crack formation and so-called deformation hardening (*State IIb*) only occurred for carbon specimens.
> The observed failure mechanism (*State III*) included yarn rupture and partial rupture with pull-out (telescopic failure).
> The overlapping length was sufficient as the load level and failure mode were comparable to specimens without splices.

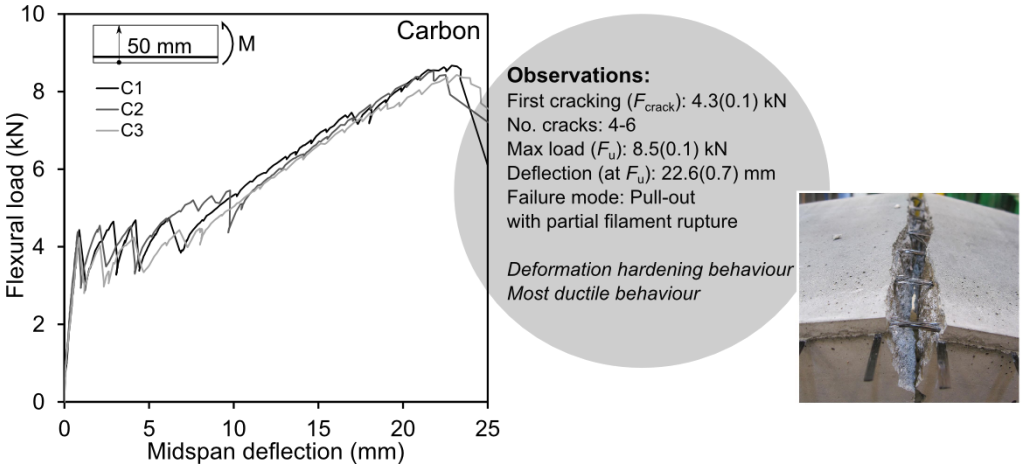

Figure 5.4 *Test series 1b – Flexural load versus midspan deflection for TRC slabs reinforced by carbon textiles, average values (std dev) (**Paper III**).*

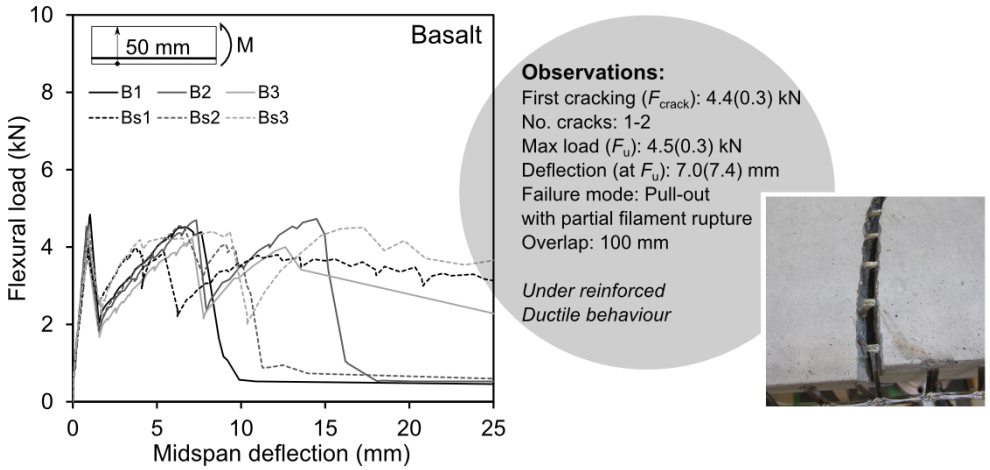

Figure 5.5 *Test series 1B – Flexural load versus midspan deflection for TRC slabs reinforced by basalt textiles, average values (std dev) (**Paper III**).*

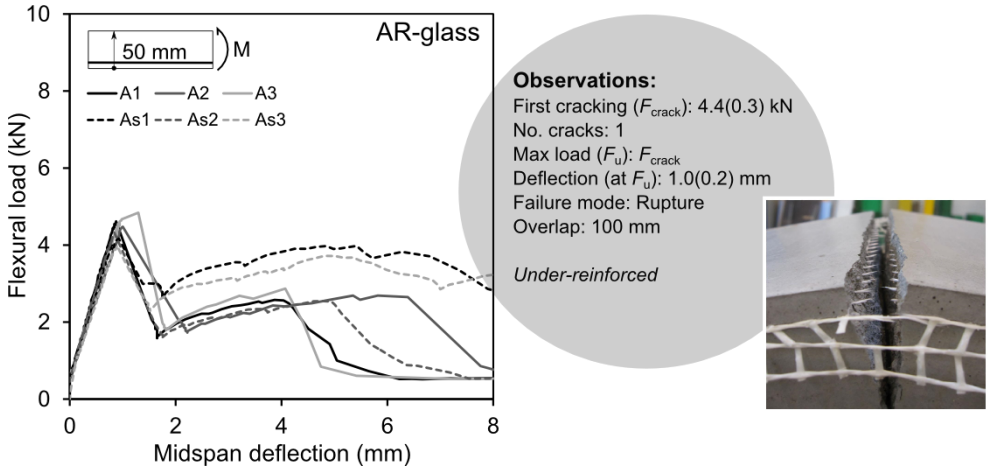

Figure 5.6 *Test series 1B – Flexural load versus midspan deflection for TRC slabs reinforced by AR-glass textiles, average values (std dev) (**Paper III**).*

Comparison

A comparison of the flexural results related to *Test series 1A* and *1B* is presented in Table 5.3 using two parameters, namely the first crack stress, σ_{cr}, and apparent flexural strength, σ_u. These parameters were calculated based on linear elastic assumptions and therefore do not yield the true flexural stress states after cracking. The first crack stress and apparent flexural strength were calculated based on the experimental first cracking flexural load, F_{cr}, and maximum flexural load, F_u, in relation to the loaded span and specimen geometry. From the results, the first cracking stress is expectedly lower for *Test series 1A* due to the larger cross-sectional area. Taking a look at the apparent flexural strength values, the 50 mm TRC specimens reinforced by carbon textiles (C1-C3) resulted in superior or so-to-say effective composite behaviour. It is interesting to note that despite the larger reinforcement ratio included in the 80 mm *Medium* slabs, the apparent flexural strength was nevertheless greater for the C1-C3 slabs likely due to improved bond or anchorage length. A general conclusion which can be drawn is that the ultimate flexural behaviour is highly governed by not only the reinforcement ratio, but foremost by the bond or utilization of the textile embedded in the concrete matrix.

Table 5.3 Four-point bending results for Test series 1A and 1B (stated in average values with std dev)

Test series	Specimen	First cracking flexural load, F_{cr} (kN)	First cracking stress, σ_{cr} (MPa)	Maximum flexural load, F_u (kN)	Apparent flexural strength, σ_u (MPa)	Midspan deflection at F_u, δ_u (mm)
1A	Carbon (Fine)	10.0	4.3	14.0	6.1	13.8
	Carbon (Medium)	10.1	4.4	18.8	8.2	8.3
	Carbon (Coarse)	9.8	4.3	12.1	5.2	2.3
1B	Carbon (C1-C3)	4.3 (0.1)	7.0 (0.1)	8.5 (0.1)	13.8 (0.2)	22.6 (0.7)
	Basalt (B1-B3)	4.5 (0.4)	7.2 (0.7)	4.6 (0.3)	7.5 (0.5)	7.5 (6.7)
	Basalt (Bs1-Bs3)	4.4 (0.3)	7.1 (0.5)	4.4 (0.3)	7.1 (0.5)	6.4 (9.4)
	AR-glass (A1-A3)	4.6 (0.2)	7.5 (0.3)	4.6 (0.2)	7.5 (0.3)	1.1 (0.2)
	AR-glass (As1-As3)	4.2 (0.2)	6.7 (0.3)	4.2 (0.2)	6.7 (0.3)	0.9 (0.0)

5.2.2 Test series 2 and 3

In *Test series 2* and *3*, thin rectangular TRC specimens of 20 mm were cast and tested at CBI. The purpose of conducting these test series was to explore the influence of numerous features on the one-way flexural behaviour: 2D versus 3D carbon textile configurations, high strength concrete mixtures, application of coatings and addition of short random fibres. These results are presented in addition to the enclosed papers.

Experimental details

The flexural behaviour was investigated using four-point bending tests based on EN 12390-5 (2009). Specimens (700 x 100 x 20 mm) were cast using a similar procedure to that applied in *Test series 1*, yet two layers of reinforcement were incorporated here. Spacing between the two layers (12 mm) was chosen to correlate with the fixed geometry of the 3D carbon grid. The corresponding cover thickness of each layer was therefore set to approximately 4 mm. After casting, the samples were removed from their formwork after 24 hours and stored in water until testing, which differed from *Test series 1*. Furthermore, the tests were conducted using a servo-mechanical testing machine (Instron 1195) and displacement-controlled load. The one-way slabs were placed on roller supports with a span of 600 mm. The load *P* was distributed by two point loads each applying a load of *P/2* onto the specimen with a distance 200 mm apart from each other. On opposite sides of the samples, two LVDTs captured the midspan displacement with respect to the top surface. An average displacement value was thereafter computed. The flexural load referred to in the following consists of the total applied load *P*.

Materials

Two types of textile reinforcements, 2D and 3D carbon, were investigated (see Figure 5.7). *Test series 2* was further split into two parts, *2A* and *2B*, wherein *2A* included a TRC reinforced by 2D carbon textile coated by 15 %-wt styrene-butadiene resin (SBR) applied by the manufacturer, while *2B* comprised a study on additional surface modifications applied to the same 2D carbon textile. The surface modification was achieved after production in the laboratory using either epoxy or another variant of *polymer* coating. The concrete applied in *Test series 2*, termed as high-performance concrete (HPC), had an f_c of 71.5 MPa at 28 days (see **Appendix A**). *Test series 3* differed from the other studies as it explored the use of reactive-powder concrete (RPC), selected short random fibres along with the 2D carbon textile from *Test series 2A*. The RPC mix applied in this test series had an f_c of 147 MPa at 28 days. Additional details related to the mix design and mechanical properties of the RPC can be found in Mueller et al. (2015). Material properties for the 2D carbon textile were presented and measured in **Paper I**. The same carbon roving (24K, bundle of 24 000 filaments) is incorporated in the 3D carbon textiles. The 3D textile also comprises a low-modulus polyester (PET) spacer which is said to merely have a function of improving the stability of the textile unit (Amzaleg et al., 2013). The tested specimen details for *Test series 2* and *3* are specified in Table 5.4.

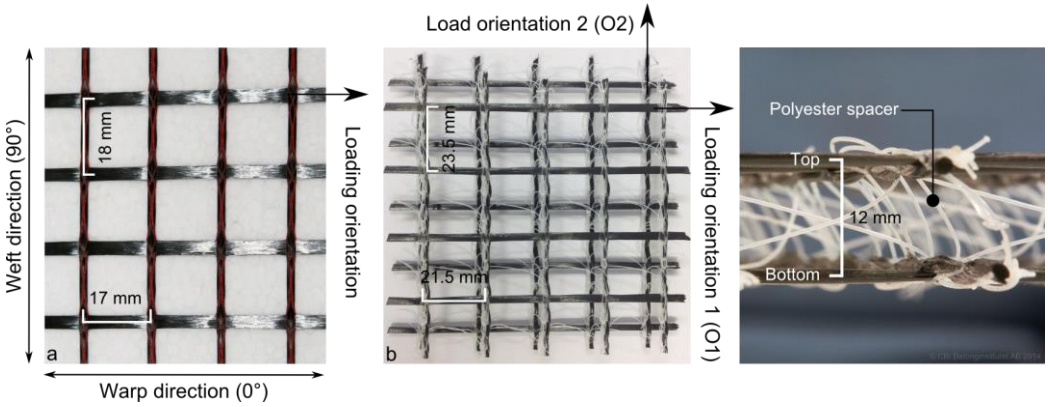

Figure 5.7 Textiles applied in Test series 2 and 3 with specified load orientation: 2D carbon textile (a) and 3D carbon textile (b).

Table 5.4 Test series 2 and 3 test matrix.

Test series	No. specimens	Concrete	Reinforcement	Average no. longitudinal yarns (both layers)	Cross-sectional area of longitudinal reinforcement, $A_{t,l}$ (mm^2)	Reinforcement ratio, ρ (%)
2A	4	HPC	2 layers, 2D carbon textile (Reference)	12	10.6	0.53
	2	HPC	1 layer, 3D carbon textile (*O1*)	9	7.9	0.40
	2	HPC	1 layer, 3D carbon textile (*O2*)	9	7.9	0.40
2B	4	HPC	2 layers, 2D carbon textile + epoxy	12	10.6	0.53
	3	HPC	2 layers, 2D carbon textile + polymer coating	12	10.6	0.53
3	4	RPC	2 layers, 2D carbon textile (Reference)	12	10.6	0.53
	4	RPC	2 layers, 2D carbon textile + carbon fibres (1 vol-%)	12	10.6	0.53
	4	RPC	2 layers, 2D carbon textile + polymer coating	12	10.6	0.53

Results: Test series 2

The experimental findings for *Test series 2A* and *2B* are presented in the form of flexural load versus midspan deflection curves and are accompanied by respective specimen documentation in this section. In all tests, the textile reinforcement did not reach its tensile strength, yet the tests were terminated according to either large deflection or effects of poor bond, i.e. pull-out of reinforcement without further crack development. The flexural behaviour of the specimens reinforced by the two layers of 2D carbon textile versus one layer of 3D carbon textile had some underlying differences (see Figure 5.8 and Figure 5.9). For the 2D carbon specimens, poor bond between the textile and matrix was observed resulting in minimal crack formation, maximum flexural loads occurring at lower midspan deflection compared to the 3D carbon specimens, followed by apparent yarn pull-out. It is thought that the PET spacer enhanced the stability and interaction of the textile reinforcement layers in the cross-section. When loaded in the *O1* direction, the PET fibres interlaced around the warp yarns appeared to improve the bond and crack development. In the *O2* direction, the weft yarns have a denser spacing due to the shift in the spacing on the top and bottom layers. As a result, a denser and finer crack pattern was noted for these specimens. The orientation of the 3D carbon textile in the specimen appeared to have an effect on the load levels by nearly half, which is likely due to the surface waviness (irregularities) and stabilisation of the warp yarns when loaded in *O2* which delayed the uniform yarn activation.

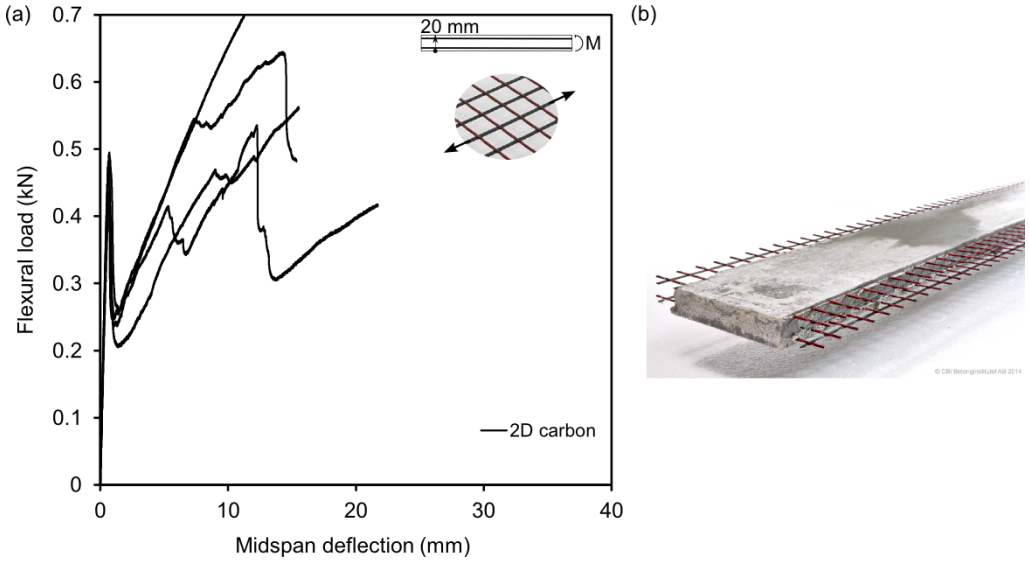

Figure 5.8 Test series 2A: Flexural load versus midspan deflection for 2D carbon textiles (a) and test specimen (b).

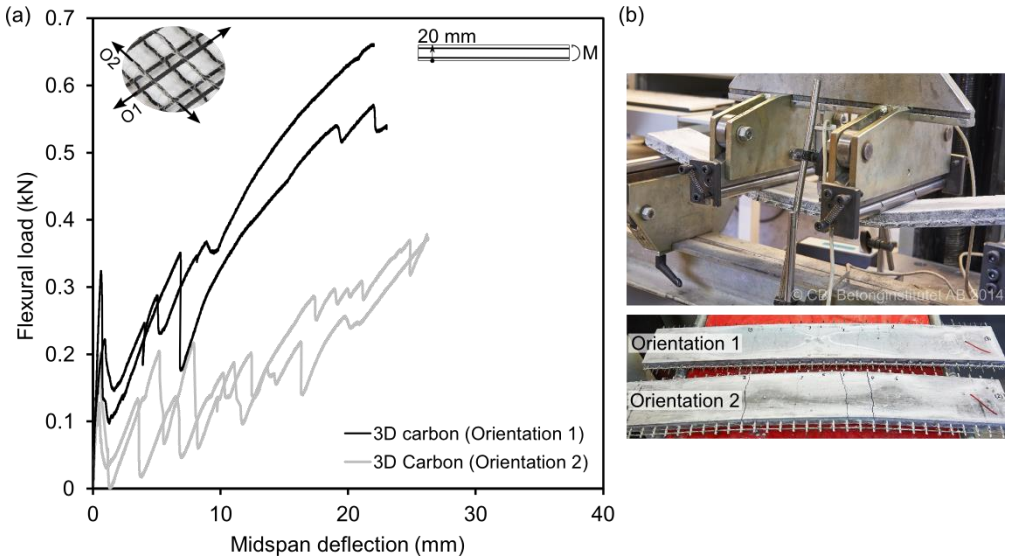

Figure 5.9 Test series 2A: Flexural load versus midspan deflection for 3D carbon textiles (a) and tested specimens (b).

To further improve the bond of the 2D carbon textile, the surface of this textile was modified as previously mentioned in *Test series 2B*. The epoxy coating was found to significantly enhance the flexural behaviour of the composite (≈ 400 % increase in maximum flexural load), while minimal improvements were noted for the *polymer* coating, as depicted in Figure 5.10. Through optical microscopy, it could be detected that the epoxy and *polymer* coatings were concentrated on the outer filaments and hardly penetrated the depth of the dense array of carbon filaments. Additionally, it is thought that the curing conditions of the specimens greatly affected the efficacy of the applied coatings, particularly SBR and the additional *polymer*. Curing in air has been reported to improve the bond between the textile and matrix (Colombo et al., 2013), but this topic is not further discussed in this scope of work. Furthermore, the crack development and spacing pertaining to the 2D carbon textile variants were compared in Figure 5.11. The epoxy coating greatly impacted the crack development in

comparison to the *polymer* which had no noticeable improvement. Pertinent findings derived from these results are further summarized in Table 5.5, along with results from *Test series 3*.

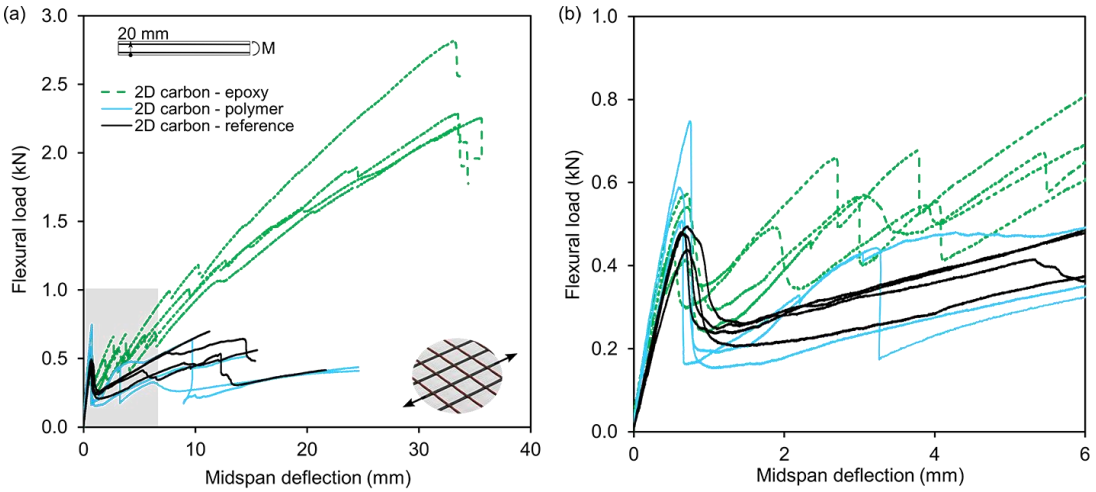

Figure 5.10 *Test series 2B: Flexural load versus midspan deflection for modified 2D carbon textiles versus reference (a) and enlargement of grey zone (b).*

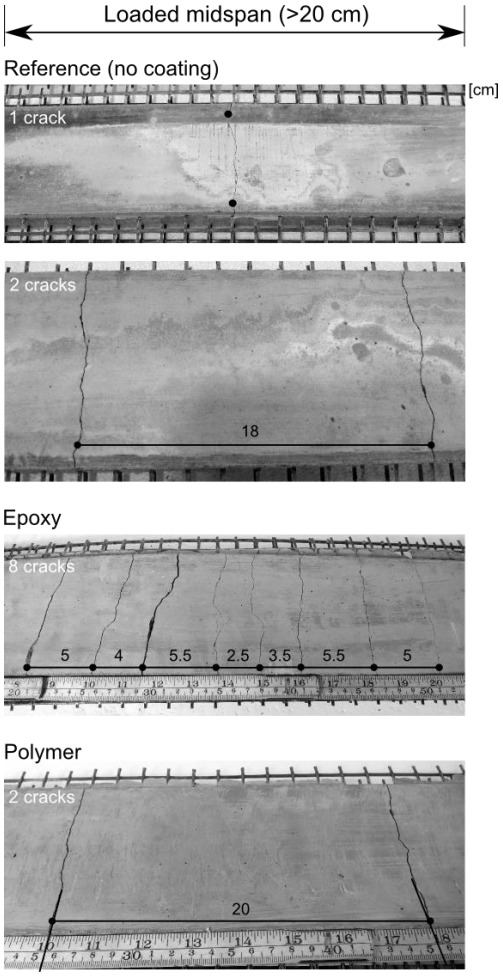

Figure 5.11 *Test series 2A & 2B: Crack spacing comparison of HPC reinforced by 2D carbon textiles with varying coatings.*

Results: Test series 3

The four-point bending results for *Test series 3* are depicted in this section. The flexural load versus midspan deflection curves are illustrated in Figure 5.12. The textile reinforcement did not reach its tensile strength in these tests, as the tests were terminated according to either large deflection, bending cracks propagating through entire specimen thickness or effects of poor bond, i.e. pull-out of reinforcement without further crack development. The poor results observed for the RPC 2D carbon grids are thought to result from a low reinforcement ratio in combination with a poor bond. In such a brittle and high strength concrete matrix, the addition of 1 vol-% short carbon fibres (Tenax® A HT C124, 12 mm) as well as the surface modification using a *polymer* coating greatly improved the bond (through crack-bridging) and toughness of the material. These applied improvements however introduced large variability within the results due to the lack of control with the fibre dispersion and uneven coating surface. These presented experimental results are further analysed and compared to those of *Test series 2* in Table 5.5.

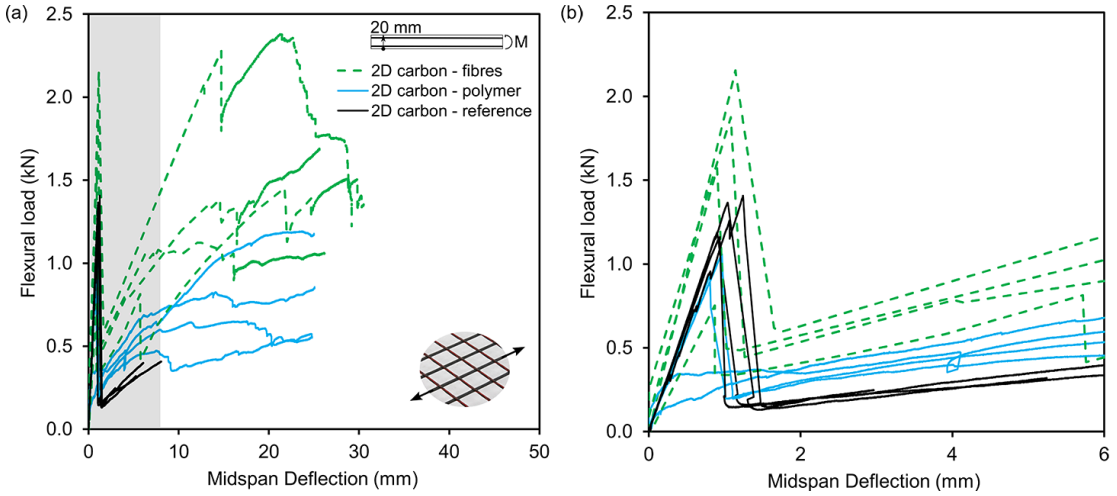

Figure 5.12 *Test series 3: Flexural load versus midspan deflection for RPC with 2D carbon textiles, 2D carbon textiles & short carbon fibres (1 vol-%), and modified 2D carbon textiles (a) and enlargement of grey zone (b).*

Comparison: Test series 2 and 3

The flexural results shown in Table 5.5 can be directly compared for specimens having the same concrete mix and reinforcement amount. In addition, similar to that presented for *Test series 1*, the apparent flexural strength was computed here for comparison purposes. In general, the apparent flexural strength values were greater for the RPC specimens (*Test series 3*) mainly due to a higher first cracking load/maximum load resulting from the higher concrete tensile strength. The reference 2D carbon grid proved to perform similarly in both HPC and RPC slabs, whereby surface modifications or the addition of short fibres were shown to improve the flexural behaviour.

Table 5.5 Summary of Test series 2 and 3 presented as average values (std dev).

Concrete matrix	Reinforcement arrangement	No. Cracks	First cracking flexural load, F_{crack} (kN)	Maximum flexural load, F_u (kN)	Apparent flexural strength, σ_u (Pa)	Deformation at F_u, δ_u (mm)
HPC	1 layer 3D Carbon (*O1*)	4-6	0.3 (0.1)	0.7 (0.1)	4.1 (1.1)	24.3 (3.3)
	Comment:	-Lower first cracking load & improved post-crack behaviour -Deformation hardening & improved crack development -Lower stress level (waviness/larger reinforcement area)				
	1 layer 3D Carbon (*O2*)	6-10	0.2 (0.1)	0.4 (0.0)	2.4 (0.8)	26.3 (0.1)
	Comment:	-Lower first cracking load & improved post-crack behaviour -Improved crack development -Lower stress level (waviness/larger reinforcement area)				
	2 layers 2D Carbon (Reference)	1	0.5 (0.0)	0.6 (0.1)	7.1 (0.4)	13.3 (1.9)
	Comment:	-Poor bond causing large pull-out and minimal crack development				
	2 layers 2D Carbon + epoxy	6-8	0.5 (0.1)	2.4 (0.3)	35.9 (4.3)	33.4 (1.4)
	Comment:	-Deformation hardening -Most ductile -Ultimate load increase by ≈ 400 %				
	2 layers 2D Carbon + polymer	1-2	0.6 (0.1)	0.6 (0.1)	9.2 (1.8)	0.7 (0.1)
	Comment:	-Poor bond causing large pull-out -Higher first cracking load -No load increase after first cracking				
RPC	2 layers 2D Carbon (Reference)	1	1.3 (0.1)	1.3 (0.1)	19.2 (1.9)	1.0 (0.2)
	Comment:	-Poor bond causing large pull-out -Low reinforcement ratio				
	2 layers 2D Carbon + short fibres (1 vol-%)	1-2	1.6 (0.6)	1.8 (0.4)	27.5 (6.0)	13.0(14.2)
	Comment:	-Higher first cracking load & improved post-crack behaviour -Added crack-bridging effect -Increased toughness -Large variability				
	2 layers 2D Carbon + polymer	1-2	0.8 (0.3)	1.0 (0.1)	15.1 (2.2)	12.6(13.5)
	Comment:	-Lower first cracking load & improved post-crack behaviour -Increased toughness -Large variability				

5.3 FE-results and discussion

It was of key interest to investigate if the material properties (Section 2) and experimental bond behaviour (Section 4) could be linked to the *global* behaviour of a TRC specimen under bending stresses through finite element analysis (FEA) (**Objective 3**). For that reason, a 2D macro-scale FE-model of a TRC one-way slab based on the carbon textile reinforced specimens presented in *Test Series 1B* (Section 5.2.1 and **Paper III**) was developed using the commercial software DIANA (DIsplacement ANAlyser) with pre- and post-processor Midas FX+.

5.3.1 Model parameters

The complete geometry of the specimen and experimental setup were modelled in order to be able to yield a crack development pattern comparable to the experimental results (see Figure 5.13). An element size of 2.5 x 2.5 mm was selected for the entire geometry based on work conducted in Pettersson et al. (2014). The element types prescribed for the individual components are summarized in **Paper III** and additional fundamental details pertaining to the element types can be found in TNO DIANA (2014). The point load was applied as a fixed deformation and equilibrium was solved using secant tangent iterations which yielded the most stable solution. The self-weight was assumed to be negligible in the analysis as it was found to have a minor influence on the overall results such that it's bending moment corresponded to 2 % of the total bending moment of the applied load. Deformation controlled loading was applied so that a more accurate computation of the behaviour could be achieved especially during the cracking state.

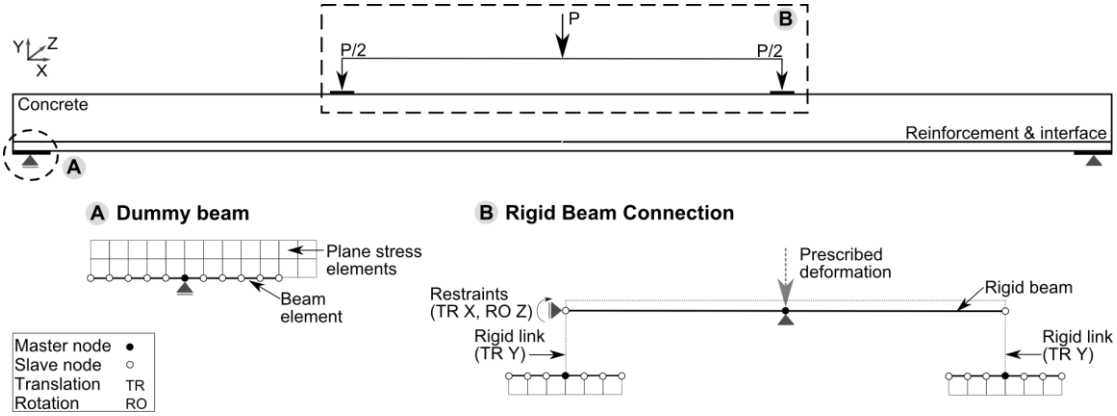

*Figure 5.13 Idealized FE-model and special features (**Paper III**).*

5.3.2 Material models

Textile reinforcement

A macroscale 2D model motivates the need for the idealization of smeared and homogenized material components and properties; as such the textile reinforcement mesh was simplified as a *monolithic bar* (see Figure 5.14). The yarns in the longitudinal direction of the specimen which are predominantly loaded under one-way bending were bundled in a monolithic yarn similar to what has been applied in other modelling approaches (Holler et al., 2004, Azzam et al., 2011, Williams Portal et al., 2013, Williams Portal et al., 2014d). A linear-elastic stress-strain law with no limiting tensile strength was assigned to the monolithic bar (refer to Section 2.2.3). The tensile properties of the carbon textile reinforcement in *Test Series 1* were not explicitly quantified. Some degree of material data was available from the producer which were related to the mesh properties as provided in **Paper III**. Alternatively, it could also be possible to characterize a more representative tensile behaviour of the textile reinforcement embedded in the matrix using a stress-strain curve obtained through uniaxial tensile tests of the TRC combination in question (see Section 6). One bond interface between the monolithic bar and concrete matrix was defined, such that the relative displacement between external and internal filaments was assumed to be negligible. Modelling with two interfaces between the external and internal filaments

have indicated insignificant differences when compared to modelling with one bond interface (Holler et al., 2004). Nonetheless, the iterative and time consuming methods required to quantify the relative displacement between the filaments would likely be more appropriate for more detailed modelling scales, i.e. meso- and microscales. Moreover, the local bond stress-slip relationship presented in Section 4.2.2 was assigned to describe this bond behaviour. The contact perimeter corresponding to each individual yarn, C_f, was summed to correspond to a so-called equivalent contact perimeter of the monolithic bar, $C_{t,l}$; the same method was applied for the equivalent area, $A_{t,l}$.

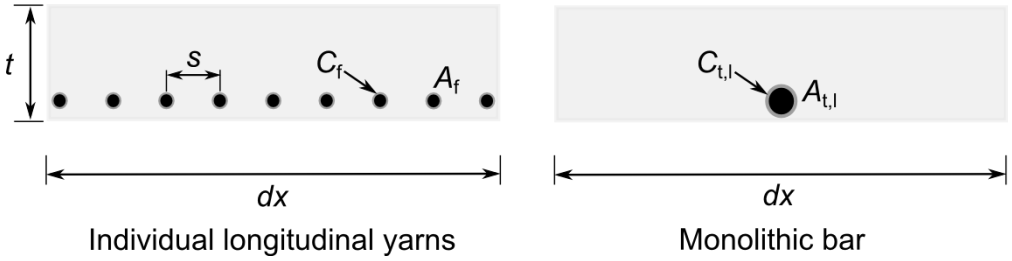

Figure 5.14 Depiction of the monolithic bar assumption (t is the thickness of the cross-section and s is the c/c yarn spacing).

Concrete

The concrete matrix was modelled as a homogeneous material using material properties presented in **Paper III** and described in Section 2.1. In essence, the compressive strength and tensile splitting strength of the corresponding concrete were quantified and the fracture energy and modulus of elasticity were estimated using fib Model Code 2010 (2013). The mechanical behaviour of the concrete material was assumed to follow typical curves for compressive and tensile behaviours provided by TNO DIANA (2014). The tension softening and compressive behaviours of concrete were incorporated in the model by means of a non-linear Hordijk tension softening model and Thorenfeldt compression curve. The Thorenfeldt curve is based on the compressive strength obtained from 300 mm long cylinder specimens (Section 2.1.2), such that correction was found to be necessary after the peak compressive strength, f_c, to take into consideration the size effect as a result of the selection of smaller element sizes in the model as suggested by Zandi Hanjari (2008). This modification allowed for the localization of strains in single element rows. In tension, a crack band width equal to the element size (2.5 mm) was chosen because the cracks generally localized in single element rows. A total strain based crack model with rotating crack was defined for the concrete elements, wherein the crack direction continuously rotates according to the principal directions of the strain vector (TNO DIANA, 2014). Other features that were taken into consideration were the *voids* in the concrete that were occupied by the lateral cross-yarns of the textile mesh in reality. As such, the tensile strength and fracture energy were reduced at these localized concrete elements. The reduction was calculated based on an estimated loss of concrete area at the lateral roving locations. Reducing the tensile strength and fracture energy could also be justified by the fact that stress concentrations and crack formation typically occur at the lateral yarn locations. By introducing this feature in the model, crack initiation was found to take place at these locations which approximately corresponded to the experimental results.

5.3.3 Results

A reasonable agreement between the numerical and experimental results was obtained in terms of crack development, deflections, maximum load, and failure mode, as summarized in Table 5.6 and shown in Figure 5.15. The analyses resulted in a slight over prediction of the ultimate capacity and indicated that failure was governed by bond which was ambiguous in the four-point bending tests.

*Table 5.6 Experimental versus FE-analysis results (**Paper III**).*

Results	Avg experimental values (Std dev)	FE-analysis	Percentage error (%)
Flexural load at first cracking, F_{cr} (kN)	4.34 (0.09)	4.01	-7
Midspan deflection at F_{cr}, δ_{cr} (mm)	0.85 (0.05)	0.91	6
Ultimate flexural load, F_u (kN)	8.54 (0.12)	9.64	13
Midspan deflection at F_u, δ_u (mm)	22.61 (0.72)	28.18	25

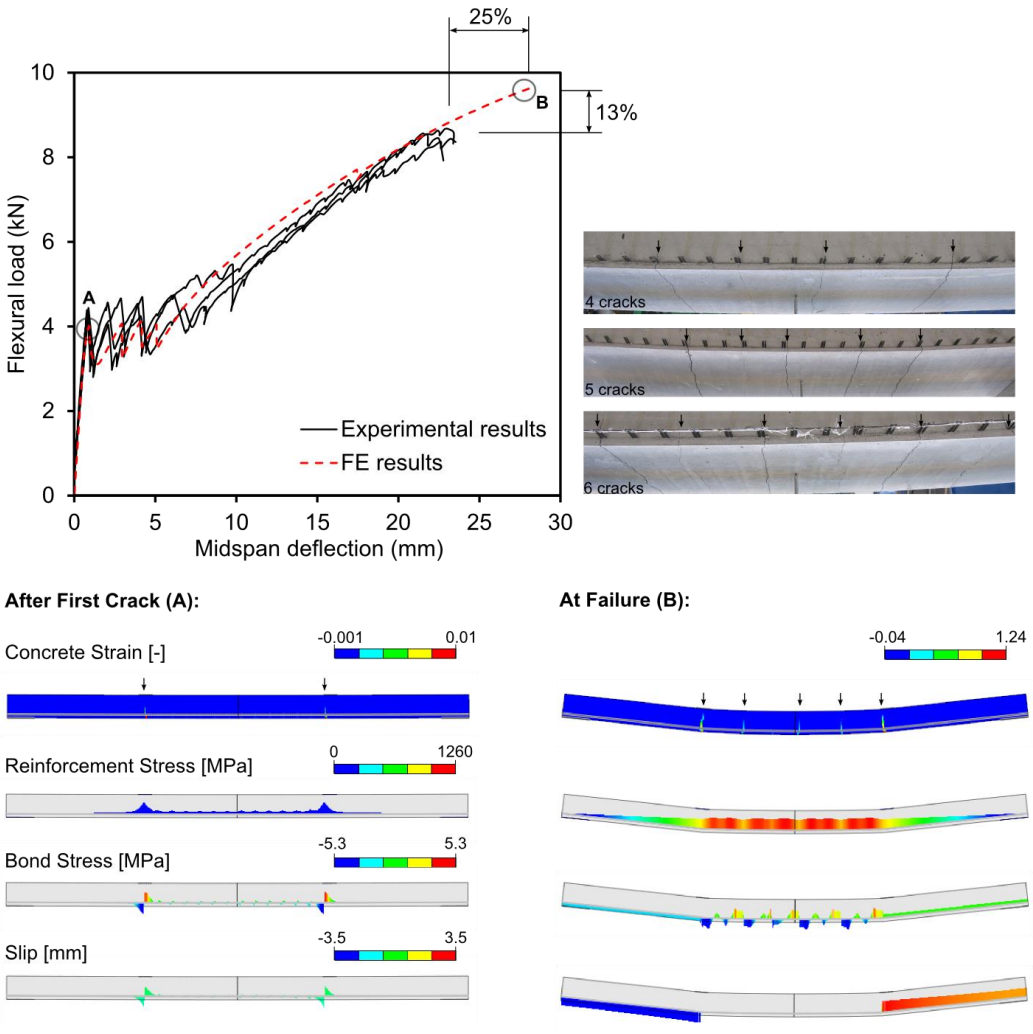

*Figure 5.15 Comparison of experimental and FE-results along with contour plots after first cracking and at failure (**Paper III**).*

5.4 Summary

The flexural behaviour of TRC specimens reinforced by available textile reinforcement was investigated using four-point bending (**Objective 1**, **Paper III**). The principle outcomes and associated commentary are:

> The 80 mm rectangular TRC specimens with the *Medium* carbon textiles resulted in the highest flexural load and crack development (*Test series 1A*).
> The 50 mm rectangular TRC specimens with the carbon textiles proved to have superior flexural behaviour (*Test series 1B*).
    - The reinforcement ratio of the other investigated reinforcement materials should be increased to be comparable to the specimens reinforced by carbon.
> Splicing of the reinforcement mesh/grid was effectively investigated for certain material combinations through four-point bending (*Test series 1B*).
    - The overlap length should be individually defined based on the applied reinforcement grid.
    - Pull-out tests could also be applied to identify an adequate overlap length.
> Casting the specimens while fastening the reinforcement mesh/grid to the formwork ensured accurate placement of the reinforcement.
    - This method is also presumed to have reduced the initial waviness of the reinforcement mesh/grid.

The additional experimental findings presented for thin TRC specimens using high performance concretes and 2D and 3D carbon textiles depicted possible material improvements and further potential applications of TRC. The apparent benefits of including additional surface coatings, short fibres and the effect of surface unevenness were discussed in this work. Overall it was observed that the interfacial bond between the matrix and reinforcement had a governing effect on the flexural behaviour, while the reinforcement ratio had a secondary effect. Further evaluations related to all test series could include: the influence of the specimen size, increased reinforcement ratio, casting method, curing conditions, and measurement technique.

An approach linking flexural tests of TRC specimens to simplified numerical models was presented. The implementation of experimental input data obtained from both *material* and *interaction* levels in macro-scale modelling was shown to be a promising approach in terms of comparing numerical results to experimental results on a *global* level, whereby improved insights in the failure mechanism could be obtained (**Objective 2, Paper III**). The main findings and suggested developments are:

> The developed non-linear FE-model can be used to understand the failure mechanism which is otherwise ambiguous to capture experimentally.
> Simplified FE-models such as presented, which are calibrated by experimental data, can be useful for preliminary design.
> The applied bond behaviour (*interaction* level – Section 4) is a critical input parameter to be able to capture the correct crack development, load-deflection relationship and failure mechanism.
    - Inclusion of bond of internal filaments could likely further improve the results, but this feature is challenging to accurately quantify and could be computationally demanding.
> The characterization of detailed input data on the *material* level (Section 2) is also paramount in order to minimize errors in numerical analyses.

6 Global Level: Tensile Behaviour

The tensile behaviour of TRC as a composite was characterized experimentally using uniaxial tensile tests. This level of investigation constitutes the *global* level of *structural performance* in this work as previously stated in Section 1.2 (**Objective 1**). The study focused on TRC specimens made of 2D and 3D carbon textiles embedded in a high-performance concrete (HPC) matrix, similar to that covered in Section 5.2.2. Digital image correlation (DIC) was utilized to evaluate the deformations and crack development over the course of testing. These presented findings are in addition to the papers included in this thesis.

Textile reinforcement is primarily incorporated in a matrix to carry the tensile loads of a structure. For that reason, the composite behaviour of TRC can be rightly captured by means of its tensile behaviour. The tensile behaviour of TRC is typically measured using uniaxial tensile tests. According to Colombo et al. (2013), the tensile behaviour characterized by means of uniaxial tensile tests can be affected by factors such as reinforcement amount and geometry, reinforcement position, curing conditions, displacement rate and size effect. The test setup, end clamping configuration and specimen geometry have also been shown to influence the experimental results (Hartig et al., 2012). The uniaxial tensile test arrangement for TRC has been extensively researched such that guidelines are provided in the draft recommendation from RILEM TC 232-TDT (Brameshuber et al., 2010b).

6.1 Overview

A parallel is drawn between the tensile behaviours of concrete/mortar and textile reinforced concrete in Figure 6.1 to highlight the possible enhancements of using TRC. It is clear that the brittle behaviour of the concrete/mortar after first cracking is eliminated with TRC allowing for the formation of multiple cracks and so-called *strain hardening*. These behavioural stages are similar to that previously described for the flexural behaviour in Section 5 and will not be further explained. A differing aspect is such that the tensile strength of the textile is typically compared to the stress-strain behaviour of TRC to observe the strain hardening effect as well as the effectivity of the interfacial bond, as emphasized in Figure 6.2. Also, it is interesting to note the positive effect of including short fibres on the tensile behaviour (see Figure 6.1). Improvements can include enhanced bond and load transfer to the reinforcement (marked by smoothness of curve), and increased tensile strength and elongation. Similar findings were also shown in Section 5 related to the flexural behaviour.

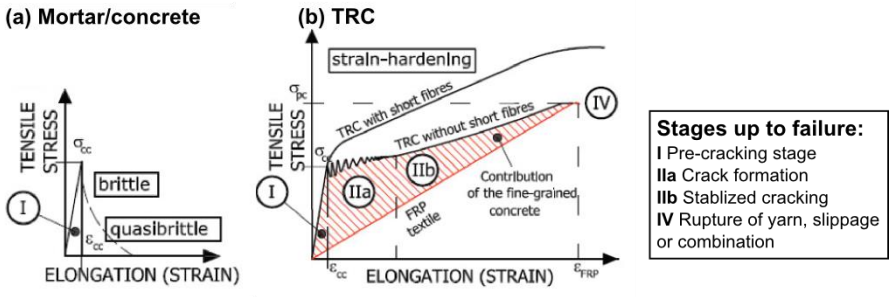

Figure 6.1 The expected tensile behaviour of a conventional mortar and concrete (a) and textile reinforced concrete (b) [Adopted from (Orosz, 2013) and (Brameshuber, 2006)].

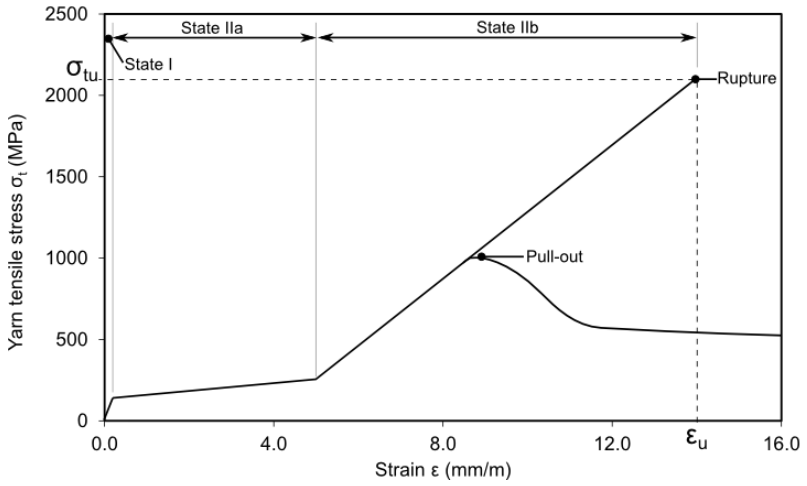

Figure 6.2 Idealized typical stress-strain relationship for TRC indicating rupture and anchorage failure [Adopted from (Lorenz et al., 2013)]

6.2 Experimental work

The tensile behaviour of TRC as a composite was characterized by means of uniaxial tensile tests based on the relevant section of the draft recommendation from RILEM TC 232-TDT (Brameshuber et al., 2010b). In this recommendation, there are two types of tests presented, namely dumbbell and rectangular, wherein the latter type was applied in this work. This type of specimen was primarily selected in order to make use of the same formwork applied for the flexural test specimens (Section 5). As such, the specimens were 700 x 100 x 20 mm and consisted of HPC (**Appendix A**) and two layers of carbon textile reinforcement grid. The 2D and 3D carbon textiles applied in the flexural tests, *Test series 2* and *3*, were also included in these tests (see Figure 5.7, Section 5). The tensile strength based on the orientation, denoted as *Orientation 1* and *2 (O1 and O2)*, of the 3D carbon textiles was tested. As previously depicted in Figure 5.7, *O1* consists of the weft yarns being placed longitudinally and rotated laterally in *O2*. Details pertaining to the tested specimens are listed in Table 6.1. The specimens were cured in water and stored in standard laboratory conditions several days prior to testing at 28 days to allow for surface preparations. The effect of the curing method is known to have a discernible influence on the tensile behaviour of TRC (Colombo et al., 2013), yet this was not further investigated in this scope of work.

Table 6.1 Tensile test specimen details.

Concrete	No. specimens	Reinforcement type	Average no. longitudinal yarns (both layers)	Cross-sectional area of longitudinal reinforcement, $A_{t,l}$ (mm^2)	Reinforcement ratio, ρ (%)
HPC	4	2 layers 2D carbon textile	12	10.6	0.53
	2	1 layer 3D carbon textile (Orientation 1- O1)	9	7.9	0.40
	2	1 layer 3D carbon textile (Orientation 2- O2)	9	7.9	0.40

6.2.1 Test setup

The uniaxial tensile tests were carried out in an electro-mechanical universal testing machine (Sintech 20D). Specimens were loaded under displacement control, while the load and machine displacement were recorded in a data acquisition system (sampling rate of 10 Hz). The ends of the specimens were clamped between two stiff steel plates (see Figure 6.3) which transfer the load to the specimen by friction. The applied clamp pressure and contact area were chosen to prevent slippage between the clamp and specimen. Additional thin neoprene rubber sheets were placed in the contact areas to avoid local stress concentrations. As depicted in Figure 6.3, the specimens and clamping devices were aligned in a frame to ensure centric loading. Thereafter, the clamps were connected to the test machine via hinged connections and the frame was removed. Moreover, metal plates painted with a speckle pattern were attached on either side of the clamping devices as reference points to measure the average deformation of the specimen related to the measuring range (see Figure 6.4). Two virtual extensometers were defined according to these reference points in a digital image correlation (DIC) system (refer to Section 6.3).

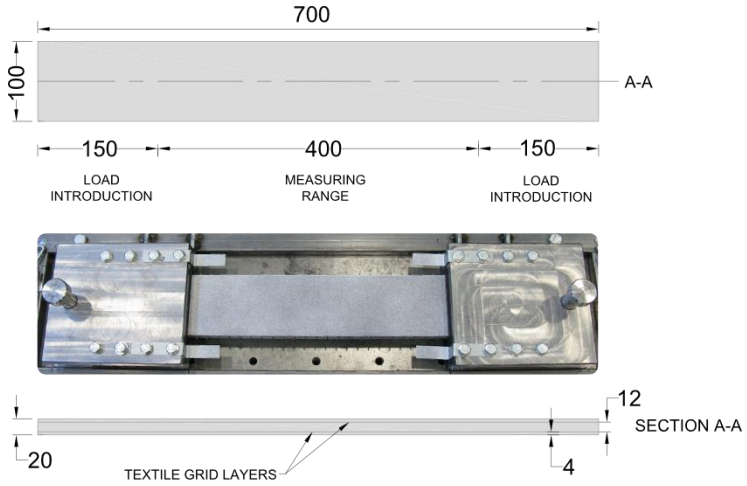

Figure 6.3 Overview of the specimen geometry and end clamp detail.

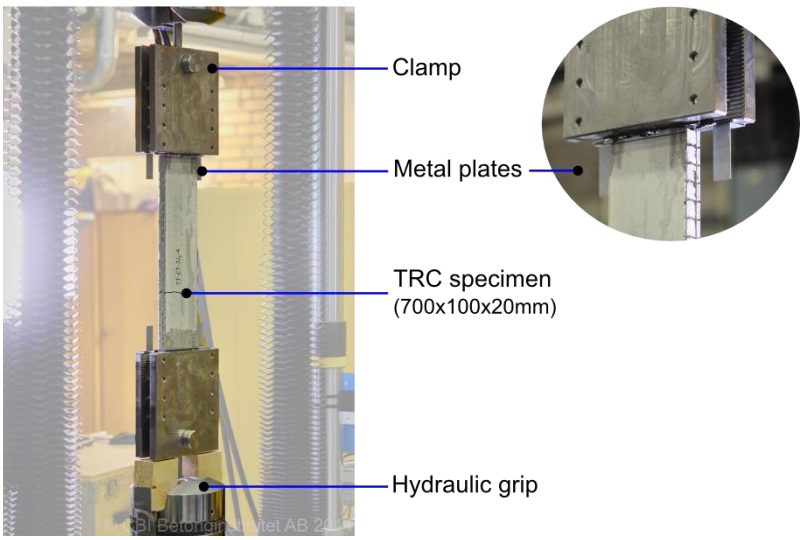

Figure 6.4 Tensile test setup and special features.

6.2.2 Results

The general expressions which were applied in this discussion are based on Brameshuber et al. (2010b). The composite stress σ_c and textile reinforcement stress, σ_t, at a given uniaxial force can be calculated based on Eq. (6.1) and (6.2), respectively. These equations can also be modified to calculate the ultimate strength of composite, σ_{cu}, or the textile reinforcement, σ_{tu}, by introducing the ultimate uniaxial force, F_u.

$$\sigma_c = \frac{F}{A_c} \quad \text{Eq. (6.1)}$$

where F is the uniaxial tensile force (N), and A_c is the concrete gross cross-sectional area, i.e. width multiplied by height (mm^2).

$$\sigma_t = \frac{F}{A_{t,l}} \quad \text{Eq. (6.2)}$$

where F is the uniaxial tensile force (N), and $A_{t,l}$ is the cross-sectional area of the longitudinal reinforcement being tested (mm^2) (see, Section 5.2.1)

The reinforcement did not reach its tensile strength in any case and testing could have continued, yet these tests were terminated due to anchorage failure marked by increased pull-out of the reinforcement seen via the DIC results (see Section 6.3). It is interesting to note that the presented tensile test results primarily differed from the four-point bending test (Section 5.2.2) because the applied pressure of the clamping devices increases the bond strength at the ends. In effect, the transfer length becomes reduced allowing for, in general, additional more closely spaced cracks and reduced crack widths.

In Section 2.2, the so-called successive loss of tensile strength from filament to composite level was discussed. This loss of strength or rather efficiency of the reinforcement in the composite form can be captured via uniaxial tensile tests. The so-called coefficient of efficiency (COE) is applied in this work to quantify the reinforcement efficiency. COE is the ratio between the maximum tensile strength of the reinforcement in the composite and the tensile strength of the yarn (Hegger et al., 2008). Alternatively, this coefficient can be calculated by dividing the maximum load of the composite by the maximum tensile force corresponding to the total reinforcement quantity acting in uniaxial tension (Colombo et al., 2013). According to work by Colombo et al. (2013), a ratio above unity signifies that the interaction between the reinforcement and matrix could lead to a tension stiffening effect, while a ratio inferior to unity indicates a weak bond strength. In this thesis, the COE was calculated using the average maximum tensile force of the carbon yarn measured to be 1.88 kN leading to a tensile strength of 2132 MPa (Section 2.2, **Paper I**).

The direct test results, load versus global deformation curves, are depicted in Figure 6.5 and Figure 6.6, while relevant experimental findings are tabulated in Table 6.2. The tensile stress at first crack corresponding to the composite, $\sigma_{c,1}$, was rather similar for all specimens, yet slightly lower for the 3D carbon reinforced panels probably because the actual amount of reinforcement area including the spacer is larger. When comparing the reinforcement stresses at first cracking, $\sigma_{t,1}$, it can be seen that higher stresses are developed for the 2D and 3D carbon textiles (*O1*). In the case of *O2*, the PET fibres interlaced around the warp yarns as well as the initial waviness of the warp yarns are thought to cause a delayed activation of the loaded yarns. It should be noted that the area of the PET fibres was assumed to be negligible

when computing the reinforcement stress. The panels reinforced by the 2D carbon textiles were able to sustain nearly the same average maximum tensile load as the samples reinforced by 3D carbon textiles. The major differences noted, however, are such that the crack development was minimal and crack openings were much larger for the 2D carbon specimens. The cause for this differentiating behaviour is the weaker bond between the reinforcement and the matrix (COE 0.53). This resulted in significantly larger pull-out of the yarns observed at the crack openings thus leading to larger displacement. The maximum tensile stress of the reinforcement, σ_{tu}, was also lower for the panels reinforced by 2D carbon textiles. Moreover, the large variability in the results for these specimens can be attributed to the fact that the amount of longitudinal yarns slightly differed within the specimen cross-section. As for the 3D carbon reinforced specimens, multiple and micro-cracking was observed particularly in the case of *O1*. The roughness of the PET fibres interlaced around the warp yarns and the spacer appears to generally increase the bond in comparison to the two individual layers of 2D carbon textile (COE 0.69-0.70). In the case of *O1*, the warp yarns placed laterally in the cross-section significantly and positively influence the crack development and resulting displacement. As for *O2*, an inferior crack development, similar to the 2D carbon textile, was noted which could possibly be owing to the smoothness of the weft yarns placed laterally in this case. This observed behaviour for *O2* greatly differs compared to the results in flexure (Section 5.2.2), where multiple cracks were noted i.e. 1-2 compared to 6-10 cracks. To explain this major difference, it is thought that the curvature of the specimen in flexure helps to increase the bond for small slips by activating the lateral cross-yarns of the top textile layer, i.e. the smooth weft yarns, which is not the case in the uniaxial tensile test. As aforementioned in Section 5.2.2, there is a shift in the spacing between the weft yarns and if both layers are so-to-say equally activated, additional stress concentrations could be introduced in the cross-section which in turn induces further crack formation.

Overall, it could be worth attempting to further improve the interfacial bond of these given TRC combinations to yield more favourable tensile behaviour. Methods to improve the bond were previously covered in Section 5 and at the beginning of Section 6. Additionally, the available anchorage length in the test configuration could be increased with the aim of reaching the tensile strength of the textile yarns. Further, to avoid cracking from occurring in the end anchorage, which was not discussed here but is in fact an underlying problem in this test, the ends could be additionally reinforced or a notch could be introduced at the centre of the specimen.

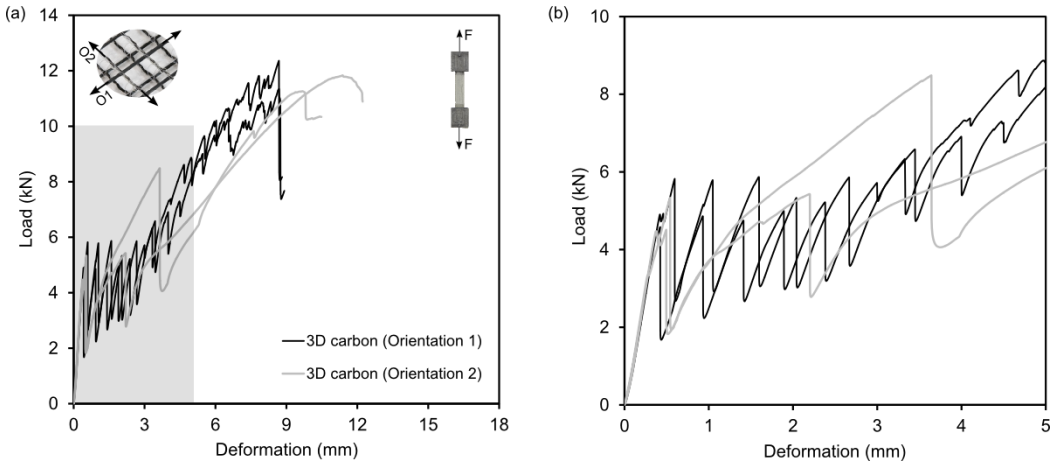

Figure 6.5 Load versus global deformation for TRC specimens reinforced by 3D carbon textiles (O1, O2): deformation of 0-18 mm (a) and 0-5 mm (b).

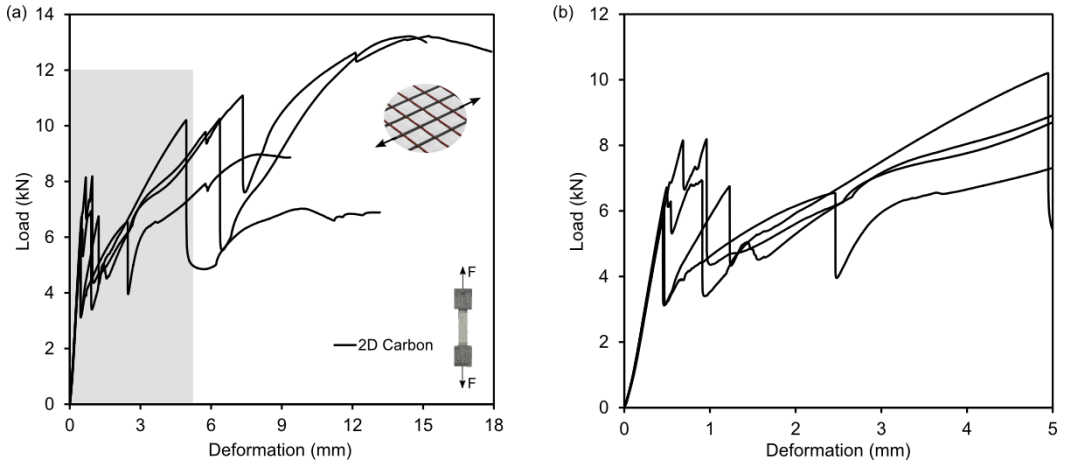

Figure 6.6 *Load versus global deformation for TRC specimens reinforced by 2D carbon textiles: deformation of 0-18 mm (a) and 0-5 mm (b).*

Table 6.2 *Summary of tensile test result presented as average values (std dev).*

Parameter	Reinforcement		
	3D Carbon (O1)	3D Carbon (O2)	2D Carbon (reference)
No. yarns	9	9	10-12
No. cracks	9-12	2	2-3
Cross-sectional area of longitudinal reinforcement, $A_{t,l}$ (mm^2)	7.9 (0.0)	7.9 (0.0)	10.1 (0.9)
Cross-sectional area of specimen, A_c (mm^2)	2006.2 (125.9)	2006.2 (125.9)	2028.0 (13.5)
First cracking load, $F_{cr,l}$ (kN)	5.6 (0.3)	4.5 (0.1)	6.7 (1.0)
Tensile stress at first crack – composite, $\sigma_{c,l}$ (MPa)	2.6 (0.4)	2.5 (0.4)	3.3 (0.5)
Tensile stress at first crack – reinforcement, $\sigma_{t,l}$ (MPa)	702.4 (41.2)	572.9 (7.7)	665.8 (118.0)
Maximum load, F_u (kN)	11.8 (0.8)	11.6 (0.3)	11.4 (2.2)
Displacement at F_u, δ_u (mm)	8.7 (0.0)	10.5 (1.2)	10.7 (5.0)
Maximum tensile stress – composite, σ_{cu} (MPa)	6.1 (0.1)	5.6 (0.3)	5.6 (1.1)
Maximum tensile stress – reinforcement, σ_{tu} (MPa)	1491.7 (98.5)	1463.0 (43.4)	1128.1 (190.7)
F_u /yarn (kN)	1.3 (0.1)	1.3 (0.0)	1.0 (0.2)
Coefficient of efficiency, *COE* (-)	0.70 (0.05)	0.69 (0.02)	0.53 (0.09)
Overall behaviour	-Multiple and micro-cracking -Superior bond to 3D carbon textile (O2) and 2D carbon textiles	-Cracks in or near support regions -Similar crack development to 2D carbon textiles -Superior bond to 2D carbon textiles	-Cracks in or near support regions -Weakest bond according to COE

6.2.3 Correlation to flexural behaviour

The COE calculated based on tensile test results presented in Section 6.2.2 were applied to calculate the bending moment resistance of the identical TRC specimens tested in flexure (*Test series 2A*, Section 5.2.2). The average bending moment resistance from experiments, M_{Rd}, and the estimated bending moment resistance, $M_{\mathrm{Rd,e}}$, can be calculated according to Eq. (6.3) and (6.4), respectively.

$$M_{Rd} = F_u \cdot \frac{L}{6} \qquad \text{Eq. (6.3)}$$

where F_u is the maximum flexural load (kN) and L is the support span (600 mm) from Section 5.2.2. This equation is based on the bending moment diagram from four-point bending test.

$$M_{Rd,e} = 0.9d \cdot COE \cdot f_t \cdot A_{t,l} \qquad \text{Eq. (6.4)}$$

where d is the effective depth (only including layer in tensile zone) (mm), COE is the coefficient of efficiency from tensile tests (-), f_t is the tensile strength of a yarn (MPa), and $A_{t,l}$ is the cross-sectional area of longitudinal yarns in the layer in the tensile zone (mm^2).

It is thought that the calculated differences between the average experimental and estimated values shown in Table 6.3 can be primarily attributed to the differing available anchorage length and the clamping featured in the uniaxial tensile test. These factors, in turn, overestimate the tensile capacity and COE compared to the flexural tests. It is also important to note that there is a larger difference calculated for the specimens with the 3D carbon textile in the orientation *O2*. The tensile behaviour of this configuration was marked by minimal crack formation, while the flexural behaviour differed greatly as previously discussed in Sections 5.2.2 and 6.2.2. It is to say that there was an improved bond in flexure for small slips but better end anchorage in the tensile test setup. Furthermore, adding a coefficient to reflect this difference could be an option as suggested in e.g. Hegger et al. (2008). However, if the failure mode in both the flexural and tensile tests would have been rupture, this difference would likely be minimized. These calculations however do illustrate the possible correlation between the tensile and flexural behaviours of TRC.

Table 6.3 Comparison of the analytical bending moment resistance based on COE and the experimental bending capacity.

Parameter	Reinforcement		
	3D Carbon (O1)	3D Carbon (O2)	2D Carbon (reference)
Average bending moment resistance, M_{Rd} (N·m), (std dev) (from Section 5.2.2)	67.1 (14.1)	39.6 (1.5)	61.0 (7.5)
COE (-)	0.70	0.69	0.53
Estimated bending moment resistance, $M_{\mathrm{Rd,e}}$ (N·m)	75.6	74.6	85.9
Difference (%)	-11	-47	-29

6.3 Evaluation using Digital Image Correlation (DIC)

During tensile testing, deformations and crack development were recorded on one side of each specimen using an optical full-field deformation measurement system ARAMIS^{TM} 12M by GOM. This system makes use of Digital Image Correlation (DIC) technique with a stereoscopic camera setup, i.e. two charge-coupled device (CCD)-cameras with 12-megapixel resolution (Figure 6.7). DIC is an accurate non-contact measurement technique which has been proven to be an applicable method for the crack opening measurement of concrete structures (Corr et al., 2007, McCormick et al., 2010, Skarzynski et al., 2013).This technique involves the sequential mapping of the deformation of a defined speckled surface area using a series of digital images captured during loading. It is to say that displacements are calculated by mapping the same pixels between a discretized subset of pixels from an undeformed reference and deformed digital image as per Figure 6.8 (Pan et al., 2009). The quality of the applied random speckled pattern can influence the results, as it acts as the deformation tracer from image to image. For additional details related to the underlying calculations involved in DIC, refer to e.g. Pan et al. (2009).

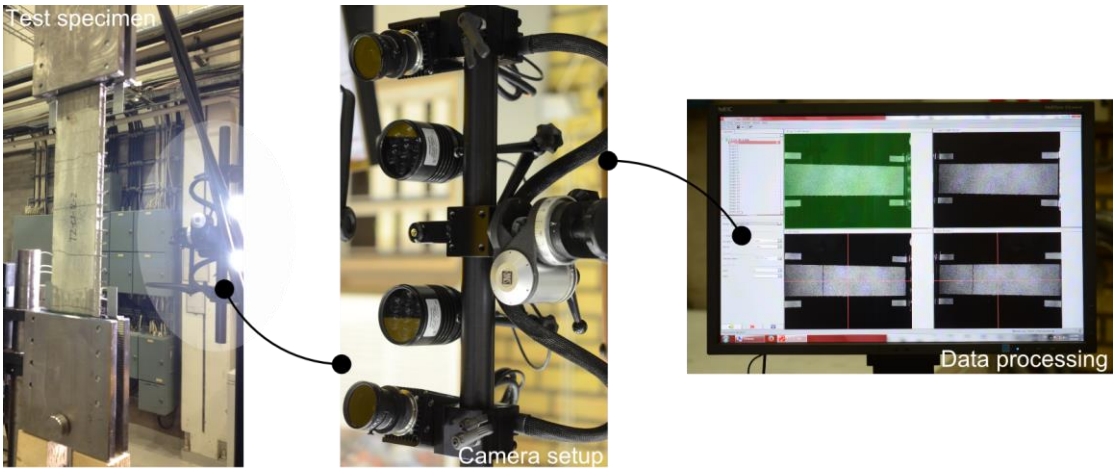

Figure 6.7 Setup of DIC method for tensile tests.

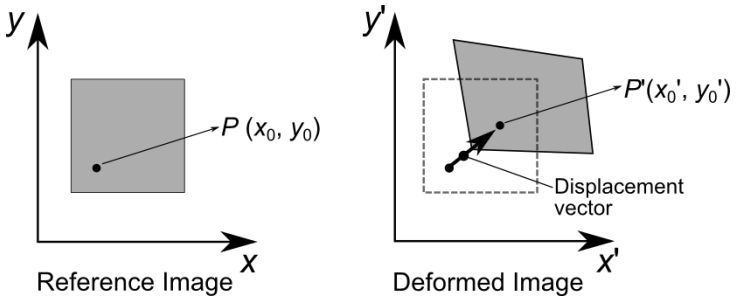

Figure 6.8 Fundamental concept of DIC [Adopted from (Pan et al., 2009)].

Within the speckled region of the TRC specimen under testing, the following features were investigated using DIC in this work (see Figure 6.9):

> Virtual extensometers were defined at relevant reference points.
  - Strains within a defined measurement area, i.e. extensometer 1 and 2, (Figure 6.10) and successive crack opening at a defined location could be evaluated (Figure 6.11).

> Cross-sectional cut was defined along the length of the specimen.
  - Major strain versus cross-sectional length could be plotted which illustrates the successive formation and location of cracks by major strain peaks (Figure 6.12).

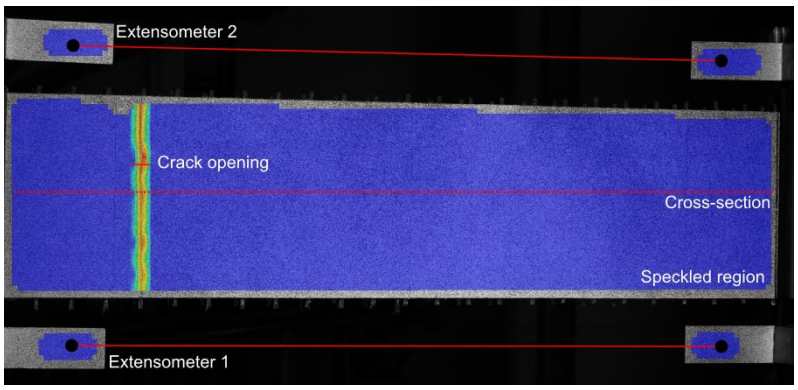

Figure 6.9 Illustration of selected features identified in the DIC system.

When comparing the reinforcement stress and the average strain extracted from the virtual extensometers, it is clear from Figure 6.10 that there was a pull-out failure of the TRC specimens reinforced by 3D carbon textiles. The stress-strain curve presented for the carbon yarn illustrates the strain hardening and rupture limits. It is to say that if the bond or anchorage length would be improved, the stress-strain curve of the specimens would shift towards the slope of the carbon yarn curve, as depicted in Figure 6.2. A similar behaviour would also be the case for the 2D carbon textiles.

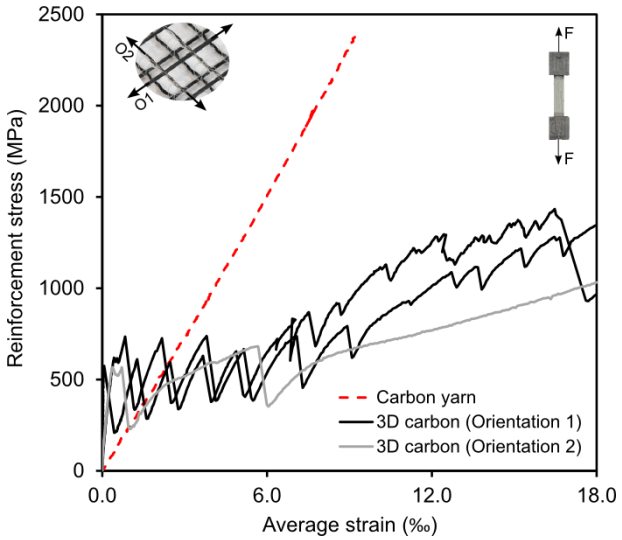

Figure 6.10 Reinforcement stress and average strain curve depicted for TRC specimens with 3D carbon textiles versus carbon yarn.

The use of virtual extensometers at prescribed crack locations is illustrated in Figure 6.11. As the loading increases, a given crack opening in terms of displacement can be followed successively. Additionally, the location of the crack formation along the length of the specimen can be monitored by means of a cross-sectional cut as shown in Figure 6.12. These two methods can be combined to retrieve detailed output data which could be useful for e.g. validation of models and design in SLS.

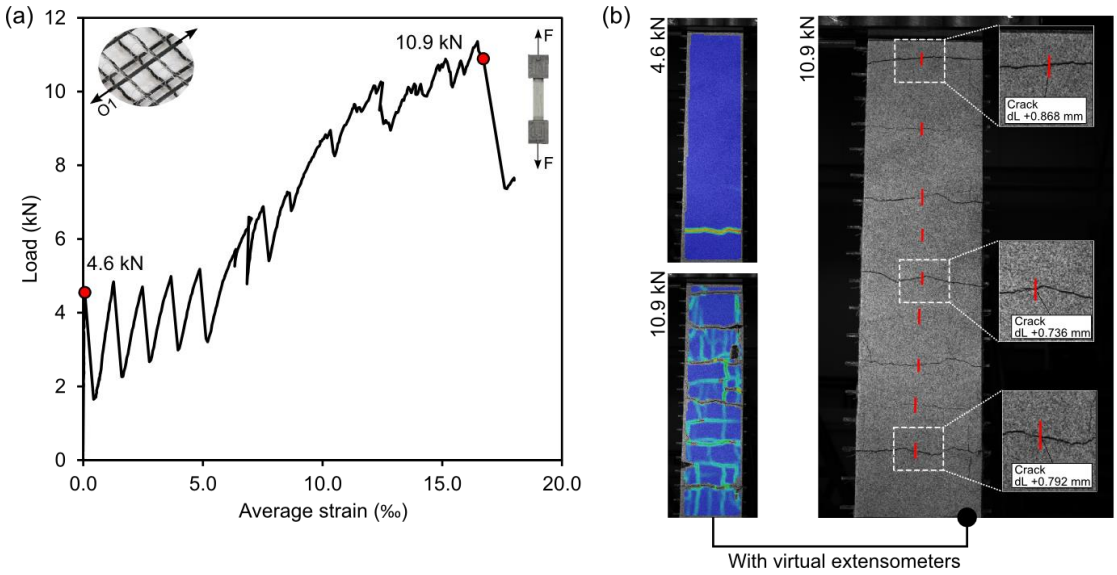

Figure 6.11 *Load versus average strain (a) and monitoring of successive crack openings with virtual extensometers (b).*

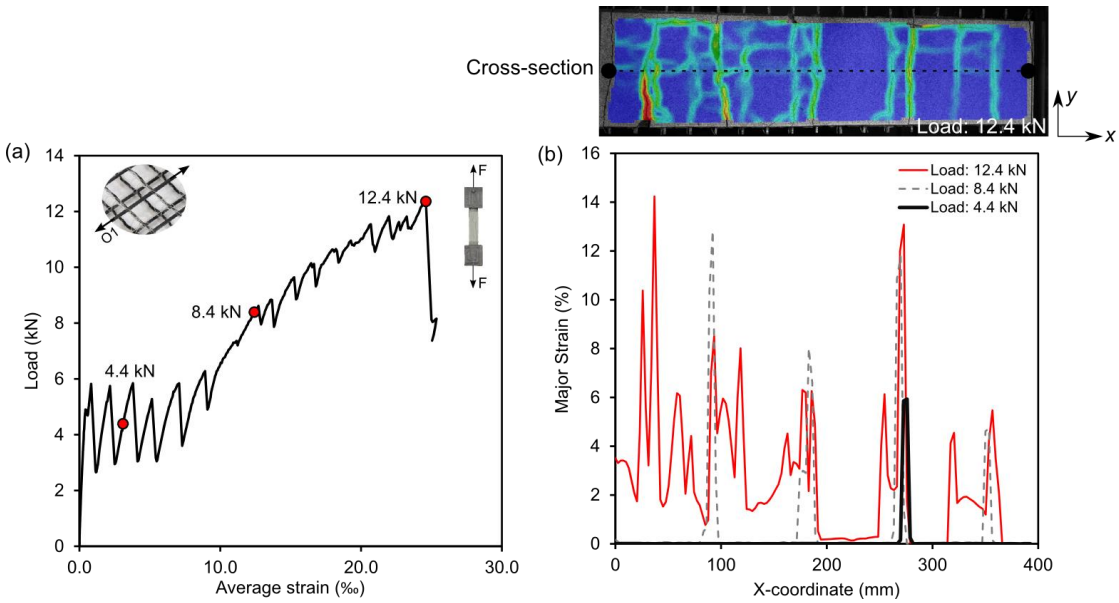

Figure 6.12 *Load versus average strain (a) and major strain versus length in x-direction for selected load levels (b).*

6.4 Summary

The tensile behaviour of TRC specimens reinforced by carbon textile reinforcement was investigated using uniaxial tensile tests (**Objective 1**). The use of digital image correlation (DIC) to further document and investigate the test results was explored in this work. The principle outcomes and associated commentary are:

> It can be concluded from these results that the bond and end anchorage are critical factors that influence the tensile behaviour of TRC.
  - Pull-out failure was observed for all tested specimens.
  - A significant difference was noted for the crack development particularly related to the 3D carbon textile in orientation *O2* compared to observations in flexure (Section 5.2.2). It appears as if the utilisation of the 3D textile (*O2*) is additionally influenced by the curvature of the specimen in flexure such that the bond was enhanced for small slips. The tensile capacity and COE are however overestimated due to the available anchorage length and clamping in the tensile test.
  - The interfacial bond between the carbon textiles and matrix can be improved by e.g. alternative curing conditions or casting methods, finer concrete matrix, surface coatings (Section 4.4, Appendix B).
  - The anchorage can also be improved by e.g. increasing the anchorage length in the test setup or increasing the strength of the specimen in the anchorage zone via epoxy or additional reinforcement.

> The correlation of the tensile and flexural behaviour was compared using the coefficient of efficiency (COE).
  - The COE was applied to calculate an estimated bending moment resistance which proved to be comparable to the experimental average results from Section 5.2.2 with a difference ranging between 11-47 %.
  - Underlying differences in the results can be primarily attributed to the differing end anchorage and clamping in the tensile and flexure tests which alter the boundary conditions.

> DIC proved to be a valuable and accurate method to measure the strains and crack development of tested TRC specimens.
  - These data can be useful when attempting to validate models or concerning the design in SLS.

7 Sustainable Potential

TRC-based research has touched upon numerous facets of this innovative composite material, for instance its structural functionality, durability, production, applicability and design. There has, however, been a lack of research related to the sustainability of this material. It is recognized that a more cyclical way of thinking is needed to fill in the gaps. It is to say that comprehensive studies touching upon health and safety, aesthetics and long-term environmental aspects are required in addition to standardization of testing and construction methods (Scheerer et al., 2015). Few publications are available regarding this topic, e.g. Nahum et al. (2015), Williams Portal et al. (2014c), and Tomoscheit et al. (2011).

Due to the fact that the term sustainability encompasses three main pillars, i.e. environmental, economic and social, it would be most adequate to assess their interaction for a given material or structure. In this thesis, the assessment of the environmental sustainability of TRC is presented resulting from **Paper IV** and answering **Objective 4**. Whereby, a Life Cycle Assessment (LCA) was applied to assess the environmental impact associated to TRC versus conventional reinforced concrete according to a *cradle-to-gate* perspective. Furthermore, the economic and social aspects are reflected upon as a final note.

7.1 Environmental sustainability

The advancement of principles for sustainable development in construction is ongoing. An example of this development is the harmonization of standards for construction materials mandated by requirement no. 7 of EU's Construction Products Regulation (Regulation (EU) No 305/2011 of the European Parliament and of the Council 2011). Currently there exist numerous methods to evaluate the so-called sustainability of materials, but there remains a lack of continuity and transparency. An underlying discrepancy exists particularly when new materials are introduced, as most often data pertaining to these materials are not available in existing life-cycle databases. In this case, the use of equivalent material data similar to the applied materials is often considered as an alternative. Then again, the collection of specific data pertaining to new materials still needs to be justified.

In this work, the environmental sustainability of TRC was evaluated using a Life Cycle Assessment (LCA) in accordance with ISO 14040 (2006) and ISO 14044 (2006). This method is typically used to evaluate the environmental impact of, e.g. building materials, assemblies or products. A *cradle-to-gate* perspective was considered in this case, signifying that the environmental impact related to the extraction to production processes were included. The main purpose of doing this analysis was to observe the associated environmental impact related to the reduction of the concrete cover in TRC slabs in comparison to a reference RC slab. Details related to the data acquisition, applied comparative case study, selected impact methods and results are provided in the following sections.

7.1.1 Impact assessment

Data acquisition

SimaPro (Version 7.3.3) was used to compute the LCA and a functional unit of 1 m^2 of reinforced concrete with a certain bending moment capacity was assumed for this study. The *cradle-to-gate* inventory data used in this study were taken from readily available databases: European Reference Life Cycle Database 3.0 (ELCD) (European Commission, 2013) and EcoInvent version 2.2 (Swiss Centre for Life Cycle Inventories, 2013). The material combinations included in this analysis were conventional steel RC, as well as carbon, basalt and glass TRC. Two studies, denoted as primary and sensitivity, were conducted to evaluate the environmental sustainability of the reinforced concrete alternatives as well as to verify the choice of inventory data in the primary study. A summary of the selected data for the respective studies is presented in Table 7.1. In the primary study, the same concrete type was assumed for all alternatives. Concrete was solely characterized by the cement content in the sensitivity study, as this constituent is considered to be the most energy-intensive in a concrete mix. It should be noted that the inventory data was selected based on the most suitable available option for the given material. For more accurate inventory data, relevant data could be collected for the specific material using standardized methods, which was out of the scope of this thesis.

*Table 7.1 Summary of inventory data used in LCA study (**Paper IV**).*

Equivalent Process	ID	Process Data Set	Database	Primary Study	Sensitivity Study
Concrete	C1	Lightweight concrete block	ELCD database 3.0	x	
	C2	Portland cement, strength class Z 52.5, at plant	EcoInvent v2.2		x
	C3	Portland calcareous cement, at plant	EcoInvent v2.2		x
Conventional steel reinforcement	S1	Steel sections (ILCD)	ELCD database 3.0	x	
	S2	Steel rebar, blast furnace and electric arc furnace route, production mix, at plant	EcoInvent v2.2		x
AR-glass fiber	G1	Continuous filament glass fiber (assembled roving)	ELCD database 3.0	x	
	G2	Glass wool, fleece, production mix, at plant	ELCD database 3.0		x
Carbon fiber	CA1	Polyacrylonitrile fibers (PAN)	ELCD database 3.0	x	x
Basalt fiber	B1	Rock wool, fleece, production mix, at plant	ELCD database 3.0	x	
	B2	Basalt, at mine	EcoInvent v2.2		x
	B3	Rock wool, at plant	EcoInvent v2.2		x

Comparative case study

To be able to objectively compare the reinforced concrete alternatives in the LCA study, it was necessary to define a comparative example. In this particular case, the one-way bending capacity of an arbitrary steel RC section (1 m x 1 m x 0.08 m) was selected as a reference, whereby the thickness fulfilled the minimum cover requirements. It was essentially of interest to observe the environmental impact of reducing the concrete cover in a TRC solution. The TRC solutions were so-to-say calibrated in terms of thickness and amount of reinforcement to meet the flexural capacity of the reference specimen. A major difference between the TRC and reference specimens is such that a coefficient of efficiency, k_1, was applied to the tensile strength of the textile reinforcement due to the effect of bond capacity when in composite form. A comparison between the one-way bending capacity and panel thickness is depicted in Figure 7.1 for considered alternatives. The input parameters and resulting calculated values for all alternatives are tabulated in Table 7.1. Details pertaining to the calculations are presented in **Paper IV**. It is without a doubt that other parameters, reference specimens, applications or mechanical behaviours could have also been used as appropriate comparative parameters.

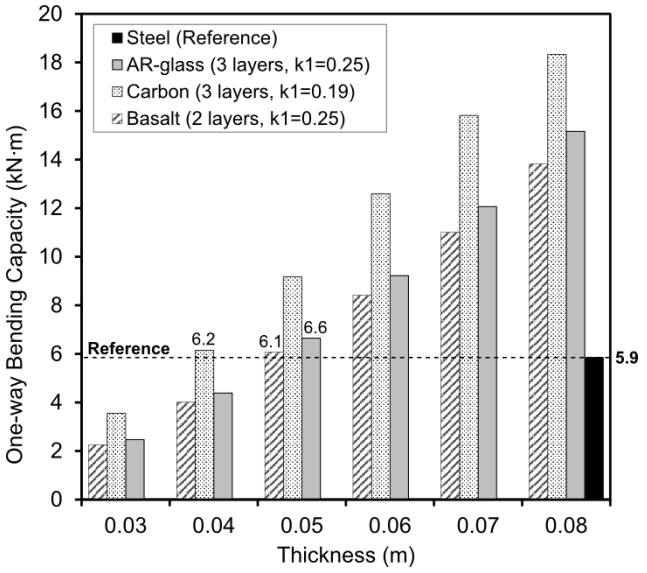

*Figure 7.1 One-way bending capacity versus thickness for reinforced concrete alternatives (**Paper IV**).*

Impact methods

The outcome of the LCA studies included the total energy consumption and environmental performance of the reinforced concrete alternatives. There are numerous standardized methods which can be used to quantify the environmental impact of a given product or material combination. In **Paper IV**, two impact assessment methods were applied: 1) Cumulative Energy Demand (CED) method and 2) CML 2001. Method 1 consists of the summation of the energy resources in MJ per functional unit, which considers both non-renewable energy resources and renewable energy resources. As for Method 2, the environmental impact, presented as a normalized score related to the World in 1990, is assessed according to baseline indicators, i.e. global warming potential (GWP100), ecotoxicity, etc. To obtain more information about the impact assessment methods refer to Pré Consultants (2010).

7.1.2 Selected results from primary study

The results based on the CED method are presented in Figure 7.2 and Figure 7.3 along with a summary of pertinent findings. In Figure 7.2, the CED is only compared between reinforcement alternatives, such that the results pertaining to 1 kg of material were compared to the values normalized according to the functional unit of 1 m^2. As for Figure 7.3, the CED results pertaining to the reinforced concrete alternatives normalized based on the functional unit are presented.

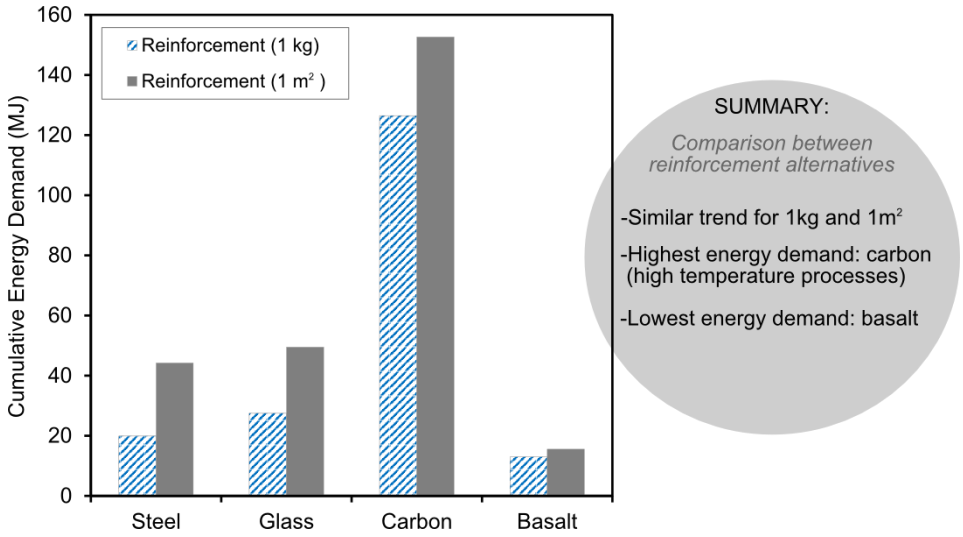

*Figure 7.2 Cumulative energy demand of reinforcement alternatives, 1 kg versus functional unit of 1 m^2 (**Paper IV**).*

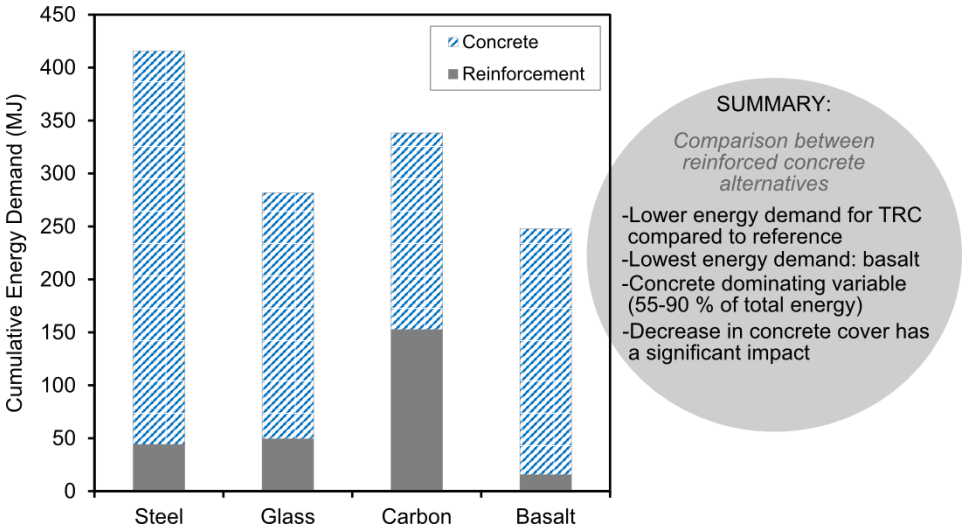

*Figure 7.3 Cumulative energy demand of primary study (reinforced concrete alternatives), functional unit of 1 m^2 (**Paper IV**).*

In **Paper IV**, the normalized environmental impact based on the CML 2001 impact method was presented for the primary study. Based on the presented baseline indicators, namely abiotic depletion, acidification, global warming (GWP 100) and total ecotoxicity, steel RC was found to have the greatest environmental impact. As for the TRC alternatives, basalt had the lowest impact, followed by carbon and glass. It is clear that a reduction in concrete thickness also plays a part in the reduction of the associated environmental impact. For further details, refer to **Paper IV**.

7.1.3 Selected results from sensitivity analysis

The choice of inventory data applied in the primary study was evaluated in the sensitivity study using the same impact methods. Other possible data options were added to the analysis to identify if there are underlying differences in the observed trends in the primary study. The additional data sets incorporated and associated acronyms are listed in Table 7.1. The results based on the CED method are presented in Figure 7.4 in addition to a summary of pertinent findings. In general, similar trends obtained in the primary study are also observed in the sensitivity study.

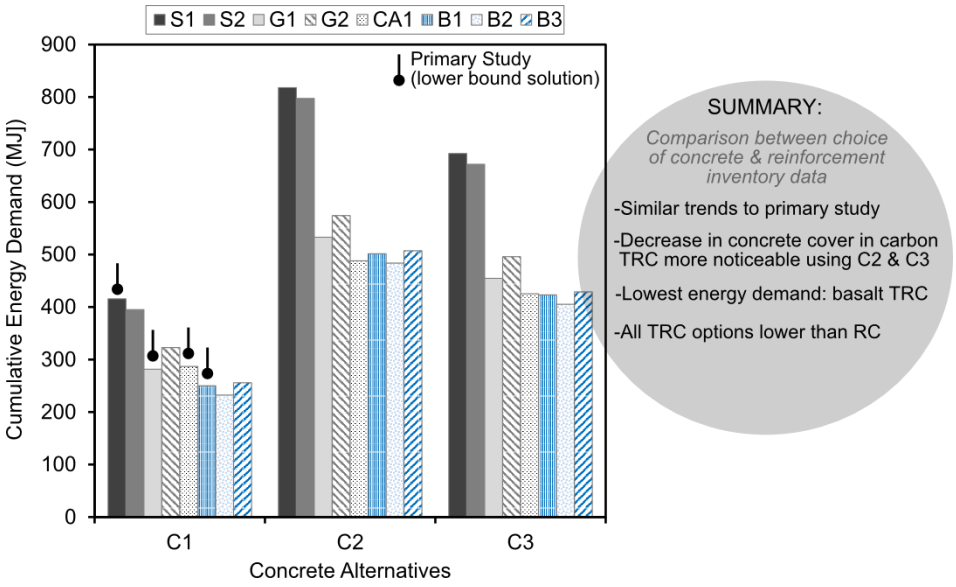

*Figure 7.4 The sensitivity of the cumulative energy demand for reinforced concrete alternatives, functional unit of 1 m^2 (**Paper IV**).*

As shown in **Paper IV**, similar to that demonstrated with the total cumulative energy demand, the primary study represented the lower-bound solution also for the normalized environmental impact. The variation of the concrete or so-to-say cement, C2 and C3, did not illustrate any notable differences; however it could be worthwhile comparing in future work to data pertaining to a normal density concrete mix. A significant difference was observed between the steel inventory data, which is believed to be due to the fact that S1 was related to larger steel sections. Concerning the TRC alternatives, the carbon alternative appeared to have a tendency to have a lower environmental impact based on the majority of the indicators. However, the sensitivity of this data selection could not be effectuated according to the available data. No significant differences could be noted between the glass data sets. Lastly, it is important to note that there was a large variation observed for the basalt TRC alternatives, such that the select basalt data sets only contributed to 0-36 % of the total impact. See **Paper IV** for additional discussion related to the environmental impact results.

7.2 Outlook on economic and social aspects

Numerous aspects need to be considered in addition to the structural performance and durability in order for TRC to become an accepted building material as a replacement or addition to conventional RC structures. As aforementioned, the sustainability of a material in terms of environmental, economic and social aspects is becoming more relevant nowadays. The environmental aspects touched upon in the previous section (Section 7.1) should ideally be evaluated in correlation to economic and social aspects to obtain a more holistic representation of the sustainability of TRC. The scope of this thesis did not include the analysis of these additional variables. Though, a comprehensive study supervised at CBI pertaining to the sustainability of TRC for renovation of buildings in comparison to commonly used solutions can be found in Carlsson et al. (2014). Even though the study is related to renovation of buildings, the assessment methods applied could also be relevant to a case study regarding new construction.

7.2.1 Economic aspects

The economic aspects can be evaluated using a Life-cycle cost analysis (LCC) and risk assessment (risk versus long-term stability) (Carlsson et al., 2014). There are many available calculation tools developed for this type of analysis which include for example a defined time perspective and projected interest rate. The incurred costs over the life-cycle of the material or structure are typically considered which are derived from production, transportation, installation, maintenance, replacement and demolition. A question which is commonly asked regarding TRC is the production costs in comparison to conventionally applied RC. Due to the fact that the production of textile reinforcement meshes for use in concrete structures is limited, particularly concerning carbon fibres, the cost is consequently higher. However, as the demand and acceptance for TRC increases, it is presumed that the cost will decrease as a result. Another relevant factor to take into consideration is the long-term performance of the building materials, which involves the maintenance and durability. Particularly TRC reinforced by carbon textiles can have a potential long-term payback, as a result of its superior durability properties.

7.2.2 Social aspects

The evaluation of social aspects is often based on a qualitative analysis of health and comfort, aesthetics as well as preservation of cultural identity. In terms of new construction, the architects and/or clients play a larger role in setting the restrictions of the building design and external appearance. There could be a demand for lightweight, flexible and aesthetically appealing structures simultaneously, which is challenging to meet. Accordingly, the boundaries of TRC are being pushed due to such demands for innovative shapes and structures. For example, new production methods are currently being developed to cast so-called folded TRC structures (Koch et al., 2015). When dealing with the sustainable renovation of dwellings, social aspects become extremely important to consider as the implementation of renovation directly affects the residents over prolonged periods. Changes effectuated to existing buildings also require that these are performed according to the buildings' prerequisites. The selected technical solutions should therefore attempt to preserve the buildings functionality and expected identity in the given context. Furthermore, the

evaluation of a sustainable renovation is effected by the existing building's prerequisites and customer's interest in relation to the client and the profit (Carlsson et al., 2014).

7.3 Summary

The sustainability, more specifically in terms of environmental aspects, was assessed for TRC in relation to RC using a case study (**Objective 4**, **Paper IV**). LCA according to a cradle-to-gate perspective was applied to assess the environmental sustainability of TRC. This study was limited to a particular case study involving the flexural behaviour of TRC slabs related to a reference RC slab. The flexural behaviour was estimated analytically, yet could be worth verifying experimentally in further studies. The main conclusions and remarks associated to this section are:

- In the primary study, the possible reduction of concrete cover thickness in TRC proved to bring upon environmental benefits whereby the cumulative energy demand and environmental impact could be reduced.
  - TRC reinforced by basalt yielded the least cumulative energy demand and carbon the least environmental impact.
  - The environmental sustainability can also be evaluated more comprehensively using numerous impact methods which cover a wider range of impact indicators or parameters.
- A sensitivity study incorporated alternative inventory data was applied to verify the results obtained from the primary study.
  - Similar trends were observed compared to the primary study, such that TRC in general appears to have superior environmental sustainability compared to RC.
- Further improvements to the LCA can include the use of a *cradle-to-cradle* perspective to identify potential long-term paybacks, as well as the use of a more homogeneous set of life-cycle inventory data. The use of uncertainty analyses can also be incorporated to further increase the certainty of the results.
- It could be worth including economic and social aspects in the assessment of the sustainable potential of TRC to further support the presented findings and overall acceptance of TRC as a building material.

8 Conclusions and Future Outlook

8.1 Concluding remarks

Structural performance, *durability* and *sustainability* aspects of TRC have been investigated by means of numerous experimental and numerical methods in this thesis. It has been established that TRC is not only a sustainable solution, yet it can be produced as structures incorporating varying thicknesses, textile materials, reinforcement ratios and shapes which could be translated into e.g. façade elements or slabs for the built environment. Textiles made of carbon fibres were found to be a promising alternative as they have superior mechanical properties as well as durability properties in an alkaline environment. In general, the bond behaviour in TRC has been identified as a critical feature which needs to be improved, particularly for carbon textiles, using e.g. surface coatings, short fibres, or alternative casting and curing methods.

Moreover, the scope of this work was further divided to address four specific objectives as presented in the introduction. The general conclusions pertaining to these objectives are summarized in this section. For a detailed account of the concluding remarks related to these objectives, refer to **Papers I-IV** as well as the summary sections included at the end of each chapter enclosed in this thesis.

Experimental and numerical methods were applied to quantify the *structural performance* of TRC on the *material*, *interaction* and *global* levels (**Objective 1**). Through these various investigations it was found that:

- The mechanical behaviour of the concrete matrix on a *material* level should be characterized using experimental methods as the available empirical expressions are not adapted for this type of fine-grained matrix.
- The experimental methods applied for concrete should be further evaluated based on the size effect of test specimens particularly when the application is dealing with thin TRC panels.
- On the *material* level, the tensile properties of the textile reinforcement should be quantified using uniaxial tensile tests based upon the corresponding level of investigation, e.g. for a structural component, the textile reinforcement mesh or yarn removed from the mesh should be characterized. The use of video extensometer techniques were found to aid in capturing the ultimate behaviour of the textile. Alternatively, uniaxial tensile tests of TRC panels leading to yarn rupture could also be applied to yield the tensile behaviour of the textile mesh in the composite.
- The *interaction* of the textile reinforcement and matrix should be experimentally quantified using pull-out tests according to the corresponding level of investigation (see the point above). For the case of a TRC structure, incorporating the textile mesh in the test specimens versus single yarns yields more representative bond behaviour as effects of mechanical anchorage are incorporated.
- A local bond stress-slip relationship can accurately be characterized from pull-out specimens having short embedment lengths as verified using simplified and complex models.
- Video extensometer techniques can be applied to more accurately capture the resulting slip of the textile yarn in relation to the specimen cross-section.

- The interfacial bond between the matrix and textile is a critical factor affecting the flexural behaviour of TRC slabs on a *global* level tested in four-point bending. The addition of coatings to the textiles (i.e. epoxy), as well as the addition of short fibres improved the bond and resulting flexural behaviour of thin carbon reinforced TRC panels.
- Similar to the flexural tests, the tensile behaviour of TRC panels reinforced by carbon textiles on a *global* level tested in uniaxial tension was also found to be greatly influenced by the interfacial bond among other factors such as the end clamping and available anchorage length.
- The extent of interaction between the textile reinforcement and matrix was measured via the coefficient of efficiency (COE) which indicated that relatively poor bond was the case for the tested carbon reinforced TRC panels, which led to pull-out failure.
- The tensile and flexural behaviours of TRC can be correlated using the COE with a certain degree of error. For example, the differing available anchorage length and end clamping in the tensile tests, which overestimate the tensile capacity and COE, are underlying reasons for the observed discrepancies.
- For the 3D carbon textile (*O2*), significantly differing crack development was observed between the tensile and flexural results. It is thought that a superior bond for small slips led to superior crack development. In flexure, the curvature of the specimen could have been responsible for the further activation of the lateral yarns in both layers.
- Digital image correlation applied in the TRC tensile tests is a valuable tool which can be applied to capture crack development and strain field during testing.

Through FE-analysis, the *structural performance* related to the experimentally quantified *material* and *interaction* level data was interconnected to the *global* level (**Objective 2**). The following conclusions can be made based on the realization of this task:

- Linking the experimental output from the *material* and *interaction* levels in a simplified macro-scale FE-model on the *global* level led to promising results, whereby insight on the actual failure behaviour was enabled. The underlying accuracy of the modelling output on the *global* level can be further improved by refining the experimental methods applied on the various levels of investigation.
- Characterizing the tensile properties of the textile reinforcement (mesh or yarn removed from mesh) on the *material* level was found to be suitable for the presented 2D macroscale FE-model. These data in combination with a bundled-bar approach appeared to be an acceptable idealization.
- The numerical output can be further improved in terms of minimizing error by incorporating: a) detailed and accurate characterization of properties on *material*, *interaction* and *global* levels; b) modifying the stress-strain curve for the textile reinforcement to include a two-branch curve with a change in stiffness to take into account the loss of stiffness within the reinforcement due to partial rupture; c) else obtaining the tensile behaviour directly from uniaxial tensile tests on TRC panels to incorporate the composite effect; d) more accurate force-slip measurements from pull-out particularly concerning the post-peak behaviour.

The *durability* of textiles was characterized by means of measuring the degradation of the tensile properties of textile products before and after accelerated chemical ageing (**Objective 3**). Through this evaluation, it was discovered that:

- The use of a standardized accelerated test method typically applied to FRP was found to be too aggressive for certain textile reinforcement products (e.g. made of basalt and AR-glass).
- The tested carbon textile reinforcement product was shown to have a superior alkali resistance based on the applied accelerated ageing test method.
- The degradation of textiles was additionally investigated using alternative exposure times, temperatures and test solutions. Degradation curves particularly for the tested basalt and AR-glass products were established based on a statistical correlation between the test conditions.
- The coatings/sizings applied to the textile reinforcement during production greatly influence the degradation of the reinforcement exposed to an alkaline environment (related to AR-glass and basalt).
- It is difficult to suggest a standardized test method for accelerated testing related to chemical attack of textile reinforcement materials in general as they degrade differently based upon their chemical composition and origin.
- It is further important to be able to correlate the accelerated time to a realistic time period for design purposes.

The environmental *sustainability* of TRC versus that of conventional RC was evaluated using LCA with a cradle-to-gate perspective (**Objective 4**). This evaluation resulted in the following:

- The reduction of the concrete cover thickness possible in TRC panels was shown to yield a reduction in cumulative energy demand and environmental impact using a comparative case study related to RC panels.
- The trends derived from the primary study were verified using comparative and available inventory data in the sensitivity study.
- Key features related to the assessment of the economic and social sustainability of TRC were deliberated. Similar assessment methods, e.g. LCC and qualitative assessment, can be applied for both new construction or renovation applications in the built environment.

8.2 Future outlook

For future research related to TRC, the following key areas are suggested:

- The continued advancement of standardization of material production processes and experimental methods is recommended to enhance the certainty of the material quality and expected performance.
- It is worthwhile to further validate and improve existing models using detailed experimental data for design purposes.
- There remains a need for real-time durability testing of textile reinforcement and TRC to validate the long-term material performance projected from accelerated testing and models.
- It could be an interesting application to consider the design of load-bearing structures using a combined solution of conventional RC with TRC (e.g. with carbon textiles) to reduce the steel reinforcement ratio and weight of the structure.
- To further enhance the prospects of TRC as an alternative building material, it is important to execute a comprehensive evaluation based on an actual case study and detailed inventory data. This study should include an environmental cradle-to-cradle perspective (LCA) in combination with economic and social aspects.

9 References

ACI 440.1 R-06. (2006): Guide for the Design and Construction of Concrete Reinforced with FRP Bars Detroit, Michigan: ACI Committee 440, American Concrete Institute.

ACI 544.1R-96. (2002): State-of-the-art report on fiber reinforced concrete. Detroit, Michigan: ACI Committee 544, American Concrete Institute.

ACI 544.5R-10. (2010): Report on the Physical Properties and Durability of Fiber-Reinforced Concrete. Detroit, Michigan: ACI Committee 544, American Concrete Institute.

ACI Education Bulletin E2-00. (2000): ACI Education Bulletin E2-00: Reinforcement for Concrete - Materials and Applications (Reapproved 2006). ACI Committee E-701, American Concrete Institute.

Aljewifi H. (2011): *Étude du comportement mécanique à l'arrachement de fils multi-filamentaires enrobés dans une matrice cimentaire et influence de l'imprégnation (Study on the mechanical behaviour of the pull-out of multi-filament yarns embedded in a cementitious matrix and the influence of impregnation).* Dissertation, Université de Cergy Pontoise.

Amzaleg E., et al. (2013): Flexural Behaviour of Cement Based Element Reinforced with 3D Fabric. VIII International Conference on Fracture Mechanics of Concrete and Concrete Structures, Toledo, Spain, 10-14 March, 2013.

ASTM D3379-75. (1989): Standard Test Method for Tensile Strength and Young's Modulus for High-Modulus Single-Filament Materials (Withdrawn 1998). West Conshohocken, PA: ASTM International.

ASTM E632-82. (1996): Standard Practice for Developing Accelerated Tests to Aid Prediction of the Service Life of Building Components and Materials (Withdrawn 2005). West Conshohocken, PA: ASTM International.

Azzam A. and Richter M. (2011): Investigation of Stress Transfer Behavior in Textile Reinforced Concrete with Application to Reinforcement Overlapping and Development Lengths. 6th Colloquium on Textile Reinforced Structures (CTRS6), Ortlepp, R. (ed.) Dresden, Germany, 2011, pp. 103-116.

Banholzer B. (2004): *Bond behaviour of a multi-filament yarn embedded in a cementitious matrix.* Dissertation, Fakultät für Bauingenieurwesen, RWTH Aachen.

Banholzer B. (2006): Bond of a strand in a cementitious matrix. *Materials and structures,* Vol. 39 (10), pp. 1015-1028.

Barhum R. and Mechtcherine V. (2012): Effect of short, dispersed glass and carbon fibres on the behaviour of textile-reinforced concrete under tensile loading. *Engineering Fracture Mechanics,* Vol. 92, pp. 56-71.

Bartos P. (1987): Brittle matrix composites reinforced with bundles of fibres. *From Materials Science to Construction Materials Engineering,* Vol. 2, pp. 539-546.

Bentland S. (2015): *Facade Elements of Vacuum Insulated Textile Reinforced Green Concrete.* Master's Thesis, Civil and Environmental Engineering, Chalmers University of Technology, pp. 34.

Bentur A. and Mindess S. (1990): *Fibre Reinforced Cementitious Composites*. Belfast, Elsevier Applied Science.

Bentur A. and Mindess S. (2006): *Fibre reinforced cementitious composites*. CRC Press.

Brameshuber W. (ed.) 2006. *Report 36: Textile Reinforced Concrete-State-of-the-Art Report of RILEM TC 201-TRC*: RILEM publications.

Brameshuber W., et al. (2010a): *Pull-out test - Test method to determine the bond properties of textile reinforced concrete.* Draft recommendations by RILEM TC 232-TDT, pp. 4.

Brameshuber W., et al. (2010b): *Uniaxial tensile test - Test method to determine the load bearing behavior of tensile specimens made of textile reinforced concrete.* Draft recommendations by RILEM TC 232-TDT, pp. 7.

Brockmann T. (2006): *Mechanical and Fracture Mechanical Properties of Fine Grained Concrete for Textile Reinforced Composites.* Dissertation, Fakultät für Bauingenieurwesen, RWTH Aachen.

Brockmann T. (2007): Mechanical and Fracture Mechanical Properties of Fine Grained Concrete for TRC Structures. *Advances in Construction Materials 2007*, Springer, pp. 119-129.

Bruckermann O. (2007): *Zur Modellierung des Zugtragverhaltens von textilbewehrtem Beton (On the modelling of pull-out behaviour of textile reinforced concrete).* Dissertation, RWTH Aachen.

Butler M., Hempel S. and Mechtcherine V. (2011): Modelling of ageing effects on crack-bridging behaviour of AR-glass multifilament yarns embedded in cement-based matrix. *Cement and Concrete Research*, Vol. 41 (4), pp. 403-411.

Butler M., Mechtcherine V. and Hempel S. (2009): Experimental investigations on the durability of fibre–matrix interfaces in textile-reinforced concrete. *Cement and Concrete Composites*, Vol. 31 (4), pp. 221-231.

Butler M., Mechtcherine V. and Hempel S. (2010): Durability of textile reinforced concrete made with AR glass fibre: effect of the matrix composition. *Materials and structures*, Vol. 43 (10), pp. 1351-1368.

Büttner T., Allessandra K. and Raupach M. (2008): Improvement of load-bearing capacity and durability of textile-reinforced concrete due to the use of polymers. 15th Congress of the Glassfibre Reinforced Concrete Association International, Prague, Czech Republic, 20-23 April, 2008: The Concrete Society.

Büttner T., et al. (2009): Einsatz von Polymeren in Textilbeton–Entwicklung polymermodifizierter Betone und Einflüsse auf die Dauerhaftigkeit (Use of polymers in textile reinforced concrete - development of polymer modified concretes and its influence on the durability). 4th Colloquium on Textile Reinforced Structures (CTRS4), Curbach, M. and Jesse, F. (eds.), Dresden, Germany, 3-5 June, 2009, pp. 197-212.

Büttner T., Orlowsky J. and Raupach M. (2011): Enhancement of the durability of AR-glass reinforcement due to an epoxy-impregnation. *Erhöhung der Dauerhaftigkeit textiler Beton-Bewehrungen durch Epoxidharztränkung,* Vol. 88 (5), pp. 263-270.

Büttner T., et al. (2010): Enhancement of the Durability of Alkali-resistant Glass-Rovings in concrete. International RILEM Conference on Material Science, Germany, 2010: RILEM Publications SARL, pp. 333-342.

Carlsson S. and Rehnmark M. (2014): *Hållbar renovering av miljonprogrammets fasader - Utvärdering av textilarmerad betong (Sustainable refurbishment of facades of the Million Programme - Evaluation of textile reinforced concrete).* Bachelor Thesis, Building Technology, Jönköping University.

CEB-FIP MC90. (1993): Design of Concrete Structures. CEB-FIP Model Code 1990. Thomas Telford.

Cohen Z. and Peled A. (2012): Effect of nanofillers and production methods to control the interfacial characteristics of glass bundles in textile fabric cement-based composites. *Composites Part A: Applied Science and Manufacturing,* Vol. 43 (6), pp. 962-972.

Colombo I., et al. (2013): Erratum to: Textile Reinforced Concrete: experimental investigation on design parameters. *Materials and Structures,* Vol. 46 (11), pp. 1953-1971.

Corr D., et al. (2007): Digital image correlation analysis of interfacial debonding properties and fracture behavior in concrete. *Engineering Fracture Mechanics,* Vol. 74 (1), pp. 109-121.

Curbach M. and Jesse F. (1999): High-Performance Textile-Reinforced Concrete. *Structural Engineering International,* Vol. 9 (4), pp. 289-291.

Cuypers H., et al. (2007a): Durability aspects of AR-glass-reinforcement in textile reinforced concrete, Part 1: Material behaviour. *In:* Grosse, C. U. (ed.) *Advances in Construction Materials 2007,* Springer Berlin Heidelberg, pp. 381-388.

Cuypers H., et al. (2007b): Durability aspects of AR-glass-reinforcement in textile reinforced concrete, Part 2: Modelling and exposure to outdoor weathering. *In:* Grosse, C. U. (ed.) *Advances in Construction Materials 2007,* Springer Berlin Heidelberg, pp. 389-395.

D'Ambrisi A., Feo L. and Focacci F. (2013): Experimental analysis on bond between PBO-FRCM strengthening materials and concrete. *Composites Part B: Engineering,* Vol. 44 (1), pp. 524-532.

D'Ambrisi A. and Focacci F. (2011): Flexural strengthening of RC beams with cement-based composites. *Journal of Composites for Construction,* Vol. 15 (5), pp. 707-720.

Dai J., Wang B. and Xu S. (2009): Textile reinforced engineered cementitious composites (TR-ECC) overlays for the strengthening of RC beams. The second official international conference of International Institute for FRP in Construction for Asia-Pacific Region, Seoul, Korea, 9-11 December, 2009, pp. 75-80.

de Andrade Silva F., et al. (2014): Effects of elevated temperatures on the interface properties of carbon textile-reinforced concrete. *Cement and Concrete Composites,* Vol. 48, pp. 26-34.

Dejke V. (2001): *Durability of FRP reinforcement in concrete: literature review and experiments.* Licentiate Thesis, Building Materials, Chalmers University of Technology.

Domone P. and Illston J. (2010): *Construction materials: their nature and behaviour*. CRC Press.

EN 1992-1-1. (2008): EN 1992-1-1:2005 Eurocode 2: Design of concrete structures. *Part 1-1: General rules and rules for buildings.* Comité Européen de Normalisation (CEN).

EN 12390-1. (2012): Testing hardened concrete - Part 1: Shape, dimensions and other requirements for specimens and moulds. Comité Européen de Normalisation (CEN).

EN 12390-3. (2009): Testing hardened concrete - Part 3: Compressive strength of test specimens. Comité Européen de Normalisation (CEN).

EN 12390-5. (2009): Testing hardened concrete - Part 5: Flexural strength of test specimens. Comité Européen de Normalisation (CEN).

EN 12390-6. (2009): Testing hardened concrete - Part 6: Tensile splitting strength of test specimens. Comité Européen de Normalisation (CEN).

EN 12390-13. (2013): Testing hardened concrete - Part 13: Determination of secant modulus of elasticity in compression. Comité Européen de Normalisation (CEN).

European Commission. (2013): *European Reference Life Cycle Database 3.0 (ELCD)* [Online]. Joint Research Centre - Institute for Environment and Sustainability. Available: http://lca.jrc.ec.europa.eu/ [Accessed February 22 2013].

Fall D. (2011): *Reinforcement in tailor-made concrete structures.* Licentiate Thesis, Chalmers University of Technology.

Fangueiro R. (2011): *Fibrous and composite materials for civil engineering applications*. Elsevier.

fib Bulletin No. 42. (2008): Constitutive modelling of high strength/high performance concrete. Lausanne: Fédération Internationale du béton.

fib Model Code 2010. (2013): Lausanne, Fédération Internationale du béton.

Fujisaki T., Nakatsuji T. and Sugita M. (1993): Research and development of grid shaped FRP reinforcement. *ACI Special Publication,* Vol. 138.

Förster T. and Mäder E. (2011): Performance of Modified Basalt Fibres. Proceedings of the 18th International Conference on Composite Materials (ICCM18), 2011: Korean Society for Composite Materials.

Förster T., et al. (2010): Challenges for Fibre and Interphase Design of Basalt Fibre Reinforced Concrete. International RILEM Conference on Material Science, 2010: RILEM Publications SARL, pp. 57-66.

Hartig J. (2011): *Numerical Investigations on the Uniaxial Tensile Behaviour of Textile Reinforced Concrete.* Dissertation, Fakultät Bauingenieurwesen, Technischen Universität Dresden

Hartig J., Häußler-Combe U. and Schicktanz K. (2008): Influence of bond properties on the tensile behaviour of Textile Reinforced Concrete. *Cement and Concrete Composites,* Vol. 30 (10), pp. 898-906.

Hartig J., et al. (2012): Influence of experimental setups on the apparent uniaxial tensile load-bearing capacity of textile reinforced concrete specimens. *Materials and structures,* Vol. 45 (3), pp. 433-446.

Hayashi R., et al. (1990): Tensile Properties of Carbon Fiber Mesh Reinforced Mortar with Various Weavings. Proceedings of the Japan Concrete Institute, 1990, pp. 1043-1048.

Hegger J. (2009): *Summary of Results for the Project INSUSHELL (Report-No. 237/2009).* RWTH Aachen University, pp. 25.

Hegger J., Goralski C. and Kulas C. (2011): A pedestrian bridge made of textile reinforced concrete. *Schlanke Fußgängerbrücke aus Textilbeton,* Vol. 106 (2), pp. 64-71.

Hegger J., et al. (2010a): Sandwich Panels Made of TRC and Discrete and Continuous Connectors. International RILEM Conference on Material Science - 2nd ICTRC - Textile Reinforced Concrete - Theme 1, Brameshuber, W. (ed.) Aachen 2010a: RILEM Publications SARL, pp. 381-392.

Hegger J., et al. (2010b): TRC Pedestrian Bridge-Design, Load-bearing Behavior and Production Processes of a Slender and Light-weight Construction. International RILEM Conference on Material Science - 2nd ICTRC - Textile Reinforced Concrete - Theme 1, Brameshuber, W. (ed.) Aachen, 2010b: RILEM Publications SARL, pp. 353-364.

Hegger J., et al. (2006): Load–bearing behaviour and simulation of textile reinforced concrete. *Materials and Structures,* Vol. 39 (8), pp. 765-776.

Hegger J. and Voss S. (2008): Investigations on the bearing behaviour and application potential of textile reinforced concrete. *Engineering structures,* Vol. 30 (7), pp. 2050-2056.

Hempel S., Butler M. and Mechtcherine V. (2015): Bond Behaviour and Durability of Basalt Fibres in Cementitious Matrices. 3rd ICTR International Conference on Textile Reinforced Concrete Brameshuber, W. (ed.) Aachen, Germany, 2015: RILEM SARL, pp. 225-233.

Holler S., et al. (2004): Computational model of textile-reinforced concrete structures. *Computers & structures,* Vol. 82 (23), pp. 1971-1979.

Häußler-Combe U. and Hartig J. (2007): Bond and failure mechanisms of textile reinforced concrete (TRC) under uniaxial tensile loading. *Cement and Concrete Composites,* Vol. 29 (4), pp. 279-289.

ISO 2062. (2009): Textiles - Yarns from packages - Determination of single-end breaking force and elongation at break using constant rate of extension (CRE) tester. Switzerland: International Organization for Standardization.

ISO 3341. (2000): Textile glass - Yarns - Determination of breaking force and breaking elongation. Switzerland: International Organization for Standardization.

ISO 4606. (1995): Textile glass - Woven fabric - Determination of tensile breaking force and elongation at break by the strip method. Switzerland: International Organization for Standardization.

ISO 5079. (1995): Textile fibres - Determination of breaking force and elongation of individual fibres. Switzerland: International Organization for Standardization.

ISO 6939. (1988): Textiles - Yarns from packages - Method of test for breaking strength of yarn by the skein method. Switzerland: International Organization for Standardization.

ISO 10406-1. (2008): Fibre-reinforced polymer (FRP) reinforcement of concrete - Test Methods. *Part 1: FRP bars and grids.* Switzerland: International Organization for Standardization.

ISO 10406-2. (2008): Fibre-reinforced polymer (FRP) reinforcement of concrete - Test methods. *Part 2: FRP sheets.* Switzerland: International Organization for Standardization.

ISO 11566. (1996): Carbon fibre-Determination of the tensile properties of single filament specimens. Switzerland: International Organization for Standardization.

ISO 13934-1. (2013): Textiles - Tensile properties of fabrics. *Part 1: Determination of maximum force and elongation at maximum force using the strip method.* Switzerland: International Organization for Standardization.

ISO 13934-2. (2014): Textiles - Tensile properties of fabrics. *Part 2: Determination of maximum force using the grab method.* Switzerland: International Organization for Standardization.

ISO 14040. (2006): Environmental management - Life cycle assessment - Principles and framework. Switzerland: International Organization for Standardization.

ISO 14044. (2006): Environmental management - Life cycle assessment - Requirements and guidelines. Switzerland: International Organization for Standardization.

Japan Society of Civil Engineers. (1997): Recommendation for design and construction of concrete structures using continuous fiber reinforcing materials.

Jun P. and Mechtcherine V. (2010): Behaviour of Strain-hardening Cement-based Composites (SHCC) under monotonic and cyclic tensile loading: Part 1 – Experimental investigations. *Cement and Concrete Composites,* Vol. 32 (10), pp. 801-809.

Katz A. and Bentur A. (1996): Mechanisms and processes leading to changes in time in the properties of CFRC. *Advanced Cement Based Materials,* Vol. 3 (1), pp. 1-13.

Koch A., et al. (2015): Locally adapted biaxial warp knitted textiles as reinforcement of folded concrete elements. 3rd ICTR International Conference on Textile Reinforced Concrete Brameshuber, W. (ed.) Aachen, Germany, 2015: RILEM SARL, pp. 419-426.

Krüger M. (2004): *Vorgespannter textilbewehrter Beton (Prestressed textile reinforced concrete).* Dissertation, Fakultät Bau- und Umweltingenieurwissenschaften, University of Stuttgart.

Kulas C., et al. (2011): Ventilated façade structures made of textile reinforced concrete - Structural behavior and construction. *Hinterlüftete Vorhangfassaden aus Textilbeton: Tragverhalten und Ausführung,* Vol. 88 (5), pp. 271-280.

Lepenies I. G. (2007): *Zur hierarchischen und simultanen multi-skalen-analyse von textilbeton (On the Hierarchical and Integrated Multi Scale Analysis of Textile Reinforced Concrete).* Dissertation, Inst. für Massivbau, Technische Universität Dresden.

Lohaus L., Tomann C. and Weicken H. (2015): Combined Formwork and Textile Reinforcement System for a Mineral Corrosion Protection Layer for Offshore Application. 3rd ICTR International Conference on Textile Reinforced Concrete Brameshuber, W. (ed.) Aachen, Germany, 2015: RILEM SARL, pp. 287-294.

Lorenz E. and Ortlepp R. (2012): Bond behavior of textile reinforcements-development of a pull-out test and modeling of the respective bond versus slip relation. *High Performance Fiber Reinforced Cement Composites 6*, Springer, pp. 479-486.

Lorenz E., et al. (2013): Textilbeton–Grundlegende Untersuchungen im Überblick. *Beton und Stahlbetonbau,* Vol. 108 (10), pp. 711-722.

Lorenz E., Schütze E. and Weiland S. (2015): Textilbeton–Eigenschaften des Verbundwerkstoffs. *Beton-und Stahlbetonbau,* Vol. 110 (S1), pp. 29-41.

Lundgren K., et al. (2012): Analytical model for the bond-slip behaviour of corroded ribbed reinforcement. *Structure and Infrastructure Engineering,* Vol. 8 (2), pp. 157-169.

Machida A. and Gakkai D. (1993): *State-of-the-art report on continuous fiber reinforcing materials*. Research Committee on Continuous Fiber Reinforcing Materials, Japan Society of Civil Engineers.

Mahadevan M. G. (2009): *Textile Spinning, Weaving and Designing*. Chandigarh, IND, Global Media.

Malaga K., et al. (2012): Textile reinforced concrete sandwich panels. International FIB Symposium - Concrete Structures for Sustainable Community, Stockholm, Sweden, 11-14 June 2012.

McCormick N. and Lord J. (2010): Digital image correlation. *Materials today,* Vol. 13 (12), pp. 52-54.

Mechtcherine V. (2012): Towards a durability framework for structural elements and structures made of or strengthened with high-performance fibre-reinforced composites. *Construction and Building Materials,* Vol. 31, pp. 94-104.

Mechtcherine V. (2013): Novel cement-based composites for the strengthening and repair of concrete structures. *Construction and Building Materials,* Vol. 41 (0), pp. 365-373.

Mehta P. K., Monteiro P. J. and Education M.-H. (2006): *Concrete: microstructure, properties, and materials*. McGraw-Hill New York.

Micelli F. and Nanni A. (2004): Durability of FRP rods for concrete structures. *Construction and Building Materials,* Vol. 18 (7), pp. 491-503.

Mobasher B. (2012): *Mechanics of fiber and textile reinforced cement composites*. CRC press.

Morales Cruz C., et al. (2015): Improving the Bond Behavior of Textile Reinforcement and Mortar Through Surface Modification. 3rd ICTR International Conference on Textile Reinforced Concrete Brameshuber, W. (ed.) Aachen, Germany, 2015: RILEM SARL, pp. 215-223.

Mueller U., et al. (2015): Reactive powder concrete for façade elements – A sustainable approach. VII International Congress on Architectural Envelopes (ICAE), San Sebastian-Donostia, Spain, 27-28 May 2015.

Mumenya S., Tait R. and Alexander M. (2010): Mechanical behaviour of Textile Concrete under accelerated ageing conditions. *Cement and Concrete Composites,* Vol. 32 (8), pp. 580-588.

Möller B., et al. (2005): Numerical simulation of RC structures with textile reinforcement. *Computers & Structures,* Vol. 83 (19–20), pp. 1659-1688.

Nahum L., Peled A. and Erez G. (2015): Structural concrete elements reinforced with textiles - sustainability perspective. 3rd ICTR International Conference on Textile Reinforced Concrete Brameshuber, W. (ed.) Aachen, Germany, 2015: RILEM SARL, pp. 295-303.

Ohno S. and Hannant D. (1994): Modeling the Stress-Strain Response of Continuous Fber Reinforced Cement Composites. *ACI Materials Journal,* Vol. 91 (3).

Orlowsky J. and Raupach M. (2006): Modelling the loss in strength of AR-glass fibres in textile-reinforced concrete. *Materials and structures,* Vol. 39 (6), pp. 635-643.

Orlowsky J. and Raupach M. (2011): Textile reinforced concrete - from research to application. *Cement Wapno Beton,* Vol. 16 (6), pp. 323-331.

Orlowsky J., et al. (2005): Durability modelling of glass fibre reinforcement in cementitious environment. *Materials and Structures,* Vol. 38 (2), pp. 155-162.

Orosz K. (2013): *Tensile behaviour of mineral-based composites.* Licentiate Thesis, Technical University of Luleå, pp. 78.

Orosz K., et al. (2010): From material level to structural use of mineral-based composites—an overview. *Advances in Civil Engineering,* Vol. 2010.

Ortlepp R., Curbach M. and Weiland S. (2008): Rehabilitation and strengthening of a hypar concrete shell by textile reinforced concrete. *Excellence in Concrete Construction through Innovation, Taylor & Francis, Kingston University, United Kingdom,* Vol., p. 357.

Ortlepp R., Schladitz F. and Curbach M. (2011): TRC strengthened RC columns. *Textilbetonverstärkte Stahlbetonstützen,* Vol. 106 (9), pp. 640-648.

Pan B., et al. (2009): Two-dimensional digital image correlation for in-plane displacement and strain measurement: a review. *Measurement science and technology,* Vol. 20 (6).

Papanicolaou C., et al. (2008): Textile reinforced mortar (TRM) versus FRP as strengthening material of URM walls: out-of-plane cyclic loading. *Materials and Structures,* Vol. 41 (1), pp. 143-157.

Parnas R., Shaw M. T. and Liu Q. (2007): *Basalt Fiber Reinforced Polymer Composites (No. NETCR63).* The New England Transportation Consortium pp. 133.

Peiffer F. (2008): *Framework for adaptive simulations applied to textile reinforced concrete.* Dissertation, RWTH Aachen University

Peled A. and Bentur A. (2003): Fabric structure and its reinforcing efficiency in textile reinforced cement composites. *Composites Part A: Applied Science and Manufacturing,* Vol. 34 (2), pp. 107-118.

Peled A., Bentur A. and Yankelevsky D. (1994): Woven fabric reinforcement of cement matrix. *Advanced Cement Based Materials,* Vol. 1 (5), pp. 216-223.

Peled A., Bentur A. and Yankelevsky D. (1998): Effects of woven fabric geometry on the bonding performance of cementitious composites: mechanical performance. *Advanced Cement Based Materials,* Vol. 7 (1), pp. 20-27.

Peled A., Bentur A. and Yankelevsky D. (1999): Flexural performance of cementitious composites reinforced with woven fabrics. *Journal of materials in civil engineering,* Vol. 11 (4), pp. 325-330.

Pettersson M. and Thorsson P. (2014): *FE-modelling of Textile Reinforced Concrete Facade Elements.* Master's Thesis, Civil and Environmental Engineering, Chalmers University of Technology, pp. 88.

Pré Consultants. (2010): *SimaPro 7 Database Manual, Methods Library v.2.4.* pp.

Purnell P. (1998): *The durability of glass fibre reinforced cements made with new cementitious matrices.* Dissertation, Aston University.

Raupach M., Orlowsky J. and Büttner T. (2011): Verbesserung der Dauerhaftigkeit von Textilbeton mittels Polymeren-Materialauswahl und Langzeitprognose (Improvement of the durability of textile reinforced concrete using polymers - Material selection and long-term predictions). 6th Colloquium on Textile Reinforced Structures (CTRS6), Curbach, M. (ed.) Berlin, Germany, 2011, pp. 227-244.

Richter M. (2005): *Entwicklung mechanischer Modelle zur analytischen Beschreibung der Materialeigenschaften von textilbewehrtem Feinbeton (On the development of mechanical models to analytically describe the material properties of fine-grained textile reinforced concrete).* Dissertation, Fakultät Bauingenieurwesen, Technischen Universität Dresden.

Richter M., Lepenies I. and Zastrau B. W. (2002): On the influence of the bond behaviour between fiber and matrix on the material properties of textile reinforced concrete. International symposium of anisotropic behaviour of damaged materials, 2002, pp. 1-24.

RILEM TC 162-TDF. (2001): Test and design methods for steel fibre reinforced concrete: Uni-axial tension test for steel fibre reinforced concrete. *Materials and Structures (RILEM).*

RILEM TC 187-SOC. (2007): Experimental determination of the stress-crack opening curve for concrete in tension: Final report.

Saertex. (2013): *Saertex - Fibre Properties* [Online]. Available: http://www.saertex.com/produkt_technik/produkte/fasereigenschaften/ [Accessed February 5 2012].

Scheerer S., Schladitz F. and Curbach M. (2015): Textile Reinforced Concrete - From the Idea to a High Performance Material. 3rd ICTR International Conference on Textile Reinforced Concrete Brameshuber, W. (ed.) Aachen, Germany, 2015: RILEM SARL, pp. 15-33.

Scheffler C., Förster T. and Mäder E. (2009a): Beschleunigte Alterung von Glasfasern in alkalischen Lösungen: Einflüsse auf die mechanischen Eigenschaften (Accelerated aging of glass fibers in alkali solutions: Influence on the mechanical properties). 4th Colloquium on Textile Reinforced Structures (CTRS4), Curbach, M. and Jesse, F. (eds.), Dresden, Germany, 3-5 June, 2009a, pp. 63-74.

Scheffler C., et al. (2009b): Aging of alkali-resistant glass and basalt fibers in alkaline solutions: Evaluation of the failure stress by Weibull distribution function. *Journal of Non-Crystalline Solids,* Vol. 355 (52), pp. 2588-2595.

Scheffler C., et al. (2009c): Interphase modification of alkali-resistant glass fibres and carbon fibres for textile reinforced concrete I: Fibre properties and durability. *Composites Science and Technology,* Vol. 69 (3), pp. 531-538.

Scheffler C., et al. (2009d): Interphase modification of alkali-resistant glass fibres and carbon fibres for textile reinforced concrete II: Water adsorption and composite interphases. *Composites Science and Technology,* Vol. 69 (7–8), pp. 905-912.

Schladitz F., et al. (2012): Bending load capacity of reinforced concrete slabs strengthened with textile reinforced concrete. *Engineering structures,* Vol. 40, pp. 317-326.

Scholzen A., Chudoba R. and Hegger J. (2012): Dünnwandiges Schalentragwerk aus textilbewehrtem Beton (Thin-walled shell structure of textile reinforced concrete). *Beton und Stahlbetonbau,* Vol. 107 (11), pp. 767-776.

Shaeffer R. E. (1992): *Reinforced concrete: preliminary design for architects and builders*. McGraw-Hill.

Shams A., Horstmann M. and Hegger J. (2014): Experimental investigations on Textile-Reinforced Concrete (TRC) sandwich sections. *Composite Structures,* Vol. 118, pp. 643-653.

Shams A., et al. (2015): Innovative sandwich structures made of high performance concrete and foamed polyurethane. *Composite Structures,* Vol. 121, pp. 271-279.

Si Larbi A., Contamine R. and Hamelin P. (2012): TRC and Hybrid Solutions for Repairing and/or Strengthening Reinforced Concrete Beams. *In:* Parra-Montesinos, G., et al. (eds.) *High Performance Fiber Reinforced Cement Composites 6*, Springer Netherlands, pp. 527-534.

Sim J., Park C. and Moon D. Y. (2005): Characteristics of basalt fiber as a strengthening material for concrete structures. *Composites Part B: Engineering,* Vol. 36 (6–7), pp. 504-512.

Skarzynski L., Kozicki J. and Tejchman J. (2013): Application of DIC technique to concrete—study on objectivity of measured surface displacements. *Experimental Mechanics,* Vol. 53 (9), pp. 1545-1559.

Smarter Building Systems. (2010): *Smarter Building Systems* [Online]. USA. Available: http://www.smarter-building-systems.com/smarter-building-basalt-faqs.html [Accessed September 10 2012].

Soukhanov A. V., et al. (2014): Modern Basalt Fibers and Epoxy Basaltoplastics: Properties and Applications. *In:* Kajzar, F., et al. (eds.) *Key Engineering Materials: Interdisciplinary Concepts and Research*, CRC Press.

SS 13 72 31. (2005): Concrete testing - Hardened concrete - Tensile strength of test specimens.

Sueki S., et al. (2007): Pullout-slip response of fabrics embedded in a cement paste matrix. *Journal of Materials in Civil Engineering,* Vol. 19 (9), pp. 718-727.

Svensk Betong. (2015): *Miljö och Hållbarhet - Koldioxidutsläpp* [Online]. Available: http://www.svenskbetong.se/bygga-med-betong/bygga-med-prefab/miljo-och-hallbarhet/koldioxidutslapp [Accessed May 10 2015].

Swiss Centre for Life Cycle Inventories. (2013): EcoInvent v3.0.

Tang L., et al. (2012): Covercrete with hybrid functions–A novel approach to durable reinforced concrete structures. *Materials and Corrosion,* Vol. 63 (12), pp. 1119-1126.

TNO DIANA. (2014): Finite Element Analysis User's Manual - Release 9.5.

Tomoscheit S., et al. (2011): Project Life INSUSHELL: Reducing the Carbon Footprint in Concrete Construction. *International Journal of Sustainable Building Technology and Urban Development,* Vol. 2 (2), pp. 162-169.

Triantafillou T. C. and Papanicolaou C. G. (2006): Shear strengthening of reinforced concrete members with textile reinforced mortar (TRM) jackets. *Materials and structures,* Vol. 39 (1), pp. 93-103.

Tysmans T., Adriaenssens S. and Wastiels J. (2011): Form finding methodology for force-modelled anticlastic shells in glass fibre textile reinforced cement composites. *Engineering Structures,* Vol. 33 (9), pp. 2603-2611.

Täljsten B., Orosz K. and Blanksvärd T. (2006): Strengthening of Concrete Beams in Shear with Mineral Based Composites Laboratory Tests and Theory. Third International Conference on FRP Composites in Civil Engineering (CICE 2006), Florida, USA, 2006, pp. 609-612.

Van de Velde K., Kiekens P. and Van Langenhove L. (Year): Basalt fibres as reinforcement for composites. *In:* Proceedings of 10th international conference on composites/nano engineering, University of New Orleans, New Orleans, LA, USA, 2003, 20-26.

Wei B., Cao H. and Song S. (2010): Tensile behavior contrast of basalt and glass fibers after chemical treatment. *Materials & Design,* Vol. 31 (9), pp. 4244-4250.

Vetrotex. (2011): *Saint-Gobain Vetrotex - Technical Information* [Online]. Available: http://www.vetrotextextiles.com/TechnicalInformation [Accessed January 14 2012].

Williams Portal N. (2013): *Sustainability and Flexural Behaviour of Textile Reinforced Concrete.* Licentiate Thesis, Structural Engineering, Chalmers University of Technology.

Williams Portal N., et al. (2015a): Implementation of Experimental Data in Analyses of Textile Reinforced Concrete Structures. 3rd ICTRC International Conference on Textile Reinforced Concrete Aachen, Germany, June 7-10 2015a: RILEM.

Williams Portal N., et al. (2014a): Alkali Resistance of Textile Reinforcement for Concrete Facade Panels. XXII Concrete Research Symposium, Reykjavik 2014a.

Williams Portal N., Lundgren K. and Malaga K. (2014b): Evaluation of Pull-out Behaviour in Textile Reinforced Concrete. 10th fib International PhD Symposium in Civil Engineering, Quebec City, Canada, 2014b, p. 97.

Williams Portal N., et al. (2014c): Sustainable Potential of Textile-Reinforced Concrete. *Journal of Materials in Civil Engineering,* Vol. 27 (7).

Williams Portal N., et al. (2013): Numerical Modelling of Textile Reinforced Concrete. VIII International Conference on Fracture Mechanics of Concrete and Concrete Structures, Toledo, Spain, 10-14 March, 2013.

Williams Portal N., et al. (2014d): Pull-out of textile reinforcement in concrete. *Construction and Building Materials,* Vol. 71, pp. 63-71.

Williams Portal N., et al. (2015b): Durability Study of Textile Fiber Reinforcement. Concrete 2015, 27th Biennial National Conference of the Concrete Institute of Australia, Melbourne, Australia, 30 August - 2 September, 2015b.

Wulfhorst B., et al. (2006): *Textile technology*. Wiley Online Library.

Xu S. (2004): Bond Characteristics of Carbon, Alkali Resistant Glass, and Aramid Textiles in Mortar. *J. Mater. Civ. Eng.,* Vol. 16 (4), p. 356.

Xu S. and Li H. (2007): Bond properties and experimental methods of textile reinforced concrete. *Journal of Wuhan University of Technology--Materials Science Edition,* Vol. 22 (3), pp. 529-532.

Zandi Hanjari K. (2008): *Load-carrying capacity of damaged concrete structures.* Licentiate Thesis, Civil and Environmental Engineering, Chalmers University of Technology, pp. 98.

Zastrau B., Richter M. and Lepenies I. (2003): On the Analytical Solution of Pullout Phenomena in Textile Reinforced Concrete. *Journal of Engineering Materials and Technology*, Vol. 125 (1), pp. 38-43.

Zhang X. B., Aljewifi H. and Li J. (2013): Failure behaviour investigation of continuous yarn reinforced cementitious composites. *Construction and Building Materials*, Vol. 47 (0), pp. 456-464.

Zhu W. and Bartos P. J. M. (1997): Assessment of interfacial microstructure and bond properties in aged GRC using a novel microindentation method. *Cement and Concrete Research*, Vol. 27 (11), pp. 1701-1711.

Appendix A

Experimental methods for concrete

Appendix A Experimental methods for concrete

A.1 Compression properties

Additional information regarding the tests conducted to determine the compression properties of concrete is presented here.

Method 2: Cylinder tests

Specimen: Cylinders were initially cast with dimensions of Ø54/200 mm in plastic cylindrical moulds and were sawn to their final length prior to testing. The specimens were demoulded and stored in water at approximately 20 °C until testing.

Test setup: Testing was conducted using a GCTS servo-hydraulic machine with a stiff load frame (load cell rated up to 1.5 MN and accuracy within 1 %). Inductive displacement transducers (range ± 2.50 mm and relative error < 1 %) were used as instrumentation for axial and circumferential deformation measurements. Refer to Figure A.1.

Test details: The tests were conducted at SP. Initially, the compressive strength, f_c, was determined in accordance with EN 12390-3 (2009) to define stress levels for the test cycle used to determine the stabilized secant modulus of elasticity, $E_{c,s}$, according to EN 12390-13 (2013) (*Method B*). A limitation of these tests is that only the compressive strength and the secant modulus are obtained, yet one of the benefits of introducing a cyclic load is to minimize the risk of potential settlement of the loading surfaces. The stress-strain relationship in compression was determined for specimens with the same concrete and dimensions. Measurements were performed in accordance with the same aforementioned standards, with the exception that the load was applied using deformation control with a displacement rate of 0.12 mm/min.

The compressive strength, f_c, was defined as the peak stress and the ultimate strain, ε_{cu}, was defined as the corresponding strain. The elastic properties, i.e. modulus of elasticity, E_c, and Poisson's ratio, ν_c, were evaluated as the secant modulus between the lower, σ_l, of 5 MPa and upper stress levels, σ_u, of $f_c/3$. The axial strain, ε_a, was calculated as the ratio of mean axial deformation and gauge length (distance between rings), while the radial strain, ε_r, was calculated from the circumferential deformation measurements. The volumetric strain, ε_{vol}, corresponded to the summation of axial strain and two times the radial strain. Poisson's ratio, ν, was determined as the ratio of radial to axial strain. See Figure A.2 for a summary of results.

In principle, both methods presented are suitable to determine the compressive properties, i.e. secant modulus and compressive strength of concrete, yet the first one is evaluated according to a standardized method and the other directly from the material's stress-strain curve. It is important to note that from Figure A.2 (b), there exists a standard deviation between the yielded compressive strength values.

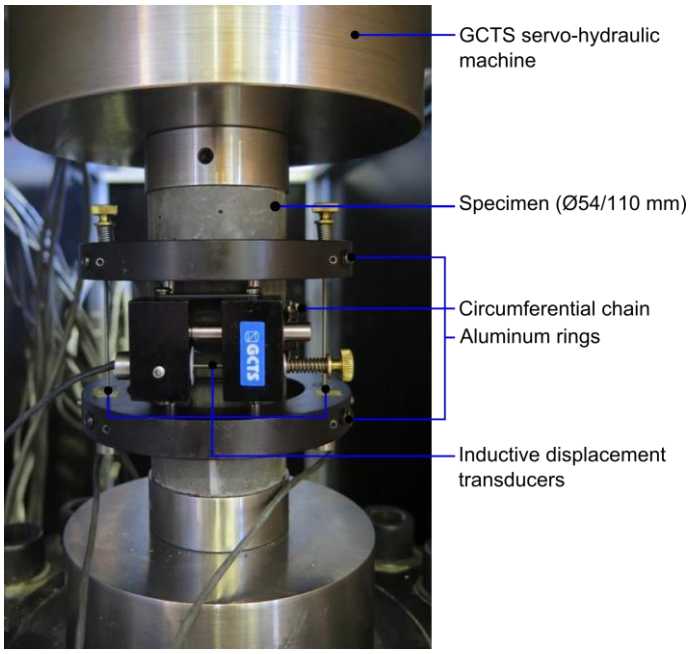

Figure A.1 *Compressive test setup and instrumentation for axial and circumferential deformation measurements.*

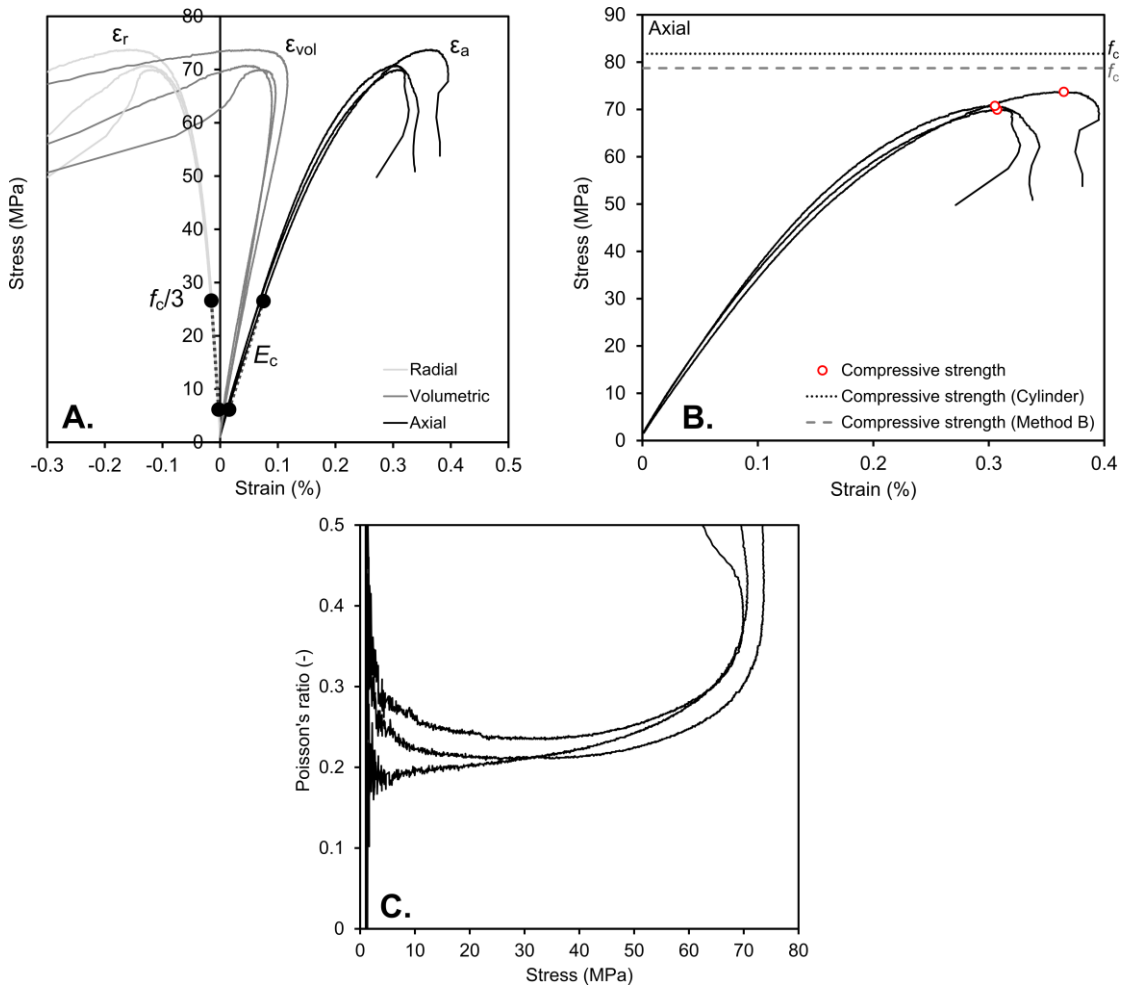

Figure A.2 *Overview of compressive test results: stress-strain diagram (a), axial stress-strain (b) and Poisson's ratio versus stress (c).*

A.2 Tensile properties

Additional information regarding the tests conducted to determine the tensile properties of concrete is presented here.

Method 2: Direct tensile test

Specimen: Cylindrical specimens (Ø54/100 mm) were tested after 28 days. The cylinders were first glued to solid steel cylindrical end caps with epoxy resin. After 24 hours of drying, the specimens along with the steel end caps were axially fixed in the test machine.

Test setup: The tests were conducted using a universal servo-mechanical testing machine with a load cell of 100 kN (Instron 1195) under load-controlled conditions wherein the loading rate was 0.05 MPa/s. Cylindrical specimens were attached to the machine by means of a hinge connection between the steel cylindrical end caps and the testing machine.

Test details: Direct tensile tests were performed according to SS 13 72 31 (2005) at CBI. The measured results include the tensile load and overall machine displacement, i.e. global displacement. The tensile strength, f_t, is obtained by dividing the failure load by the cross-sectional area of the specimen. The end conditions applied in this test setup did not allow for the characterization of the softening behaviour. The test setup and an example of tensile stress versus global displacement results are presented in Figure A.3.

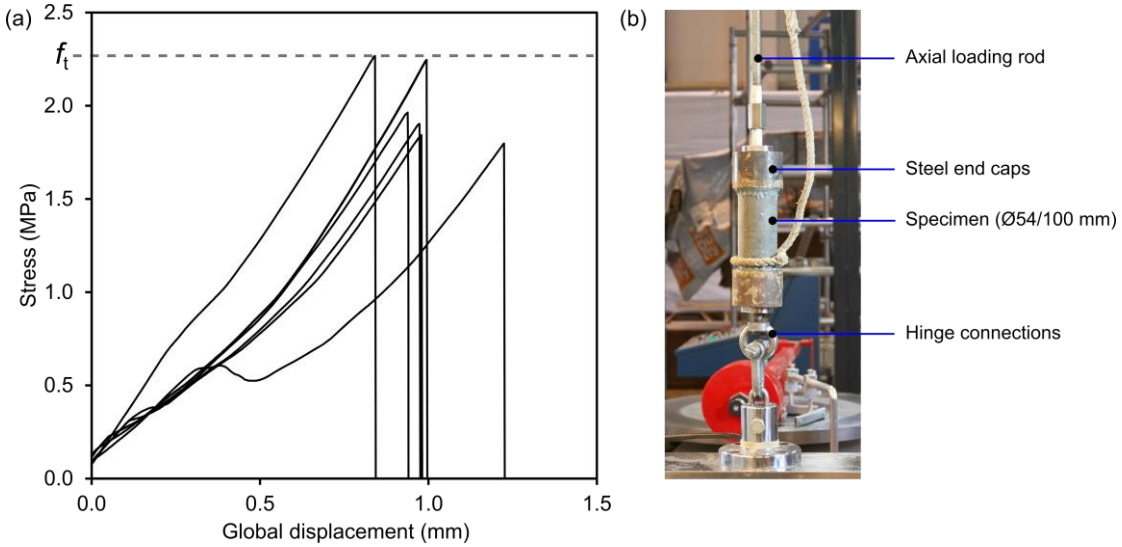

Figure A.3 Overview of tensile test results (a) and test setup (b).

Method 3: Uniaxial tension test (UTT)

Specimen: Tests were performed on notched cylinders (Ø 100/100 mm) with fixed end conditions after 28 days of curing. Cylinders were initially cast with dimensions of Ø 100/200 mm in steel cylindrical moulds and were sawn to their final length prior to testing. The notches were sawn on each side of the centreline of the specimen with a depth of 15 mm and width of 3 mm (see Figure A.4 (a)), whereby amounting to a combined depth of 30 % of the specimen width. The diameter across the notch was

measured at three separate locations along the perimeter and the average value was used to calculate the corresponding cross-sectional area at the notch.

Test setup: The same testing device as previously specified for *Method 2: Cylinder tests* was used in order to suppress rotations of the load platens that could lead to bending failure (see Figure A.4 (b)). As well, the device was pre-tensioned with a load of 150 kN and the load cell was rated up to 200 kN. The deformation was applied at a rate of 0.003 mm/min and measured locally over the cylinder notch with three inductive displacement transducers with a gauge length, l_g, of 30 mm. The deformation was calculated as the mean value of the three displacement gauges.

Test details: The tests were conducted at SP based on RILEM TC 187-SOC (2007) and RILEM TC 162-TDF (2001). The stress-deformation curve shown in Figure A.5 was used to derive the softening behaviour of the concrete material according to equations provisioned in RILEM TC 187-SOC (2007). The tensile stress, σ, was derived by dividing the load by the effective cross-section, A_{eff}, at the notch. The tensile strength, f_t, is defined as the peak stress and deformation at peak stress, δ_{tu}, which takes place at the onset of macro cracking. The crack opening w, in the post-peak regime, was calculated by subtracting the elastic deformation, δ_e, from the measured deformation, δ. Since the notch obstructed the direct measurement of the modulus of elasticity in tension, the ratio E/l_g was replaced by the elastic stiffness, K, which was evaluated directly from the tensile stress-deformation curve. The fracture energy G_F was thereafter calculated from the area under the stress-crack opening relationship.

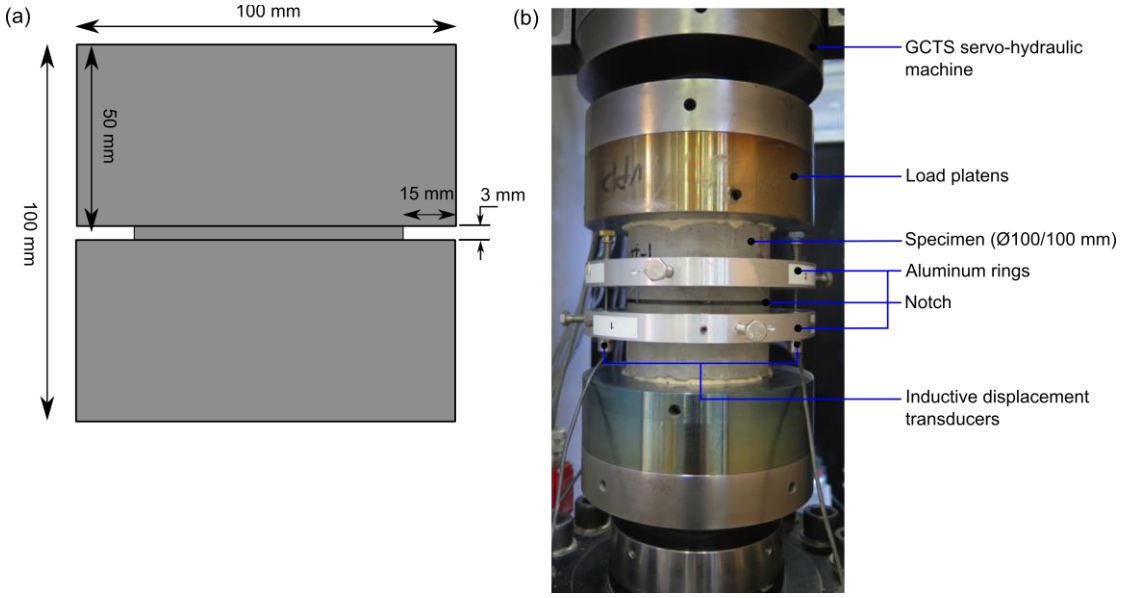

Figure A.4 Tensile test specimen geometry (not to scale) (a) and experimental test setup for the uniaxial tensile test (UTT) (b).

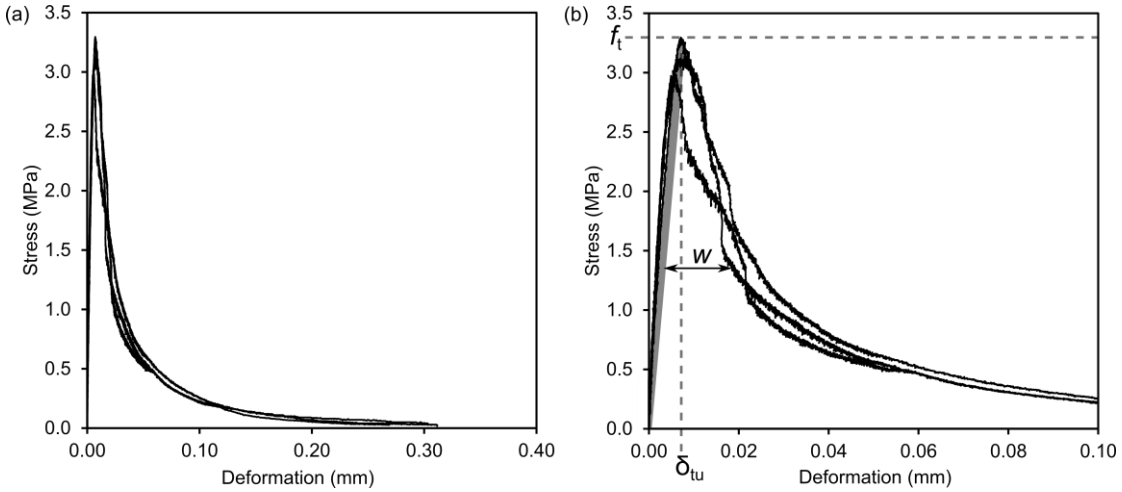

Figure A.5 Overview of UTT results: stress-deformation curve (a) and definition of crack-opening relationship (b).

References

EN 12390-3. (2009): Testing hardened concrete - Part 3: Compressive strength of test specimens. Comité Européen de Normalisation (CEN).

EN 12390-13. (2013): Testing hardened concrete - Part 13: Determination of secant modulus of elasticity in compression. Comité Européen de Normalisation (CEN).

RILEM TC 162-TDF. (2001): Test and design methods for steel fibre reinforced concrete: Uni-axial tension test for steel fibre reinforced concrete. *Materials and Structures (RILEM).*

RILEM TC 187-SOC. (2007): Experimental determination of the stress-crack opening curve for concrete in tension: Final report.

SS 13 72 31. (2005): Concrete testing - Hardened concrete - Tensile strength of test specimens.

Appendix B

Pull-out testing of TRC

Appendix B Pull-out testing of TRC

Details related to the additional pull-out investigations for TRC are presented here.

Test method

A modified double-sided pull-out test was studied in addition to the content presented in the enclosed papers. The main simplification of this method is such that the embedded length is defined by means of cutting away a part of the yarn within the anchorage length as previously illustrated. A video extensometer technique (Messphysik Video Extensometer ME46 with pattern recognition) was used instead of physical extensometers to capture the active end-slip of the reinforcement relative to the concrete end.

Preliminary study

A preliminary study was conducted to evaluate the modified pull-out test method according to Table B.1. The pull-out tests were performed on specimens reinforced by either one layer of carbon textile grid or reinforced by an individual carbon yarn in order to determine the effect of the grid structure and cross-threads on the bond behaviour. Surface modifications were also studied using a *polymer* coating and epoxy (see Section 5.2.2). The embedment length was chosen to be 100 mm, however several embedment lengths will be tested in future experiments to obtain a pull-out force versus embedment length relationship for a given TRC configuration. A step-by-step procedure applied in the preliminary round of tests is presented in Figure B.1.

Table B.1 Preliminary test matrix.

Textile reinforcement type	2D carbon textile		
Surface coating	Reference (no coating)	Polymer coating	Epoxy
No. specimens – grid	3	3	3
No. specimens – roving	3	3	3
Embedment length, L_e (mm)	100		
Anchorage length, L_a (mm)	100		
Free length of roving (mm)	150		

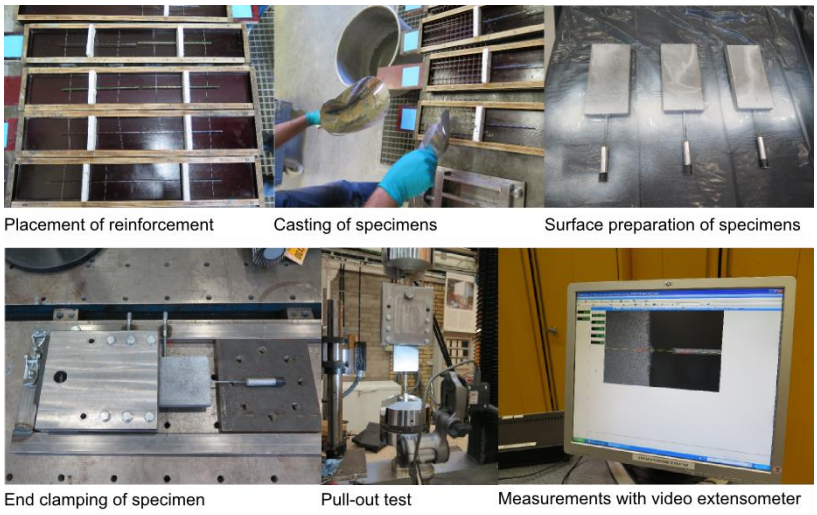

Figure B.1 Overview of the step-by-step procedure applied.

Results and added value of method

Images captured via video extensometer techniques along with the associated force versus active end slip curves are shown in Figure B.2 for both grid and roving. For the reference case, the effect of the cross-threads (spacing of 18 mm) becomes apparent by sudden load dips signifying that any *defect* or *change of area* related to the tested roving can inherently affect the bond. The reference grid had more mechanical anchorage which generally decreased the bond strength, yet further experiments are required to make conclusive remarks due to the observed uncertainty. The epoxy grid versus roving had on average superior bond strength and less active slip due to the enhanced stiffness and mechanical anchorage provided by the entire grid structure. Overall, the addition of epoxy to the roving or grid was shown to increase the bond strength and also led to a more homogeneous distribution of stresses to the reinforcement resulting in e.g. the rupture of the roving in the case of the grid.

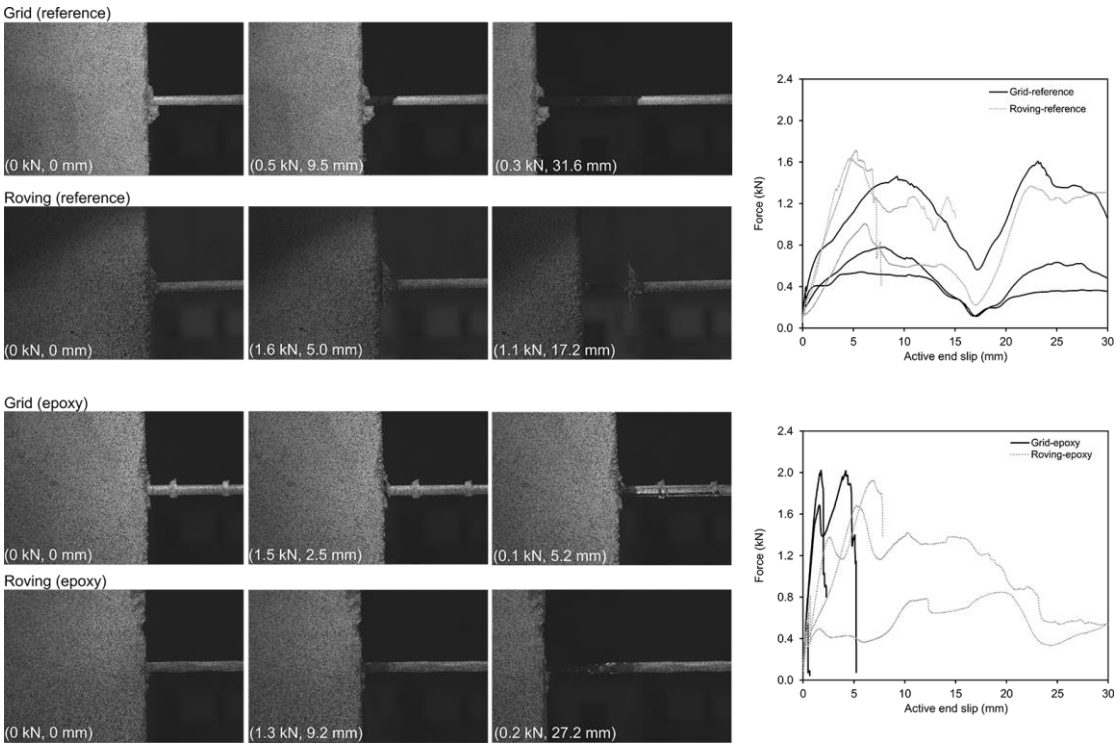

Figure B.2 Images of the end slip and force versus active end slip for reference and epoxy coated grid and roving.

The added value of this developed pull-out method compared to the two-sided method applied in Section 4 (**Paper II**) is summarized in Table B.2.

Table B.2 Summary of added value of the developed pull-out method.

Feature	Remark	Disadvantages	Modifications
Casting method/ specimen type	No need to cut the specimen to create a 'breaking point' after casting which is common in other methods.	Additional reinforcement preparation and sizing.	Improve the precision of the reinforcement placement. Could create more customized formwork.
End anchorage of reinforcement	Similar solution applied for the tensile tests of the rovings (Section 2)	Additional preparation and epoxy drying time prior to testing (24 hrs)	–
End clamping of specimen	Similar solution applied for the uniaxial tensile tests of TRC (Section 6).	–	–
Test setup	Similar test setup that is used for uniaxial tensile tests of TRC (Section 6), such that there is no need for supplemental apparatuses.	–	–
Measurement of active end slip	Accurate measurement of active end slip relative to concrete using video extensometer technique	Additional surface preparations.	–
Measurement of passive end slip	Not measured.	More challenging casting procedure.	Could include an 'opening' in the specimen at the end of the roving to capture this slip.